Efficient support of DNA replication functions by DNA ligase 3 in vertebrate cells

Inaugural-Dissertation

zur

Erlangung des Doktorgrades

Dr. rer. nat.

der Fakultät für Biologie

an der

Universität Duisburg-Essen

vorgelegt von

Theresa Christin Bednar

aus Brilon

Juni 2013

Die der vorliegenden Arbeit zugrunde liegenden Experimente wurden am Institut für Medizinische Strahlenbiologie der Universität Duisburg-Essen durchgeführt.

1. Gutachter: Prof. Dr. Georg Iliakis

2. Gutachter: PD Dr. Jürgen Thomale

Vorsitzender des Prüfungsausschusses: Prof. Dr. Hemmo Meyer

Tag der mündlichen Prüfung: 11.09.2013

Es ist fast unmöglich, die Fackel der Wahrheit durch ein Gedränge zu tragen, ohne jemandem den Bart zu versengen.

Georg Christoph Lichtenberg (1742-1799)

Parts of the results have been published:

Paul, K., Wang, M., Mladenov, E., Bencsik-Theilen, A.A., Bednar, T., Wu, W., Arakawa, H., and Iliakis, G. (2013). DNA ligases I and III cooperate in alternative non-homologous end-joining in vertebrates. PLoS One *8*, e59505.

Arakawa, H., Bednar, T., Wang, M., Paul, K., Mladenov, E., Bencsik-Theilen, A.A., and Iliakis, G. (2012). Functional redundancy between DNA ligases I and III in DNA replication in vertebrate cells. Nucleic Acids Res *40*, 2599-2610.

Singh, S.K., Bednar, T., Zhang, L., Wu, W., Mladenov, E., and Iliakis, G. (2012). Inhibition of B-NHEJ in Plateau-Phase Cells Is Not a Direct Consequence of Suppressed Growth Factor Signaling. Int J Radiat Oncol Biol Phys *84*, e237-e243.

Table of contents

List of abbreviations

4HT	4-hydroxytamoxifen
Ab	Antibody
ADP	Adenosine 5’-diphosphate
AMP	Adenosine 5’-monophosphate
A-T	Ataxia-telangiectesia
ATM	Ataxia-telangiectasia-mutated
ATP	Adenosine 5’-triphosphate
ATR	Ataxia-telangiectasia and RAD3 related kinase
ATR	ATM and Rad3 related
BER	Base excision repair
BFP	Blue Fluorescent Protein
BRCA1	Breast cancer susceptibility protein 1
BRCT	BRCA1 C-terminal domain
BrdU	5-Brom-2-desoxyuridine
BSA	Bovine serum albumin
bsr	Blasticidin
Cdc9	Cell division cycle protein 9
cDNA	Complementary DNA
Chk	Checkpoint kinase
CNS	Central nervous system
Cre	Causes recombination

DAPI	4',6-diamidino-2-phenylindole
DBD	DNA-binding domain
DMEM	Dulbecco's modified eagle medium
DMSO	Dimethyl sulfoxide
DNA-PK	DNA-dependent protein kinase
DNA-PKcs	DNA-dependent protein kinase catalytic subunit
DSB	DNA double strand breaks
DsRed	Red fluorescent protein from Discosoma
EdU	Ethynyl-2’-deoxyuridine
EGFP	Enhanced green fluorescent protein
et al.	Et alii
FEN1	Flap endonuclease 1
FITC	Fluorescein isothiocyanate
GAPDH	Glyceraldehyde 3-phosphate dehydrogenase
IF	Immunofluorescence
IRES	Internal ribosome binding site
LIG1	DNA ligase 1
LIG3	DNA ligase 3
LIG4	DNA ligase 4
MEF	Mouse embryonic fibroblast
MEM	Minimum Essential Medium
Mer	Mutated estrogen receptor
mts-hLIG1	Human LIG1 with a mitochondrial targeting signal

NAD^+	Nicotinamide adenine dinucleotide
NER	Nucleotide excision repair
NHEJ	Non-homologous end-joining
NTase	Nucleotidyltransferase
OB-fold	Oligonucleotide/oligosaccharide binding-fold
PARP1	Poly (ADP-ribose) polymerase 1
PBS	Phosphate-buffered saline
PCNA	Proliferating cell nuclear antigen
PCR	Polymerase chain reaction
PI	Propidium iodide
PIKK	Phosphoinositide 3-kinase-like kinase
PIP	PCNA-binding motif
pol α	DNA polymerase α
pol δ	DNA polymerase δ
RFC	Replication factor C
RPA	Replication protein A
RSV	Rous sarcoma virus
RT	Room temperature
S. cerevisiae	*Saccharomyces cerevisiae*
SCE	Sister chromatid exchange
SDS	sodium dodecyl sulfate
SV40	Simian virus
TBP1	TATA-binding protein 1

V(D)J	Variable (diversity) joining
WCE	Whole cell extract
XLF	XRCC4-like factor
XRCC1	X-ray cross-complementing protein 1
XRCC4	X-ray cross-complementing protein 4
ZnFn	Zinc finger

List of figures

List of tables

1 Introduction

1.1 DNA ligases

The joining of breaks in the phosphodiester backbone of the DNA is of great importance in maintaining genomic stability in all phases of the cell cycle and is carried out by enzymes collectively called DNA ligases. Joining of strand ends at the DNA is required during the removal of DNA lesions generated by DNA damaging agents, but also of spontaneously generated DNA lesions. Indeed, approx. 2×10^5 DNA single-strand breaks are spontaneously generated per mammalian cell per day, whereas 1 Gray (Gy) of ionizing radiation only causes 600-1000 single-strand breaks and 16-40 double-strand breaks (Barnes and Lindahl, 2004; Ward, 1988). This form of joining in the phosphodiester backbone is of even greater importance during DNA replication, where approx. 2×10^7 Okazaki fragments are generated by discontinuous lagging strand DNA synthesis; ligation of these fragments is crucial for completing DNA replication. Furthermore, programmed DNA double-strand breaks are generated in a number of cell types such as immune cells undergoing immunoglobulin gene rearrangements (Bassing and Alt, 2004; Yao et al., 1996).

In 1967 the joining of DNA ends was first described in extracts of *Escherichia coli* and 1 year later also in extracts of mammalian cells (Lehman, 1974). The required high energy co-factor divides the DNA ligases into 2 sub-families: The first family of ligases uses Nicotinamide adenine dinucleotide (NAD^+) as a cofactor, while the second family of ligases uses adenosine 5'-triphosphate (ATP). All known eukaryotic ligases are ATP dependent, whereas in bacteria, archea and viruses members of both families have been found (Ellenberger and Tomkinson, 2008). As in this thesis the contribution of DNA ligases to replication in vertebrates is studied, the following discussion focuses on ATP-dependent ligases.

1.1.1 Catalytic Activities of DNA ligases

The 3 step mechanism by which DNA ligases catalyze the formation of the phosphodiester bond is shown in Figure 1. The mechanism is universal and shared by all DNA ligases and also by RNA ligases (Nandakumar et al., 2006; Shuman, 2009). In the first step, an adenosine 5'-monophosphate (AMP) is transferred from ATP to a lysine in the active site of the ligase. In the second step, the ligase bound AMP is transferred to the 5' phosphate of the DNA substrate. The 5' AMP activates the 5' phosphate of the DNA substrate for phosphodiester bond formation and during step 3 the 3' hydroxyl of an adjacent DNA strand attacks this end to replace the AMP and covalently joins the DNA strands (Ellenberger and Tomkinson, 2008; Tomkinson et al., 2006). As each reaction by itself is energetically highly favorable, this process is effectively irreversible. Therefore, it is likely that, even in the absence of a suitable substrate, ligases in the cell are adenylated. This adenylation also enhances the specificity of DNA binding, which is known as nick sensing (Ellenberger and Tomkinson, 2008; Sriskanda and Shuman, 1998).

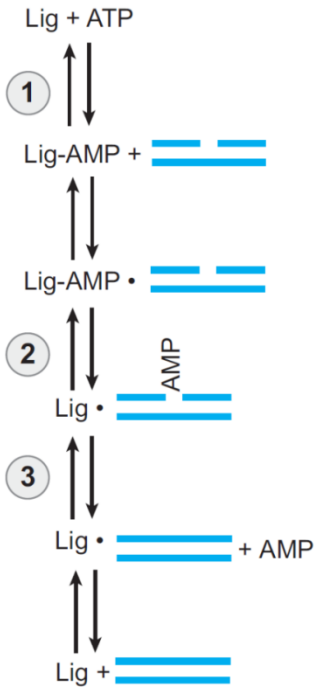

Figure 1: Schematic representation of the enzymatic ligation of DNA (Ellenberger and Tomkinson, 2008)

1.1.2 Structural features of eukaryotic DNA ligases

Recent advances in the research of the structure of DNA ligases reveal that all ligases except the simplest viral ligases completely encircle the DNA substrate, using a multidomain architecture with sufficient flexibility to open and close around the DNA. Tomas Lindahl first provided biochemical and immunological evidence that there is more than one species of DNA ligases in mammalian cells; these species have recently been extensively characterized (Ellenberger and Tomkinson, 2008; Lindahl and Barnes, 1992).

All DNA ligases share a conserved catalytic domain, the catalytic core, consisting of the nucleotidyltransferase (NTase) domain flexibly tethered through a polypeptide linker to an oligonucleotide/oligosaccharide binding (OB)-fold domain. This domain, typically associated with single-strand DNA-binding proteins, binds double stranded DNA in the minor groove and contacts the 3'-OH and 5'-PO_4 ends of DNA during the last 2 steps of ligation.

While the NTase and OB-fold domains are conserved in all known DNA and RNA ligases and form the minimal catalytic unit, mammalian ligases are endowed with additional N- and C-terminal domains. These domains serve as protein-protein and/or protein-DNA-binding domains and are therefore crucial for biological activity. One of these domains is shared by all eukaryotic DNA ligases: the N-terminal DNA-binding domain (DBD). It interacts with the minor groove and contacts the DNA upstream and downstream of the nick. It stabilizes the DNA in underwound conformation and makes protein-protein interactions with the catalytic core completing a ring shaped structure that encircles the DNA (Cotner-Gohara et al., 2008; Pascal et al., 2004). Homologs of the DNA ligase 1 (LIG1) and DNA ligase 4 (LIG4) genes appear to be present in all eukaryotes. In contrast, the DNA ligase 3 (LIG3) gene appears to be restricted to vertebrates. The characteristic features of the DNA ligase polypeptides are described below.

1.1.3 DNA Ligase 1

CDC9, the homolog of human *LIG1* gene in *Saccharomyces cerevisiae* (*S. cerevisiae*), is essential for cell survival and its mutation leads to hypersensitivity to DNA damage, which links Cdc9 to DNA replication and repair (Hartwell, 1974; Johnston, 1979; Johnston and Nasmyth, 1978). There are 2 translation initiation sites generating 2 forms of Cdc9 (Figure 2).

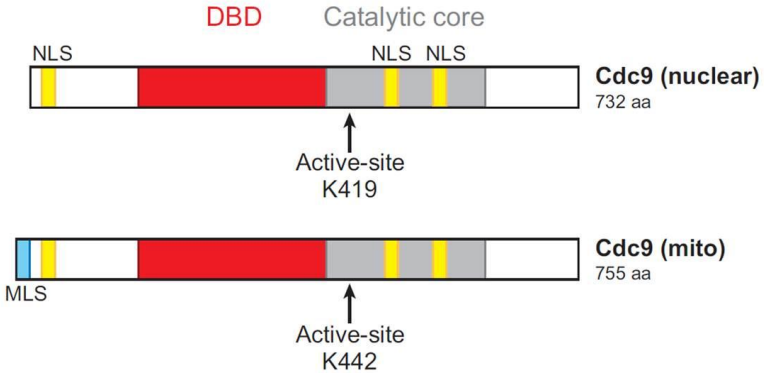

Figure 2: Schematic representation of nuclear and mitochondrial Cdc9 (Ellenberger and Tomkinson, 2008) NLS: nuclear localization signal (yellow), DBD: DNA-binding domain (red), OB-fold domains (gray), MLS: Mitochondrial leader sequence (blue)

One is directed to the nucleus, the other one has an N-terminal mitochondrial leader sequence which results in mitochondrial localization of the protein to maintain the genome in this organelle (Willer et al., 1999). Unlike *CDC9*, the human *LIG1* gene does not encode a polypeptide that is targeted to mitochondria, as in vertebrates the *LIG3* gene encodes the mitochondrial DNA ligase (Figure 3).

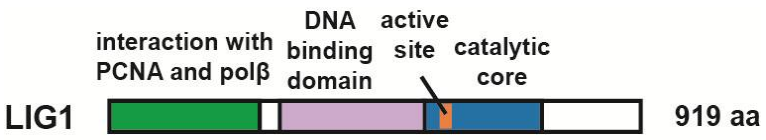

Figure 3: Schematic representation of vertebrate LIG1. (Arakawa et al., 2012)

The N-terminal region of LIG1 could not be associated with nicked DNA but contains sequences required for nuclear localization of LIG1 to replication forks and is involved in protein-protein interactions that are discussed in detail below

(Cardoso et al., 1997; Montecucco et al., 1998; Montecucco et al., 1995; Pascal et al., 2004). Further regulation of the functions of this domain is afforded by serine phosphorylations mediated by cyclin dependent kinases and by casein kinase II (Ferrari et al., 2003; Montecucco et al., 1998; Rossi et al., 1999; Song et al., 2007).

1.1.3.1 LIG1 and Okazaki fragment maturation

In eukaryotes, replication of double-stranded DNA is an essential preparatory step for cell division and takes place during the S-phase of the cell cycle. The genetic material is duplicated with high efficiency and accuracy. DNA replication is initiated at multiple origins on each chromosome and proceeds bi-directionally from each and every replication origin forming a replication fork. (Zheng and Shen, 2011). Due to the 5’ to 3’- directionality of DNA polymerases, replication proceeds by continuous synthesis on the leading strand and discontinuous synthesis on the lagging strand (Balakrishnan and Bambara, 2011). Both, leading and lagging strand synthesis, are progressing with similar speed, which is likely due to some sort of coordination between leading and lagging strand synthesis (Pandey et al., 2009). As at the leading strand, continuous involvement of DNA ligases is not necessary, only the synthesis of the lagging strand will be described in more detail.

Lagging strand synthesis is initiated by RNA primers and continues with the formation of DNA segments, the Okazaki fragments, which have a length of approx. 100 to 200 nucleotides in eukaryotes and consist of an 8 to 11 nucleotides long RNA primer followed by a short stretch of DNA (Balakrishnan et al., 2010; Okazaki et al., 1968). The first short RNA primer and a short portion of DNA are synthesized by the primase, which is a hetero-tetramer of RNA polymerase and DNA polymerase α (pol α) and then prolonged by polymerase δ (pol δ) (Zheng and Shen, 2011). Pol δ displays both polymerase and proofreading function and can therefore correct errors made by pol α (Balakrishnan and Bambara, 2011). Replication protein A (RPA) binds to the single stranded DNA immediately after unwinding by DNA helicases and thus protects the DNA from cellular nucleases. Furthermore, it acts as an assembly

point for replication-associated proteins like the primase (Wold, 1997). The interaction of replication factor C (RFC) with pol α triggers the switch from initiation of replication to elongation with the help of pol δ, and pol α is replaced with the former and the proliferating cell nuclear antigen (PCNA) is loaded on the DNA (Tsurimoto et al., 1990). When pol δ has filled the gap between 2 adjacent Okazaki fragments, it cannot remove the RNA segment because it does not possess a 5'-3'-exonuclease function. This function is most of the times carried out by flap endonuclease 1 (FEN1) binding to the RNA primer, cleaving it and leaving only a nick which can be joined by LIG1 (Figure 4) (Balakrishnan and Bambara, 2011; Gloor et al., 2010).

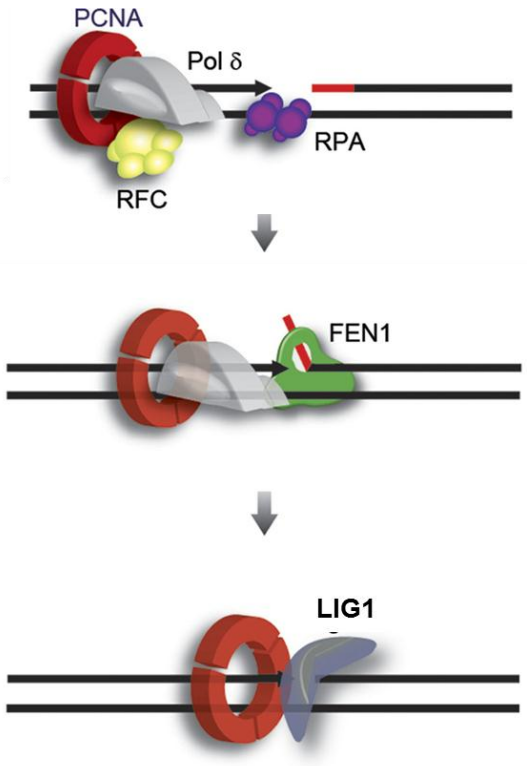

Figure 4: Eukaryotic Okazaki fragment maturation. Modified from (Balakrishnan et al., 2010)

Efficient and precise eukaryotic nick translation is a coordinated effort of PCNA, pol δ, and FEN1, which is demonstrated by the inability of mutants lacking the PCNA binding site of FEN1 to carry out nick translation (Burgers, 2009; Li et al., 1995).

In addition to their function in replication, LIG1 and FEN1 are also involved in long patch base excision repair (BER) (correction of a patch of 2-12 nt). In short patch repair (correction of a single nucleotide) another endonuclease is involved and also another ligase, LIG3 (see below) (Balakrishnan and Bambara, 2011; Matsumoto and Kim, 1995).

1.1.3.2 LIG1 protein partners

Several LIG1-interacting proteins have been identified by LIG1 affinity chromatography, among them PCNA (Levin et al., 1997; Levin et al., 2004; Song et al., 2007). The interaction is primarily mediated by a conserved PCNA-binding motif (PIP) at the N-terminus of LIG1 (Levin et al., 2000; Song et al., 2007) (Figure 5a).

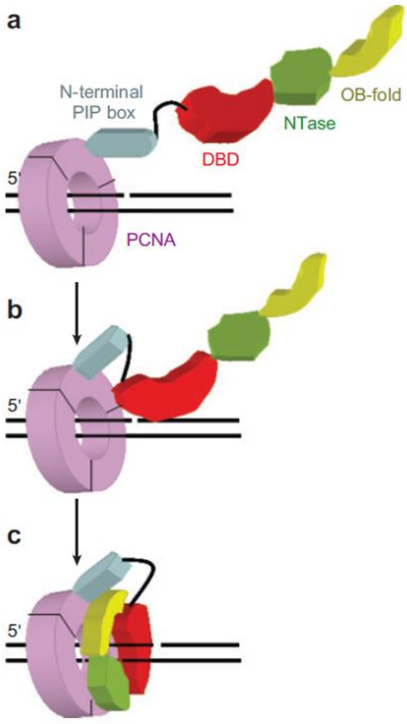

Figure 5: Model for the interaction of human LIG1 with DNA-linked homotrimeric PCNA. a) Docking of LIG1 onto the PCNA ring via an interaction between the N-terminal PIP box and the interdomain connector loop of a PCNA monomer. **b)** Initial docking facilitates an interaction between DBD and PCNA **c)** Interaction of DBD with nicked DNA orchestrates the transition of the catalytic region of LIG1 from the extended to a closed ring conformation with each of the domains containing the DNA (Ellenberger and Tomkinson, 2008).

It is assumed that the region adjacent to the PIP box is flexible and allows the catalytic core of the protein to engage both PCNA and DNA (Ellenberger and Tomkinson, 2008) (Figure 5c). The PIP box of LIG1 is essential for its localization to replication factories. Inactivation of the LIG1 PIP box not only abolishes the targeting of LIG1 to replication foci, but also affects the complementation of the Okazaki fragment joining and long-patch base excision repair defects in the LIG1-deficient human cell line 46BR (Montecucco et al., 1998; Song et al., 2007)

PCNA also interacts with the replicative DNA polymerases δ and ε, RFC and the FEN-1 nuclease, which makes it likely that PCNA coordinates their activity at replication forks (Kelman, 1997; Mossi et al., 1997; Tomkinson et al., 2006).

In addition to interacting with DNA sliding clamps and clamp loaders, LIG1 also interacts with DNA polymerase β within a base excision repair complex that was purified from bovine testes (Prasad et al., 1996).

Although PCNA is of great importance in replication, it also has diverse roles in cell cycle control and checkpoint processes (Kelman, 1997). Interestingly, PCNA is also known to interact with X-ray cross-complementing protein 1, (XRCC1) a known interaction partner of LIG3 (see below) (Fan et al., 2004).

1.1.3.3 LIG1 deficiency

As mentioned above, knockout of *CDC9* in yeast is a lethal event. There is a wealth of evidence confirming that LIG1 is the main ligase involved in joining DNA replication intermediates. LIG1 expression and activity correlate closely with the rate of cell proliferation; the protein localizes to multiprotein replication complexes and functions in lagging-strand DNA replication *in vitro* (Levin et al., 2000; Tom et al., 2001; Waga et al., 1994; Waga and Stillman, 1994). The inactivation of the vertebrate *LIG1* gene was therefore expected to be incompatible with survival. Indeed, cell lethality was observed in mouse embryonic stem cells upon inactivation of both *LIG1* alleles (Petrini et al., 1995). Notably, however, mouse embryos harboring homozygous deletions of the 3’ end of the *LIG1* gene without taking out the active site were found to develop

normally until midgestation (Bentley et al., 2002; Bentley et al., 1996). Mouse embryonic fibroblast (MEF) cell lines generated from such embryos proliferate normally, show normal sensitivity to DNA damaging agents, but have a defect in Okazaki fragment joining and increased genomic instability, but no elevated level of spontaneous sister chromatid exchanges (SCE) (Bentley et al., 2002; Bentley et al., 1996). Although in the study of 1996, the 3′ end of the gene was removed and neither *LIG1* transcripts nor LIG1 protein could be detected in mutant embryos, it was suggested that the inactivation of the gene might not have been complete, mainly because the active site of the protein had not been removed (Mackenney et al., 1997).

LIG1 deficient cell lines could also be derived from the only known case of a human with mutated *LIG1* gene, a young woman with growth retardation, sun sensitivity and immunodeficiencies, who died aged 19 with lymphoma and showed 2 different missense mutations at the *LIG1* locus on chromosome 19, one in each allele (Barnes et al., 1992; Webster et al., 1992). The SV40 immortalized cell line 46BR 1N encodes the same mutation in both alleles, a C to T transition in the codon for Arg771, which causes this residue to be replaced by Trp (Barnes et al., 1992). This mutation, though not decreasing the actual amount of protein, diminishes the activity of LIG1 to approx. 10%, without completely abolishing it (Barnes et al., 1992). 46BR cells show no obvious defects in proliferation, but show a marked defect in Okazaki fragment joining and hypersensitivity to UV-light suggesting a function of LIG1 in NER (Aboussekhra et al., 1995). In addition, cells are hypersensitive to ionizing radiation (IR) as well as to simple alkylating agents owing to a defect in the long-patch subpathway of BER (Bentley et al., 2002; Bentley et al., 1996; Henderson et al., 1985; Levin et al., 2000; Lönn et al., 1989). They also show an increased level of spontaneous SCEs, once again linking SCEs to replication and suggesting genomic instability (Painter, 1980; Sonoda et al., 1999; Webster et al., 1992; Wolff, 1977).

Although the above results suggest that in vertebrates another ligase could substitute for LIG1 in DNA replication, the identity of this ligase remained conjectural before the results presented in the present thesis were generated.

1.1.4 DNA Ligase 3

While almost all eukaryotes have homologs of the *LIG1* and *LIG4* genes, the *LIG3* gene is less widespread. Initially, the *LIG3* gene was thought to be restricted to vertebrates, but with the sequencing of more genomes, it has now been found in about 30% of eukaryotes, including members of 4 of the 6 ancestral eukaryotic groups (Simsek and Jasin, 2011). Unlike the *LIG1* and *LIG4* genes, the *LIG3* gene encodes 4 different DNA ligase polypeptides (Figure 6).

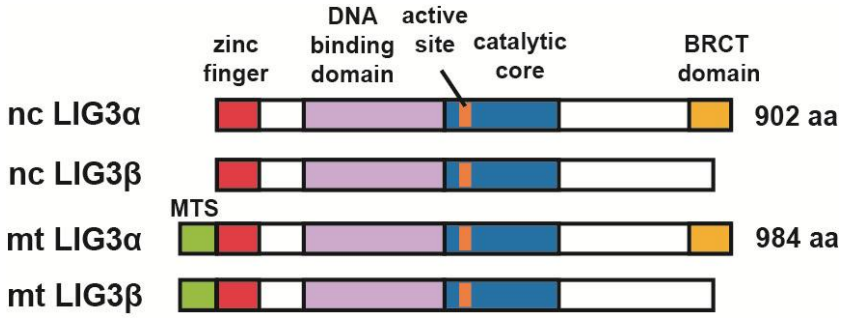

Figure 6: Schematic representation of the different form of vertebrate LIG3. (Arakawa et al., 2012)

Mitochondrial and nuclear versions of LIG3 are generated in all cells by alternative translation initiation (Lakshmipathy and Campbell, 1999; Perez-Jannotti et al., 2001). The *LIG3* mRNA open reading frame encodes an N-terminal mitochondrial leading sequence that is cleaved off during entry into the mitochondria. Thus, the mitochondrial DNA ligation functions are transferred from *LIG1* in lower eukaryotes to *LIG3* in vertebrates. There is no obvious nuclear localization signal within the LIG3 polypeptide and it remains unclear how the nuclear localization of LIG3 is accomplished. It may be that the interaction with its protein partner XRCC1 is crucial for this localization (Caldecott, 2003).

In addition a germ-cell-specific alternative splicing mechanism which replaces the terminal 3'-coding exon of LIG3α by a shorter exon lacking the breast cancer susceptibility protein (BRCA) 1-related C-terminal (BRCT) domain, generates LIG3β (Mackey et al., 1997; Perez-Jannotti et al., 2001). Similar to

LIG1, LIG3 adopts a flexible extended conformation in the absence of DNA (Figure 7). Though only sharing approx. 21% amino acid identity, the structure of the catalytic core of LIG3 bound to DNA still closely resembles the structure of the catalytic core of the DNA bound LIG1 (Cotner-Gohara et al., 2010).

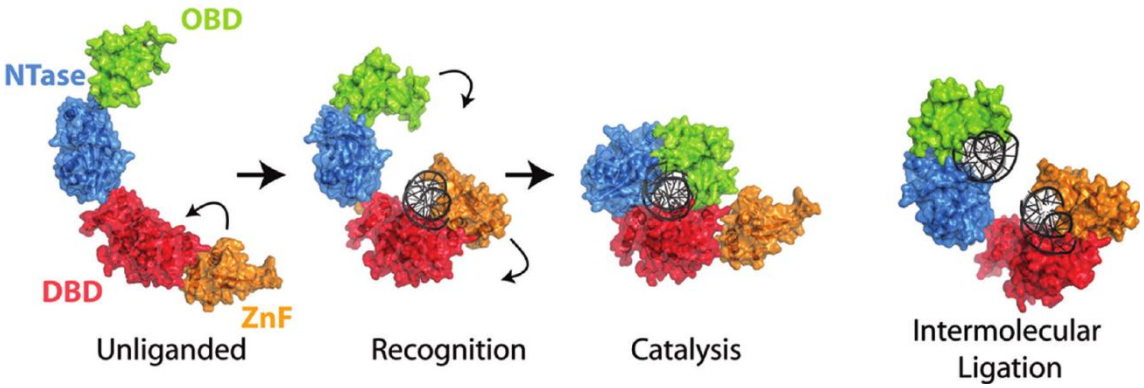

Figure 7: Jackknife mechanism of DNA substrate recognition (Cotner-Gohara et al., 2010)

A unique feature of the ligases encoded by *LIG3* is an N-terminal zinc finger (ZnFn) that is structurally related to the pair of ZnFns at the N-terminus of poly (ADP-ribose) polymerase 1 (PARP1) that binds to DNA nicks and gaps and serves as a nick sensor (Mackey et al., 1999). This domain is not required for DNA nick joining by LIG3, but it significantly broadens the substrate range of the enzyme and enables it to join breaks even at high salt concentrations (Mackey et al., 1999). The zinc finger and the DBD form a second nick-binding module in addition to the one formed by NTase and OB-domain, which tolerates different nick structures including gaps, whereas the first module preferentially binds to ligatable nicks (Cotner-Gohara et al., 2008). Based on these properties, the jackknife model for ligation of intermolecular gaps was proposed (Figure 7) (Cotner-Gohara et al., 2010; Cotner-Gohara et al., 2008). This model suggests that the ZnFn-DBD-module acts as nick sensor that engages the DNA breaks. If the nick is ligatable, it initiates a conformational change, replacing the ZnFn-DBD-module with the NTase/OB-domain module, then forming the compact clamp structure with the DBD around the DNA nick (Figure 7). Among the DNA ligases, LIG3 has the most robust intermolecular DNA joining activity (Chen et al., 2000). This activity is not solely dependent on the ZnFn, but also requires key residues inside the DBD (Cotner-Gohara et al., 2010; Cotner-Gohara et al.,

2008). A possible scenario is that both modules engage one of the DNA ends enabling LIG3 to ligate them (Cotner-Gohara et al., 2010).

Biochemical and cell biology studies link the nuclear LIG3α and XRCC1 to the short patch subpathway of BER and the repair of single strand breaks (Frosina et al., 1996; Okano et al., 2003; Okano et al., 2005). Nuclear LIG3α is also a key component of a nucleotide excision repair (NER) subpathway that operates in dividing cells but is particularly important for the repair of UV lesions in non-dividing cells (Moser et al., 2007). There is also evidence that LIG3α is a component of an alternative pathway of non-homologous end-joining (NHEJ) functioning as a backup (B-NHEJ) to the DNA dependent protein kinase (DNA-PK) dependent pathway of NHEJ (D-NHEJ) (Wang et al., 2005).

1.1.4.1 LIG3 protein partners

The 77 C-terminal residues that distinguish LIG3α from LIG3β constitute a BRCT domain (Bork et al., 1997). The BRCT motif mediates the interaction of LIG3 with XRCC1; this interaction stabilizes LIG3 and mediates some of its functions (Caldecott et al., 1995; Caldecott et al., 1994; Dulic et al., 2001; Mackey et al., 1997; Nash et al., 1997). XRCC1 interacts with several other proteins involved in base excision and single strand repair such as PARP1 and PCNA (Fan et al., 2004; Okano et al., 2003). LIG3α, as well as XRCC1, interacts with PARP1 and is therefore recruited to single strand breaks (Okano et al., 2005).

XRCC1 is absent from mammalian mitochondria which suggests that the mitochondrial version of LIG3α has different protein partners in this organelle. The mitochondrial DNA polymerase, polymerase γ, has been identified as an interaction partner binding not the BRCT domain of LIG3, but the central catalytic region. This suggests an interplay of these enzymes during mitochondrial DNA replication and repair (De and Campbell, 2007).

1.1.4.2 LIG3 deficiency

Although the confirmed specific functions of the peptides generated by the *LIG3* gene appear restricted to DNA repair, the deletion of *LIG3* has consequences significantly severer than the deletion of either *LIG1* or *LIG4* and causes early embryonic lethality that cannot be rescued by deletion of p53 (Puebla-Osorio et al., 2006). Whereas this result may be explained by the function of LIG3α in mitochondria DNA metabolism or in BER and other repair pathways, this observation is intriguing and required further in depth investigation (Lakshmipathy and Campbell, 1999). One of the main goals of the work presented here is to fill this gap of knowledge.

Interestingly, in non-dividing monocytes LIG3 and also its close interaction partner XRCC1 are not detectable at protein level (Bauer et al., 2011; Bauer et al., 2012). When these cells mature to dendritic cells or macrophages, the expression of these proteins is reestablished and reaches normal levels after 6 d for dendritic cells and 3 d for macrophage maturation (Bauer et al., 2012). However, the mRNA level of *LIG3* is not changed during maturation and it is therefore likely that some residual protein might be produced that is unstable without sufficient levels of XRCC1, which is expressed in a maturation dependent manner (Bauer et al., 2011).

1.1.5 DNA Ligase 4

The second family of ligases found in all eukaryotes is that of LIG4 and the main function attributed to these polypeptides is the ligation step during the repair of DNA double strand breaks (DSBs). This function is supported, both in yeast and in vertebrates, by a C-terminal extension of the central core with 2 tandemly arrayed BRCT motifs (Schär et al., 1997; Teo and Jackson, 1997; Wei et al., 1995; Wilson et al., 1997) (Figure 8). Through these domains, LIG4 interacts with XRCC4 and becomes integrated in a pathway of DSB repair (D-NHEJ), which in vertebrates also comprises XRCC4-like factor (XLF) and the DNA-PK complex consisting of the Ku heterodimer and the catalytic subunit, DNA-PKcs (Critchlow et al., 1997; Grawunder et al., 1997). LIG4 is one of the

targets of DNA-PK (Wang et al., 2004). Through its domain structure and possibly through adaptations in its central core, LIG4 has the unique ability of joining DNA ends that are non-complementary ignoring mismatches or short gaps (Gu et al., 2007). Unlike LIG1 and the nuclear LIG3α, which participate in several DNA repair pathways, LIG4 appears to function only in D-NHEJ, except in specialized cells of the immune system, where it also completes variable (diversity) joining (V(D)J) recombination (Grawunder et al., 1998a).

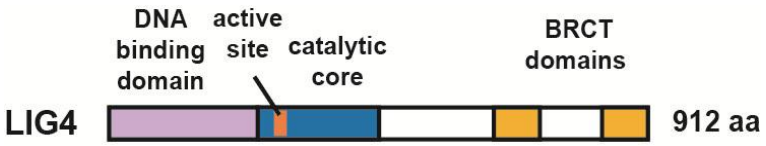

Figure 8: Schematic representation of vertebrate LIG4. (Arakawa et al., 2012)

1.1.5.1 LIG4 protein partners

As mentioned above, LIG4, like LIG3, has a close interaction partner which stabilizes the protein: XRCC4. Without XRCC4, LIG4 is unstable and cells deficient in XRCC4 are also functionally deficient in LIG4, which emphasizes the importance of this interaction (Bryans et al., 1999). The region between the BRCT motifs interacts with a region on the coiled-coils of XRCC4 and appears to block tetramer formation by XRCC4 which suggests that the LIG4-XRCC4 complex is composed of one LIG4 molecule and 2 XRCC4 molecules (Grawunder et al., 1998b; Sibanda et al., 2001; Tomkinson et al., 2006). There are physical and functional interactions between LIG4-XRCC4 and Ku as well as between LIG4-XRCC4 and the catalytic subunit of DNA-dependent protein kinase (DNA PKcs) in NHEJ (Chen et al., 2000; Hsu et al., 2002; Kysela et al., 2003; McElhinny et al., 2000).

1.1.5.2 LIG4 deficiency

The predominant function of LIG4 in DSB repair is further supported by the phenotype of its inactivation in the mouse. Embryonic lethality occurs late, after multiple normal DNA replication cycles, and is caused by massive apoptosis in

the central nervous system (CNS) (Barnes et al., 1998; Frank et al., 1998; Frank et al., 2000). Live births are possible when CNS apoptosis is rescued by the concomitant loss of either p53 or Ataxia-telangiectasia-mutated (ATM) function, but *LIG4*$^{-/-}$/*p53*$^{-/-}$ MEFs are highly radiosensitive and show defects in DSB repair owing to defective D-NHEJ (Frank et al., 2000; Lee et al., 2000; Sekiguchi et al., 2001).

Although LIG4 is firmly linked to D-NHEJ, it remains open whether it can substitute for the functions of other ligases.

1.2 Cell cycle checkpoints

The maintenance of genomic stability is crucial for every cell. DNA damage or incomplete replication jeopardizes this stability and can therefore result in cell death or cancer (Aguilera and Gomez-Gonzales, 2008; Branzei and Foiani, 2008; Friedberg, 2003; Hoeijmakers, 2001). Therefore, when the cell is at risk, it activates surveillance mechanisms, which detect problems and co-ordinate a global response to maintain genome integrity (Harrison and Haber, 2006; Zhou and Elledge, 2000). As some repair processes are slow, the checkpoint triggers an arrest in the cell cycle to provide sufficient repair time. Checkpoint deficiency causes genomic instability and has also been associated with carcinogenesis in studies of cancer-predisposition syndromes (Hartwell and Kastan, 1994; Shiloh, 2003).

The checkpoints are designed to prevent cells from going from one cell cycle phase to another, if they have residual DNA damage that might jeopardize processes of the upcoming cell cycle phase. In contrast to the other checkpoints which stop the cells from progressing to the next cell cycle phase, the inter-S-phase, or DNA replication checkpoint, does not stop ongoing replication, but prevents the firing of unreplicated origins – particularly late firing origins (Costanzo et al., 2000; Santocanale and Diffley, 1998; Tercero and Diffley, 2001).

Checkpoint response proteins can generally be divided into 4 subgroups: Sensors, which recognize the damaged DNA, Mediators, which simultaneously associate with damage sensors and signal transducers at certain phases of the cell cycle, Signal transducers, namely checkpoint kinase 1 (Chk1) and Chk2, and Effectors, which actually give the checkpoints their unique identities (Sancar et al., 2004). As in this study we were interested in the induction of the checkpoints only, we will focus on the DNA damage sensors.

Although the G1/S, intra-S, and the G2/M checkpoints are distinct, the damage sensor molecules that activate the various checkpoints appear either to be shared by all 3 pathways or to play a primary sensor role in one pathway and a back-up role in the others. Two important damage sensors for checkpoint response are the 2 phosphoinoside 3-kinase-like kinase (PIKK) family members, ATM and ATR (ATM and Rad3 related) (Melo and Toczyski, 2002; Sancar et al., 2004). Mutations in ATM cause ataxia-telangiectasia (A-T) in humans, a condition primarily characterized by cerebellar degeneration, immunodeficiency, genome instability, clinical radiosensitivity and cancer predisposition (Shiloh and Kastan, 2001). ATR knockout results in embryonic lethality and partial loss of activity in humans share features with the phenotype of ATM mutations (Brown and Baltimore, 2000; de Klein et al., 2000; O'Driscoll et al., 2003). As ATM and ATR are of great importance at very early stages of the checkpoint signaling, the inhibition of these proteins results in abrogated or greatly reduced checkpoint response.

2 Goal of the thesis

In vertebrates there are 3 different forms of DNA ligases which differ in their known functions. LIG1 plays its main role in DNA replication through its interaction with PCNA and is seen as the replicative ligase; it also functions in the long-patch subpathway of BER. LIG4 has its main known contribution in the repair of double strand breaks and V(D)J recombination. LIG3 has its function in the short-patch subpathway of BER, the repair of single strand breaks and a NER subpathway.

The knockout of the *LIG1* homolog in yeast, *CDC9*, is lethal for the cells. In accordance with this result, the knockout of *LIG1* in vertebrates is embryonically lethal but there are both mouse and human cell lines with impaired activity of LIG1 which grow with similar characteristics as LIG1 proficient cells, despite a marked defect in Okazaki fragment joining. Although these mutants have residual activity or are incomplete knockouts, these results suggest the presence of a backup replicative ligase in vertebrate cells.

In the present study, the impact of ligase knockout (all 3 families) on cell survival and replication functions was investigated. We measured the impact of these knockouts on cell growth, replicating potential, the maturation of Okazaki fragments and the induction of spontaneous SCEs.

The observations, gathered with the help of a unique set of DT40 mutants, enables us to draw conclusions about an impressive functional flexibility between the DNA ligases and allow a deeper understanding of the interplay among them. In future work, the mechanistic foundation of this functional flexibility should be investigated in more detail. In particular, it will be important to characterize the protein domains enabling this flexibility and identify the potential interaction partners involved.

3 Material and Methods

3.1 Materials

Table 1: Laboratory Apparatus.

Apparatus	Provider
63x/1.4 oil immersion objective	Leica Microsystems, Mannheim, Germany
Aluminum filter	GE Healthcare, USA
Cell counter, Multisizer™ 3 and Coulter Z2	Beckman Coulter, Germany
Centrifuge, Avanti™ J-20 XP	Beckman Coulter, Germany
Centrifugal elutriation rotor, JE-6	Beckman Coulter, Germany
Centrifugal rotor, JA 25.50	Beckman Coulter, Germany
Centrifuge, Rotana 460 R	Hettich, Germany
Dry Block Heater/Cooler	HLC, Oehmen, Germany
Electrophoresis chambers, Horizon 11•14 and 20•25	Life Technologies™, USA
Electrophoresis chamber, Mupid-One	Advance Co. Ltd., Japan
Falcon™ Express™ Pipet-Aid®	BD Biosciences, Germany
Flow cytometer, Epics XL and Gallios	Beckman Coulter, Germany
FluorImager, Typhoon 9400	Molecular Dynamics, Germany
iBlot® Dry Blotting System	Invitrogen, Life Technologies, Germany
Inverted phase contrast microscope	Olympus, Germany
Laminar flow hood, HeraSafe	Heraeus, Thermo Scientific, Germany
LC Carousel Centrifuge 2.0	Roche Diagnostics, Germany
LightCyler 2.0	Roche Diagnostics, Germany
Magnetic stirrer, MR Hei-Standard	Heidolph, Germany
MCO-18 O_2/CO_2 incubators	Sanyo, Germany
Metafer Slide Scanning Platform	MetaSystems, Germany
Micro Centrifuge, IR	Carl Roth, Germany
NanoDrop™ 2000	Thermo Scientific, Germany
Nucleofector® 2b Device	Amaxa, Lonza, Germany
Odyssey® infrared imaging system	LI-COR Biosciences, Germany
pH-Meter, FE20 – FiveEasy™ pH	Mettler Toledo, Germany
Pipettes, Pipet-Lite™	Mettler Toledo, Germany
Power supply, PowerPac™ Basic	Bio-Rad, Germany
PTB dosimeter	Physikalisch-Technische Bundesanstalt, Germany
Pump drive, MCP Standard	Ismatec®, Idex Health & Science, Germany

Pumphead, Easy-Load® II	Ismatec®, Idex Health & Science, Germany
SDS-PAGE apparatus	Bio-Rad, Germany
SDS-PAGE mini gels, Mini PROTEAN	Bio-Rad, Germany
Seifert Isovolt 320 HS X-ray tube	Seifert, GE Measurement & Control, USA
Rocky shaker	Oehmen, Germany
Tabletop centrifuge, Biofuge fresco	Heraeus, Thermo Scientific, Germany
Thermo-mixer	Eppendorf, Germany
Ultracentrifuge, Optima Max	Beckman Coulter, Germany
Ultracentrifuge rotor, MLN80	Beckman Coulter, Germany
UV spectrophotometer	Shimadzu, Germany
Vacuum gas pump	VWR, Germany
Vortexer, IKA MS 3 basic	IKA, Germany
Water bath	GFL, Germany
Weighing balance, 572-43	Kern, Germany
Weighing balance, VWR-124	Sartorius, Germany

Table 2: Disposable Products and Commercial Kits.

Disposable Product / Commercial Kit	Provider
0.5, 1.5 and 2 ml reaction tubes	Greiner, Germany
2, 5, 10, 25 ml pipette	Greiner, Germany
3 mm diameter glass tubes	CM Scientific Ltd., UK
15 and 50 ml tubes	Greiner, Germany
20 mm glass cover slips	Invitrogen, Life Technologies, Germany
60, 100 mm bacteria and cell culture dishes	Greiner, Germany
150 mm culture dishes	TPP, Switzerland
Click-iT® EdU Alexa Fluor® 647 Imaging Kit	Invitrogen, Life Technologies, Germany
Cuvettes, Q-VETTES Halbmikro	Ratiolab®, Germany
Filter tips	Greiner, Germany
fluorescence microscope, AxioImager Z2	Zeiss, Germany
Glass flasks, beakers and cylinders	Schott Duran, Germany
High pure RNA isolation kit	Roche Diagnostics, Germany
Maxima First strand cDNA Synthesis Kit	Fermentas, Thermo Scientific, Germany
Microscope Slides, H872	Carl Roth, Germany
Minisart®, 0.45 µm sterile filter	Sartorius, Germany
NucleoBond Xtra Midi/Maxi Plus EF purification kit	Macherey-Nagel, Germany
NucleoSpin Tissue Kit	Macherey-Nagel, Germany
Peha-soft® nitrile FINO gloves	Hartmann, Germany
Phase Lock Gel, 1.5 ml Heavy	Eppendorf, Germany
Pipettes	Greiner, Germany
Pipette tips	Greiner, Germany
LightCycler® capillaries	Roche Diagnostics, Germany
LightCycler® FastStart DNA Master^{PLUS} SYBR Green I Kit	Roche Diagnostics, Germany
iBlot® blotting stacks, Nitrocellulose and PVDF	Invitrogen, Life Technologies, Germany

Table 3: Chemical Reagents

Chemical	Provider
1,4 Dithiothreitol	Carl Roth, Germany
Acetic acid	Carl Roth, Germany
Agarose, LE	Lonza, Germany
Ampicillin	Carl Roth, Germany
β-Mercaptoethanol	Sigma-Aldrich, Germany
Blasticidin S	InvivoGen, Germany
Boric acid	Carl Roth, Germany
Bovine serum albumin fraction IV	Carl Roth, Germany
Bromophenol blue	Sigma-Aldrich, Steinheim, Germany
Caspase Inhibitor III, BOC-D-FMK	Calbiochem®, Merck Millipore, Germany
Chicken serum	Gibco®, Life Technologies, Germany
Chloramphenicol	Carl Roth, Germany
Chloroform	Sigma-Aldrich, Germany
Colcemid	Biochrom, Germany
Coomassie brilliant blue R 250	SERVA, Germany
CsCl	Crescent Chemical, USA
DAPI	Sigma-Aldrich, Germany
Dimethyl sulfoxide	Sigma-Aldrich, Germany
Dulbecco's Modified Eagle Medium	Gibco®, Life Technologies, Germany
Dulbecco's Modified Eagle Medium: Nutrient Mixture F-12	Gibco®, Life Technologies, Germany
EDTA	Roth, Germany
Entellan	Merck, Heidelberg, Germany
Ethanol	Sigma-Aldrich, Germany
Ethidium bromide	Roth, Germany
Fetal bovine serum	Biochrom, Germany; PAA, Coelbe, Germany; Gibco®, Life Technologies, Germany
G418	InvivoGen, Germany
Gelatine	Calbiochem®, Merck Millipore, Germany
GeneRuler™ 1 kb DNA Ladder	Fermentas, Thermo Scientific, Germany
GeneRuler™ 100 bp Plus DNA Ladder	Fermentas, Thermo Scientific, Germany
Giemsa stain	Carl Roth, Germany
Glycerol	Carl Roth, Germany
HCl	Carl Roth, Germany
HEPES	Carl Roth, Germany
LB agar	USB®, Affymetrix®, USA
LB medium	USB®, Affymetrix®, USA
KCl	Carl Roth, Germany
KH_2PO_4	Carl Roth, Germany
KOH	Carl Roth, Germany

Ku55933	Calbiochem®, Merck Millipore, Germany
Mc Coy's 5A medium	Sigma-Aldrich, Steinheim, Germany
Methanol	Sigma-Aldrich, Germany
Methylcellulose	Sigma-Aldrich, Germany
$MgCl_2$	Merck, Darmstadt, Germany
Minimum Essential Medium	Gibco®, Life Technologies, Germany
NaCl	Carl Roth, Germany
NaF	Carl Roth, Germany
$NaHCO_3$	Carl Roth, Germany
NaH_2PO_4	Merck Millipore, Germany
Na_2HPO_4	Carl Roth, Germany
NLS	Merck, Heidelberg, Germany
Non-fat dry milk	Carl Roth, Germany
*Not*I	Fermentas, Thermo Scientific, Germany
NU7441, KU-57788	Tocris Bioscience, USA
Orange G	Carl Roth, Germany
Paraformaldehyde	Carl Roth, Germany
Phenol	Carl Roth, Germany
Phosphoric acid	Carl Roth, Germany
Phenylmethylsulfonyl fluoride	Carl Roth, Germany y
Poly-L-lysine	Biochrom AG, Berlin, Germany
Primer	Invitrogen, Germany
ProLong® Gold antifade reagent	Invitrogen, Germany
Protease inhibitor cocktail	Sigma-Aldrich, Germany
Propidium iodide	Sigma-Aldrich, Germany
Puromycin	InvivoGen, Germany
RIPA buffer	Thermo Scientific, Germany
RNase A	Sigma-Aldrich, Germany
Rotiphorese® Gel 30 (37.5:1)	Carl Roth, Germany
Page Ruler, Prestained Protein Ladder	Fermentas, Thermo Scientific, Germany
Sodium dodecyl sulfate	Carl Roth, Germany
Sorenson's buffer	Gibco®, Life Technologies, Germany
Streptomycin	Calbiochem®, Merck Millipore, Germany
Sucrose	Sigma-Aldrich, Germany
SYBR Gold	Molecular Probes, Life Technologies, Germany
Tetramethylethylenediamine (TeMeD)	Sigma-Aldrich, Germany
Tris base	Carl Roth, Germany
Triton X-100	Sigma-Aldrich, Germany
Trypsin	Biochrom, Germany
Tween 20	Carl Roth, Germany
VE-821	Haoyuan Chemexpress Co., China
Xylene Cyanol	Sigma-Aldrich, Germany

Table 4: Antibodies

Antibody	Provider
Alexa Fluor 488 (mPAb, rPAb)	Invitrogen, Germany
GAPDH (mMAb)	Millipore, Germany
GFP (mMAb) ab1218	Abcam, UK
IRDye 680 (mPAb, rPAb)	LI-COR Biosciences, Germany
IRDye 800 (mPAb, rPAb)	LI-COR Biosciences, Germany
LIG1 (mMAb) 10H5	GeneTex, USA
LIG3 (mMAb) 1F3	GeneTex, USA
PCNA (mMAb) PC10	Dako, Germany
PCNA (rMAb) EPR3821	GeneTex, USA
XRCC1 (mMAb) 33-2-5	Abcam, UK
XRCC1 (rPAb)	GeneTex, USA

3.2 Methods

3.2.1 Cell lines

3.2.1.1 DT40 Parental cell line and generation of mutants

The DT40 mutants used here were designed by Dr. Hiroshi Arakawa (exceptions are mentioned explicitly) and were derived from the DT40-Cre1 cell line that conditionally expresses Cre recombinase to allow genome editing and v-myb to enhance gene conversion (Arakawa et al., 2002; Arakawa et al., 2001). Cre recombinase is expressed from a human β-actin promoter as a chimera, MerCreMer, of 2 mutated estrogen receptors (Mer), only responding to tamoxifen or 4-hydroxytamoxifen (4HT), and Cre recombinase (Arakawa et al., 2002; Arakawa et al., 2001; Zhang et al., 1996). In the absence of 4HT, MerCreMer is efficiently sequestered by heat shock proteins in the cytoplasm. This interaction is rapidly disrupted upon administration of 4HT and causes the translocation of the protein to the nucleus, where Cre exerts recombination activity at loxP sites (Arakawa et al., 2012). The targeting strategies used have been extensively described in Arakawa et al 2012. Briefly, the different ligases within the chicken genome were identified by Blast search, and large portions of

the functional domains including the active site which is highly conserved among the species were taken out. The deletions after knockout are depicted in Figure 9. Some of the mutants had to be made inducible as the knockout was lethal. For this purpose we applied a conditional targeting system, taking advantage of the loxP system. The mutants were designed in such a way that the portion of gene, which was to be deleted was flanked by 2 loxP-sites which enables the induction of the knockout upon addition of 20 nM 4HT, as described earlier (Arakawa et al., 2012).

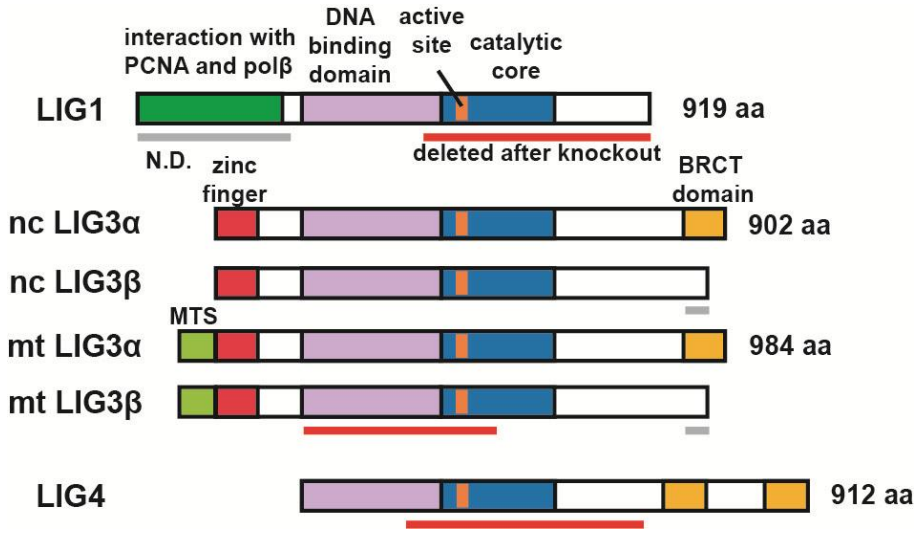

Figure 9 Schematic comparison between the 3 DNA ligases in vertebrates and the part deleted after knockout Nc: nuclear; mt: mitochondrial. Red bars indicate regions deleted in the mutants generated. The β form of LIG3 is inferred, as the corresponding exon could not be identified (Arakawa et al., 2012).

The generation of mutants which lack the nuclear form of LIG3, but are left with the mitochondrial version, was achieved by inactivation of the M2 translation initiation site in one allele of the LIG3 gene, while the other one was flanked by flanked by loxP sites (*LIG3*$^{2loxP/M2I}$) to induce the knockout or taken out completely (*LIG3*$^{-/M2I}$), depending on the mutant (Arakawa et al., 2012; Paul et al., 2013).

All knockouts were checked at the DNA level by polymerase chain reaction (PCR) and at the RNA level with real-time-PCR (RT-PCR).

In addition to the knockouts, we also designed mutants stably overexpressing certain genes. These constructs were integrated into the DT40 genome with the help of a vector which targets a defined intergenic locus on chromosome 8, without destroying or grossly disturbing nearby genes. The vector included a Rous sarcoma virus (RSV) promoter, which is followed by an internal ribosome binding site (IRES), the blasticidin (*bsr*) selection marker and the Simian virus (SV40) polyA signal.

Table 5: Summary of DT40 mutants used (Arakawa et al., 2012; Paul et al., 2013)

Cell line	Description
***LIG4*$^{-/-}$ •**	*LIG4* knockout
***LIG1*$^{2loxP/-}$ •**	*LIG1* conditional knockout
***LIG1*$^{-/-}$ •**	*LIG1* knockout
***LIG3*$^{2loxP/-}$ ***	*LIG3* conditional knockout
***LIG3*$^{2loxP/M2I}$ •**	conditional nuclear *LIG3* knockout
***LIG3*$^{-/M2I}$ •**	nuclear *LIG3* knockout
***LIG3*$^{2loxP/-}$*cdc9* •**	*LIG3* conditional knockout overexpressing *CDC9* (*LIG1* homolog in yeast)
***LIG3*$^{-/-}$*cdc9* •**	*LIG3* knockout overexpressing *CDC9* (*LIG1* homolog in yeast)
***LIG1*$^{-/-}$*LIG4*$^{-/-}$ •**	*LIG1* knockout; *LIG4* knockout
***LIG3*$^{2loxP/-}$*LIG1*$^{-/-}$ •**	*LIG3* conditional knockout; *LIG4* knockout
***LIG3*$^{-/M2I}$*LIG1*$^{2loxP/-}$ •**	nuclear *LIG3* knockout; *LIG1* conditional knockout
***LIG3*$^{-/2loxP}$*LIG4*$^{-/-}$*mts-hLIG1* $^{+}$**	*LIG3* conditional knockout; *LIG4* knockout overexpressing human mitochondrial *LIG1*
***LIG3*$^{-/-}$*LIG4*$^{-/-}$*mts-hLIG1* $^{+}$**	*LIG3* knockout; *LIG4* knockout overexpressing human mitochondrial *LIG1*
***LIG3*$^{-/M2I}$*LIG1*$^{2loxP/-}$*hLIG3β* ***	nuclear *LIG3* knockout; *LIG1* conditional knockout overexpressing human *LIG3β*
***LIG3*$^{-/M2I}$*LIG1*$^{2loxP/-}$ *hLIG3α*-ZnFn Cl1 ***	nuclear *LIG3* knockout; *LIG1* conditional knockout overexpressing human *LIG3α* without Zinc Finger domain, Clone 1
***LIG3*$^{-/M2I}$*LIG1*$^{2loxP/-}$ *hLIG3α*-ZnFn Cl2 ***	nuclear *LIG3* knockout; *LIG1* conditional knockout overexpressing human *LIG3α* without Zinc Finger domain, Clone 2

• Mutants generated by H. Arakawa.
$^{+}$ Mutants generated by K. Paul.
* Mutants generated by T. Bednar.

The yeast LIG1 homolog, *CDC9*, human LIG1 with a mitochondrial leader sequence (*mts-hLIG1*), the human LIG3α and its truncated mutants were cloned into this vector and knocked into DT40 chromosome 8 (Arakawa et al., 2012; Paul et al., 2013). The mutants used are summarized in Table 5.

3.2.1.2 46BR 1N, 46BR PBAHL and MRC5 SV cell lines

The 46BR 1N cell line is a human cell line mutated in the LIG1 gene. The effect of this mutation on the patient the cells were derived from, are described in 1.1.3.3.

46BR PBAHL cells have been generated by transfecting the LIG1 deficient 46BR cells with a *LIG1* expressing vector carrying the neo gene as selection marker.

MRC5 SV cells serve as control as they are an SV40-transformed normal fibroblast cell line (Huschtscha and Holliday, 1983).

3.2.1.3 PF20 and PFL13 cell lines

PF20 (wild type) and LIG1-deficient immortalized mouse cell line (PFL13) are spontaneously immortalized mouse fibroblasts. They were derived from normal or LIG1 deficient mice (Bentley et al., 2002). Although defined as LIG1 deficient there have been some doubts about the reliability of these mutants, as only exons 23 to 27 were knocked out, which do not include the active core of LIG1 (Bentley et al., 2002).

3.2.1.4 EM9 cells

EM9 cells were produced during a screening for DNA repair-deficient mutants of CHO cells (Thompson et al., 1980). An XRCC1 expressing plasmid was found to give an approx. 80% correction of EM9 (Thompson et al., 1990).

3.2.2 Cell culture

All cells were routinely maintained in the logarithmic phase of growth and incubated in a humidified incubator supplemented with 5% CO_2.

3.2.2.1 DT40 cell culture

DT40 cells were grown at 41ºC in a mixture of Dulbecco's Modified Eagle Medium (DMEM)/F12 growth medium supplemented with 10% fetal bovine serum, 1% chicken serum and 50 µM β-mercaptoethanol.

Stable transfectants were selected in 15 µg/ml of blasticidin S, 1 µg/ml mycophenolic acid, or 1 µg/ml of puromycin, as appropriate. Targeted clones were screened by PCR according to Arakawa et al. (Arakawa et al., 2002).

3.2.2.2 Culturing 46BR 1N, 46BR 1N and MRC5 SV cells

46BR 1N, 46BR PBAHL and MRC5 SV1 cells were grown in Minimum Essential Medium (MEM) supplemented with 10% fetal bovine serum at 37°C.

3.2.2.3 PF20 and PFL13 cell lines

PF20 and PFL13 were cultured in DMEM supplemented with 10% fetal bovine serum and non-essential amino acids at 37°C.

3.2.2.4 EM9 cells

EM9 cells were cultured in McCoy’s 5A medium supplemented with 10% fetal bovine serum at 37°C.

3.2.3 Drug treatments and irradiation

Irradiations of cells were carried out at room temperature (RT) using an X-ray machine (General Electric-Pantak), operated at a maximum energy of 320 keV. Controls were mock irradiated.

All inhibitors used in this work were dissolved in dimethyl sulfoxide (DMSO) and added to the studied cells 1 h before irradiation or start of surveillance. Inhibitors used are summarized with the concentrations used in Table 6.

Table 6: Summary of inhibitors used

Inhibitor	Mode of action	Working-concentration
Caspase Inhibitor III (BOC-D-FMK)	Inhibits activity of caspase family proteases and blocks apoptosis	50 µM
ATR inhibitor (VE-821)	Potent and selective ATP competitive inhibitor of ATR	5 µM
ATM inhibitor (Ku55933)	Potent, selective and competitive ATM kinase inhibitor	10 µM

3.2.4 Electroporation

3.2.4.1 Electroporation of DT40 cells

For knock-in of the truncated LIG3 genes in DT40, 1-10x10^6 cells were electroporated with 5 to 10 µg linearized plasmid DNA, with program B23 using commercially available equipment and protocols (Amaxa).

3.2.4.2 Electroporation of 46BR 1N, MRC5 SV and EM9 cells

For transient transfection with pDsRed-*LIG1*, pTagBFP-*PCNA* and pEGFP-*XRCC1* plasmids, 1.2 to 2 million cells were transfected with 1 µg plasmid DNA of each plasmid. 46BR 1N and MRC5 SV were electroporated with program P22, EM9 cells were electroporated with program U23 using commercially available equipment and protocols (Amaxa).

3.2.5 Analysis of DNA replication by BrdU incorporation and analysis of cell cycle distribution by flow cytometry

Exponentially growing cells were incubated with 10 µM 5-Brom-2-desoxyuridine (BrdU) for 1 h and fixed in 70% ethanol. After washing with 0.9% NaCl, the cell pellet was incubated for 10 min at 37°C in a pepsin-HCl solution (0.5 g pepsin, 55 mM HCl ad 100 ml). Subsequently, cells were then incubated in 2 M HCl for 20 min at RT and washed in 1x phosphate-buffered saline (PBS; 137 mM NaCl, 2.7 mM KCl, 7.4 mM Na_2HPO_4, 1.5 mM KH_2PO_4, pH 7.4) supplemented with 0.05% Tween20 (PBS-T) before incubation for 30 min at 4°C with an anti-BrdU antibody (1:50 dilution, Becton Dickinson) in the same solution. After washing with PBS-T-BSA (1%), a fluorescein isothiocyanate (FITC) conjugated secondary antibody (1:100 dilution, Sigma) was applied for 30 min at 4°C in the same solution. Finally, cells were stained with propidium iodide (PI) and analyzed by flow cytometry (Arakawa et al., 2012).

For all other flow cytometric analyses cells were also fixed in pre-chilled 70 % ethanol or stained directly in 100 mM Tris pH 7.0, 100 mM NaCl, 5 mM $MgCl_2$, 0.05% Triton X-100 containing 40 µg/ml PI and 62 µg/ml RNase A at RT for at least 10 min. If fixed with ethanol, cells were collected by centrifugation and resuspended in PBS containing 40 µg/ml PI and 62 µg/ml RNase A. Samples were incubated at 37ºC for 20 min and 20,000 cells were measured. The fraction of cells in the different phases of the cell cycle was calculated using the Wincycle® software.

3.2.6 Cell fractionation in G1 or G2 phase of the cell cycle by centrifugal elutriation

To get a clean population for studying sister chromatid exchanges (SCE), cells were enriched in G2 by centrifugal elutriation, which separates cells on the basis of their size. For cell cycle progression measurement, cells were enriched in G1 phase of the cell cycle and further cultivated for experiments. The method

is based on 2 opposite forces applied in a conical separation chamber, containing a non-synchronized cell population: the continuous flow rate of the medium is directed against the centrifugal force.

DT40 cells were grown for 24h to a cell concentration of 1.5 x 10^6 cells per ml. 2-3 x 10^8 cells were elutriated at 4°C in a Beckman J2-21M high speed centrifuge and a Beckman JE-6 elutriation rotor (Beckman-Coulter, Krefeld, Germany). During the separation process, the cells in G1-phase are firstly elutriated (cells of smaller size), followed by fractions of S- and G2-subpopulations (larger cells). After cell cycle analysis by FACS, depending on the experiment, G1 or G2 subpopulations were further cultivated for experiments.

3.2.7 Sister chromatid exchanges

G2 enriched cells were cultivated for 2 generations with medium containing 20 µM BrdU and with 0,05 µg/ml colcemid during the last 2 h of cultivation. Cells were collected by centrifugation at 1200 rpm for 7 min at 4°C, supernatant was removed and cells were resuspended in hypotonic solution (0.075 M potassium chloride (KCl)), incubated for 10 min at RT and centrifuged again. Cell pellets were fixed in 3 parts methanol and 1 part acetic acid, and fixed cells were dropped on a clean glass slide. The slide was air dried in the dark overnight, stained with 5 µg/ml Hoechst 33258 in Sorensen buffer (10582-013, Gibco, Invitrogen) and covered with a coverslip. The slides were placed on a slide warmer at 55°C and exposed to a black light fluorescent lamp (Radium SupraBlack HBT 125-281) at a distance of 2 cm for 10 min. After removing the coverslip, the slides were stained in 2.5 ml of ready to use Giemsa stain (Carl Roth GmbH & Co.) diluted in 50 ml of Sorenson's buffer (10582-013, Gibco, Invitrogen) for 20 min. SCE pictures were taken using a 40x objective in an automated analysis station equipped with a bright field microscope (AxioImager Z2, Zeiss) and controlled by Metafer software (MetaSystems). The images were analyzed using the Ikaros software (MetaSystems). For each cell line, at least 2 independent experiments were performed, counting 100 metaphases in each.

The sister chromatid which has incorporated BrdU is stained more lightly, which enables us to tell the sister chromatids from one another, and to visualize potential exchanges between sister chromatids. The SCEs in the representative pictures are marked with red arrows for better visualization.

3.2.8 Reverse transcription reaction and real-time PCR

The RNA was prepared according to the protocol of the High Pure RNA Isolation Kit (Roche) with the exception that 3 million cells were used for total RNA isolation. RNA concentration was determined with a spectrophotometer (NanoDrop; Thermo Scientific). cDNA was prepared from 1 µg total RNA by reverse transcription using the "Transcriptor First Strand cDNA Synthesis Kit" (Roche) according to the manufacturer's instructions. This cDNA was used as input in real-time PCR reactions according to the protocol suggested in the LightCycler® FastStart DNA Master^{PLUS} SYBR Green I kit (Roche). Briefly, 1 µl of cDNA, 0.5 µl of sense and antisense primer solution, 2 µl of LightCycler® FastStart DNA Master^{PLUS} SYBR Green I Master Mix and 6 µl H_2O were mixed together in a 10 µl reaction mixture in a LightCycler® Capillary. Capillaries were placed in the sample carousel of the LightCycler® (Roche).

Table 7: Protocol for Real-time PCR

Temperature	Time	Cycles	PCR step
95°C	10 min	1	Denaturation
95°C	10 s	45	Denaturation
62°C	5 s		Annealing
72°C	10 s		Amplification
65°C – 95°C	0.1°C/s		Melting Curve
37°C	1 min		Cooling

The settings for the thermal cycles are summarized in table 7, the primer used for DNA ligase expression analysis can be looked up in table 8. TATA-binding protein 1 (TBP1) is the housekeeping gene used as reference.

Table 8: Primer sequences used in DT40 for Real time PCR

Oligo nucleotide	Sequence
Chk LIG1-F7	CATCTGCAAGATAGGCACTG
Chk LIG1-R7	CCCAAATCGTCACCAAACAG
Chk LIG3-F	GATGACCCCAGTTCAGCCTA
Chk LIG3-R	GTGGGCTACTTTGTGGGGAA
Chk LIG4-F	CCCCATTAACAGGCAGGATA
Chk LIG4-R	CCACGTTTGTCAGGCTTGTA
Chk TBP1-F	CAGCACCAACAGTCTGTCCA
Chk TBP1-R	GGGGCTGTGGTAAGAGTCTG

3.2.9 Extract preparation and immunoprecipitation reactions

Whole cell extracts (WCE) for immunoprecipitation were prepared with ready-to-use RIPA buffer (Pierce) according to the manufacturer's protocol, and the protein concentration was determined using the colorimetric Bradford assay with BSA as standard. For immunoprecipitation reactions, we used mouse and rabbit TrueBlot IgG agarose beads. 50 µl beads were incubated with 300 µg WCE and 5 µg of antibody for at least 2 h on a shaker at 4°C. Non-specific bound proteins were removed by washing the beads 3 times with 500 µl of IP buffer (50 mM Tris HCl pH 8.0, 150 mM NaCl, 1% NP-40 (Igepal CA-630)). Bound proteins were denatured by adding 60 µl 2xLaemmli buffer (Tris-HCl 126 mM, glycerol 20%, SDS 4%, bromophenol blue 0,02%, pH 6,8, 0,2% 2-mercaptoethanol) to each tube, heated to 95°C for 5 min and run on a 10% SDS polyacrylamide gel, before blotting onto a nitrocellulose membrane.

3.2.10 SDS-PAGE and Western blotting

Protein gel electrophoresis under denaturing conditions was carried out using 10% polyacrylamide gels. For further analysis, the proteins were blotted onto a 0.2 µm nitrocellulose membrane using an iBlot dry-transfer system (Invitrogen). To ensure equal loading of protein, the concentration was determined using the

colorimetric Bradford assay with BSA as standard and detection of GAPDH as loading control where possible. After transfer, membranes were incubated in blocking buffer (5% non-fat dry milk in 0.05% Tween-20, 150 mM NaCl, 25 mM Tris-HCl, pH 7.6) for 2 h at RT. Subsequently, membranes were incubated overnight at 4˚C with primary antibody appropriately diluted (anti-LIG3 1:500, anti-PCNA 1:1000, anti-XRCC1 1:1000, anti-LIG1 1:1000, GAPDH 1:10,000) in blocking buffer. After 3 washes for 10 min with PBS-T (PBS, supplemented with 0.05% Tween-20), membranes were incubated for 1 h with secondary antibody (IRDye680 or IRDye800 (Li-COR) 1:10,000) diluted in PBS-T and washed again 3 times. After immunoblotting, membranes were visualized using Odyssey Infrared Imaging System (LI-COR Biosciences GmbH, Bad Homburg, Germany) according to the manufacturer's instructions.

3.2.11 Assay for DNA replication intermediates

The assay for analyzing the DNA replication intermediates was conducted as described in Bentley et al., 2002 with only slight modifications (Bentley et al., 2002). Briefly, exponentially growing human and mouse fibroblasts were cultured in 30 mm dishes and were rinsed twice with warm serum-free medium. Human and mouse cells were incubated at 37°C for 10 min in serum-free medium containing 2 µCi of [methyl-^{3}H]- thymidine (25 Ci/mol) per ml. The medium containing radioactive thymidine was removed and 2 ml of warm supplemented medium containing 2 mM thymidine was added and incubated at 37°C for the required chase period (2, 5, 10, 15 or 30 min). After chasing time, the cells were scraped, covered with 1 ml ice cold PBS, pelleted by brief centrifugation and resuspended in 20 µl buffer A (10 mM Tris-HCl (pH 8.0), 50 mM NaCl, 0.1 M EDTA). 60 µl of molten 1.5% low-melting point agarose was added to the suspension, mixed and left to set on ice for 5 min. DT40 cells were handled in a similar way, but scraping was not required; instead, they were collected by centrifugation and incubated at 41°C. The plugs were incubated for 18 h at 50°C in 1 ml lysis buffer supplemented with 2% (w/v) *N*-laurylsarcosine and 0.2 mg/ml proteinase K. Subsequently, plugs were transferred to 5 ml buffer A for 1 h. The nascent DNA was separated on a 1% agarose gel as

described ((Sambrook et al., 1989). The electrophoresis was carried out at 2 V/cm for 6 h at RT. After electrophoresis, the gel was soaked in neutralization buffer (1 M Tris-HCl (pH 7.6), 1.5 M NaCl) for 1 h and sliced into 1 cm fractions, ranging from <0.2 to >23 kb using size markers as a guide. Agarose pieces corresponding to the different sizes were soaked in 0.1 M HCl for 1 h, melted by heating in a microwave oven and the [^{3}H] present was counted in a scintillation counter. The results were plotted as the percentage of cpms measured in agarose sections comprising DNA smaller than 2 kbp, which was compared to the total cpms in the corresponding lane.

3.2.12 Immunofluorescence microscopy

Three coverslips were put in 1 60 mm cell culture dish. 5 ml poly-L-lysine was added and incubated for at least 30 min. Directly after electroporation, cells were transferred to pretreated dishes and left to attach for at least 8 h. After initial incubation, cells were washed twice with pre-warmed PBS and fresh pre-warmed growth medium was added. 24 h after electroporation, 10 µM 5-ethynyl-2'-deoxyuridine (EdU) was added to the growth medium for 20 min to 1 h at 37°C, dependent on the cell line used. Cells were fixed for 20 min in 2% paraformaldehyde in PBS. After washing 3 times with PBS, cells were permeabilized for 5 min in P-solution (0.5% Triton X-100 in 100 mM Tris, 50 mM EDTA), washed again as indicated and blocked in PBG solution (PBS, 0.5 % BSA, 0.2 % gelatine) overnight at 4°C.

For visualization of GFP, coverslips were incubated for 90 min at RT with an anti-GFP mouse monoclonal antibody (ab1218, Abcam) diluted 1:500 in PBG solution. Coverslips were washed once in PBS and an anti-mouse IgG antibody, conjugated with AlexaFluor488 (Invitrogen), was added for 60 min at RT in 1:400 dilution in PBG solution. For visualization of EdU, the Click iT®-EdU Imaging system (Invitrogen) was used after antibody staining. 50 µl of Click iT® reaction cocktail was added to each coverslip for 30 min. Coverslips were washed once with PBS and were mounted on slides using Prolong-Gold Antifade (Invitrogen). BFP and dsRed signals could be rescued after fixation without any additional antibody staining. After solidification of the mounting

media at RT, 3D-images were captured in a Leica confocal microscope TCS SP5 (Leica Microsystems GmbH, Wetzlar, Germany) using the Leica Application Suite Advanced Fluorescence (LAS-AF) software.

3.2.13 Plasmid preparation and digestion

Chemically competent bacteria were transformed with the desired plasmid with heat-shock transformation and plated onto a 10 cm LB agar plate containing the appropriate antibiotic and incubated overnight at 37°C. Mini-cultures containing 3 ml of LB- medium with antibiotics were inoculated with 1 colony from the agar plate and incubated on an orbital shaker at 37°C for 8 h. 200 ml of LB-medium with antibiotics were inoculated with 200 µl pre-culture and incubated for 16 h on an orbital shaker at 37°C. The bacteria were collected after incubation and the bacteria pellets were processed using a NucleoBond Xtra Midi/Maxi Plus EF purification kit (Macherey-Nagel) following the instruction manual of the manufacturer.

For linearization of plasmid DNA for transfection of DT40, plasmids were digested with *Not*I (Fermentas) following the manufacturer's manual. Agarose gel electrophoresis was applied to test the completeness of digestion. The completely digested plasmid was purified with phenol/chloroform extraction precipitated with isopropanol, and the precipitate was washed with 70% ethanol. The air-dried plasmid was dissolved in 1 x TE buffer (10 mM Tris, 1 mM EDTA, pH 7.5) to a final concentration of 1 µg/µl. Plasmid concentration was determined using a NanoDrop spectrophotometer (Thermo Scientific).

3.2.14 Measurement of apoptotic index

To determine the apoptotic index of a cell population, cells were collected by centrifugation and fixed in 70% ethanol. Ethanol fixed cells were resuspended in 4',6-diamidino-2-phenylindole (DAPI) staining solution (0.1 M Tris, pH 7.0, 0.1 M NaCl, 5 mM $MgCl_2$, 0.05% Triton X-100 and 2 µg/ml DAPI) and incubated at RT

for 5 min. After staining, cells were analyzed under a fluorescent microscope by counting the fraction of pycnotic and fragmented nuclei in 1000 cells.

4 Results

There are hints in the literature that LIG1 might not be the only replicative DNA ligase in vertebrates. In support of this, it has been reported that a human cell line derived from a patient with a mutation in *LIG1* gene could effectively undergo DNA replication despite an evident defect in Okazaki fragment maturation (Barnes et al., 1992; Webster et al., 1992). Moreover, a genetic approach using mouse embryos with a knockout of *LIG1* showed that although the knockout resulted in no viable mouse embryos, the fibroblasts generated from these embryos were viable and had growth kinetics similar to that of wild type (wt) cells (Bentley et al., 1996).

Nevertheless, there were some limitations with the above models so that a complete lack of LIG1 could not be unequivocally ensured in neither experimental approaches, a complete elimination of the LIG1 activity could not be demonstrated. In fact, in the human cell line, residual LIG1 activity was documented, and in the mouse system the gene fragment encoding the catalytic core of LIG1 was not completely disrupted. As a result, the assertion that some derivative products retaining LIG1 activity could not be ruled out (Barnes et al., 1992; Mackenney et al., 1997).

4.1 LIG3 but not LIG1 or LIG4 are essential for cell survival

4.1.1 LIG4 is dispensable for replication

Although the knockout of LIG4 is embryonically lethal, there are several cell lines that are viable in the absence of functional LIG4, particularly when the p53 gene is additionally inactivated. Moreover, there is no single report suggesting that LIG4 deficiency compromises DNA replication (Barnes et al., 1998; Frank et al., 1998; Frank et al., 2000). To confirm the above findings, *LIG4* was

knocked out first and the DT40 mutants were checked for their growth characteristics and their DNA replication activity (Figure 10).

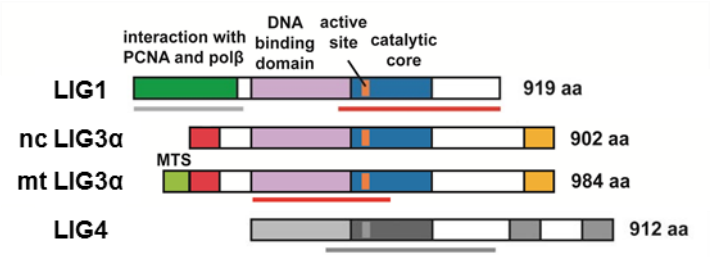

Figure 10: Schematic representation of the active ligases in *LIG4*$^{-/-}$ cells. Deleted ligase is depicted in grey, expressed ligases are shown in color (modified from (Arakawa et al., 2012)).

As expected, *LIG4* knockout cells in DT40 (*LIG4*$^{-/-}$) were viable and showed no shifts in the cell cycle distribution; only a slightly slower growth rate in comparison to the wt cell line was observed (Figure 11).

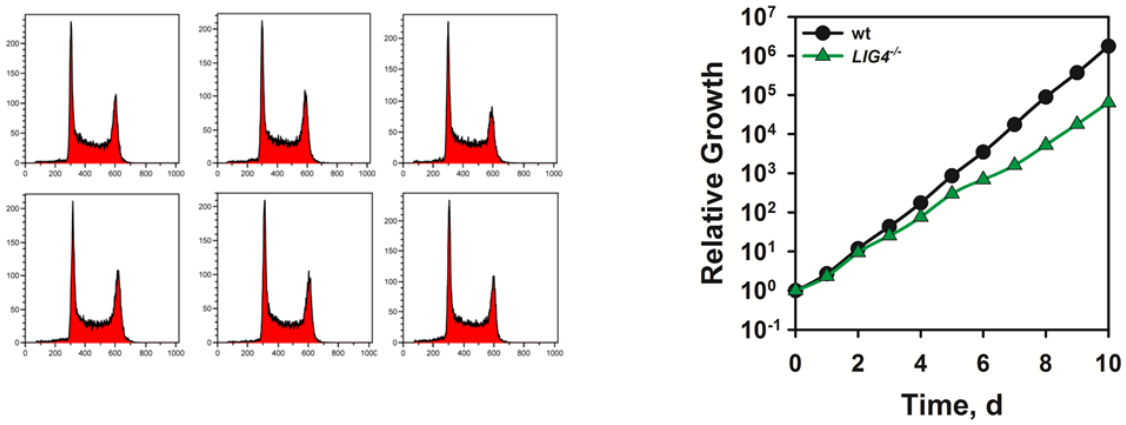

Figure 11: *LIG4* knockout does not change the growth kinetics of *LIG4*$^{-/-}$ cells. Cells were diluted daily in fresh growth medium to maintain exponential growth. The cell numbers are normalized to the initial number of cells seeded.

For a more in depth analysis of actively replicating cells, DNA replication was measured using a 2-parametric flow-cytometry approach. In this protocol, DNA content was analyzed by PI staining and the fraction of actively replicating cells was determined by BrdU incorporation. This analysis is particularly useful because, in addition to the total fraction of cells in S-phase as estimated by DNA content (PI-signal), it also provides the fraction of cells actually engaged in

semi-conservative DNA replication (BrdU-positive). For quantitation, we defined the parameter “Fraction of active S-phase cells,” which is calculated by dividing the number of BrdU positive cells by the total number of cells within the PI limits shown in Figure 12. By convention, the gating for this analysis was set between the end of the G1 and the beginning of the G2 peaks. Similar to the growth kinetics, there was no obvious difference between the wt and the LIG4 mutants in the percentage of actively replicating S-phase cells (Figure 12).

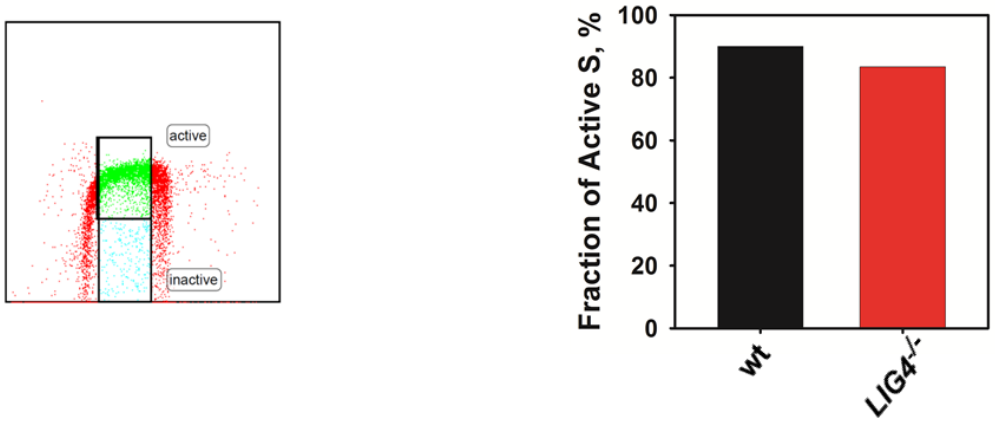

Figure 12: BrdU incorporation of *LIG4*$^{-/-}$ and wt DT40 cells. Left: Representative dot plot of BrdU-labeled *LIG4*$^{-/-}$ cells showing the gates applied to calculate the active S-phase fraction. Right: Calculated fraction of actively replicating cells.

As the induction of SCEs is intimately associated with DNA replication, we investigated whether the knockout of LIG4 changes the frequency of SCEs – which might indicate alterations in homologous recombination repair activity for example through replication stress (Painter, 1980; Sonoda et al., 1999; Wolff, 1977). The frequency of SCEs in LIG4 deficient cells was slightly higher than that of the wt cell line. However, this difference is quite small and not statistically significant (p value of 0.25 after Wilcoxon Signed Rank Test) (Figure 13). These results, in aggregate, support the notion that there are no severe consequences on DNA replication associated with LIG4 deficiency. Therefore, it was concluded that LIG4 knockout has no effect on replication in DT40.

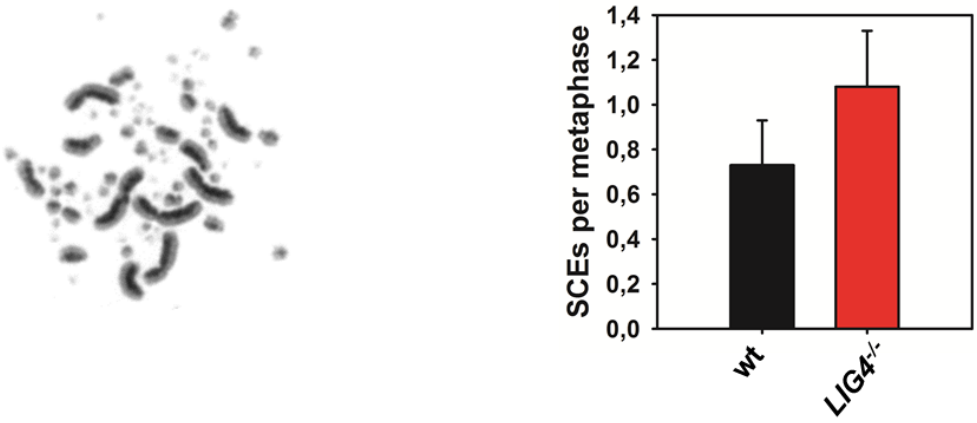

Figure 13: Spontaneously induced SCE in *LIG4*$^{-/-}$ and wt DT40 cells. Left: Representative image of *LIG4*$^{-/-}$ metaphase incubated for two cell cycles with BrdU and stained with a Giemsa protocol allowing the detection of SCE (see under "Material and Methods"). The red arrow points to SCE in this exemplary metaphase. Right: Calculation of SCE frequency per metaphase. Error bars represent standard error of the mean.

4.1.2 *LIG1* knockout has no measurable impact on DNA replication

As it was likely that the LIG1 knockout would be lethal, we applied a conditional genetic system to eliminate the LIG1 activity as described under "Material and Methods" (3.2.1.1.). Briefly, one allele of the *LIG1* gene was excised from the genome while the other one was flanked by 2 loxP sites, which are recognized by the Cre recombinase. In our DT40 cells, the sequences encoding a chimera between Cre recombinase and the mutated estrogen receptor (MER) are integrated into the genome. This ensures continuous expression of MerCreMer protein under the control of the human β-actin promoter (Arakawa et al., 2012; Arakawa et al., 2002; Arakawa et al., 2001; Zhang et al., 1996). In the absence of 4-hydroxytamoxifen (4HT), MerCreMer is efficiently sequestered by heat shock proteins in the cytoplasm. This interaction is rapidly disrupted upon administration of 4HT resulting in translocation of the protein to the nucleus, where Cre exerts recombination activity at loxP sites (Arakawa et al., 2012).

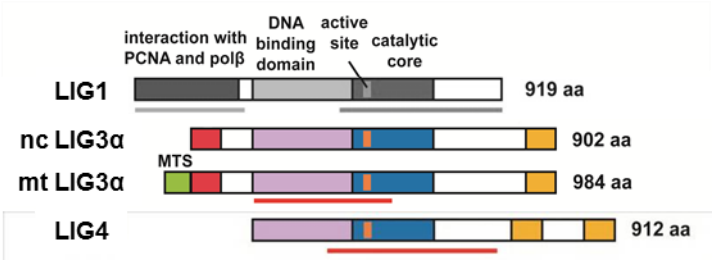

Figure 14: Schematic representation of the active ligases in *LIG1*$^{-/-}$ cells. Deleted ligase is depicted in grey, expressed ligases are shown in color (modified from (Arakawa et al., 2012)).

After administration of 4HT to the above cell line, the *LIG1* mRNA amount drops to undetectable levels in a timeframe of 8 to 12 h (Figure 15). Unfortunately, it was not possible to correlate the LIG1 mRNA level with the disappearance of the LIG1 protein as antibodies recognizing the chicken form of LIG1 could not be found (data not shown).

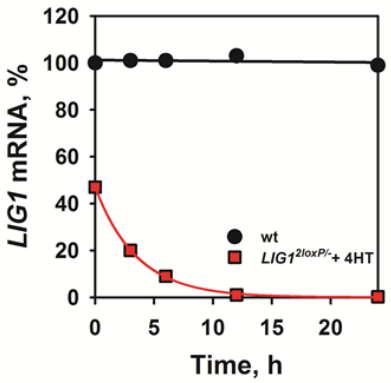

Figure 15: *LIG1* mRNA level in 4HT treated *LIG1*$^{2loxP/-}$ cells. *LIG1* mRNA level in *LIG1*$^{2loxP/-}$ cells as a function of time after induction of the total knockout by incubation with 4HT, measured by RT-PCR.

In further experiments, the growth kinetics of *LIG1*$^{2loxP/-}$ cells were followed after induction of *LIG1* knockout by 4HT treatment, and the fraction of actively replicating S-phase cells was also monitored over time (Figure 16A, B). It turned out that knockout of *LIG1* to generate *LIG1*$^{-/-}$ does not significantly change the growth kinetics and the fraction of active S-phase cells over time (Figure 16A, B).

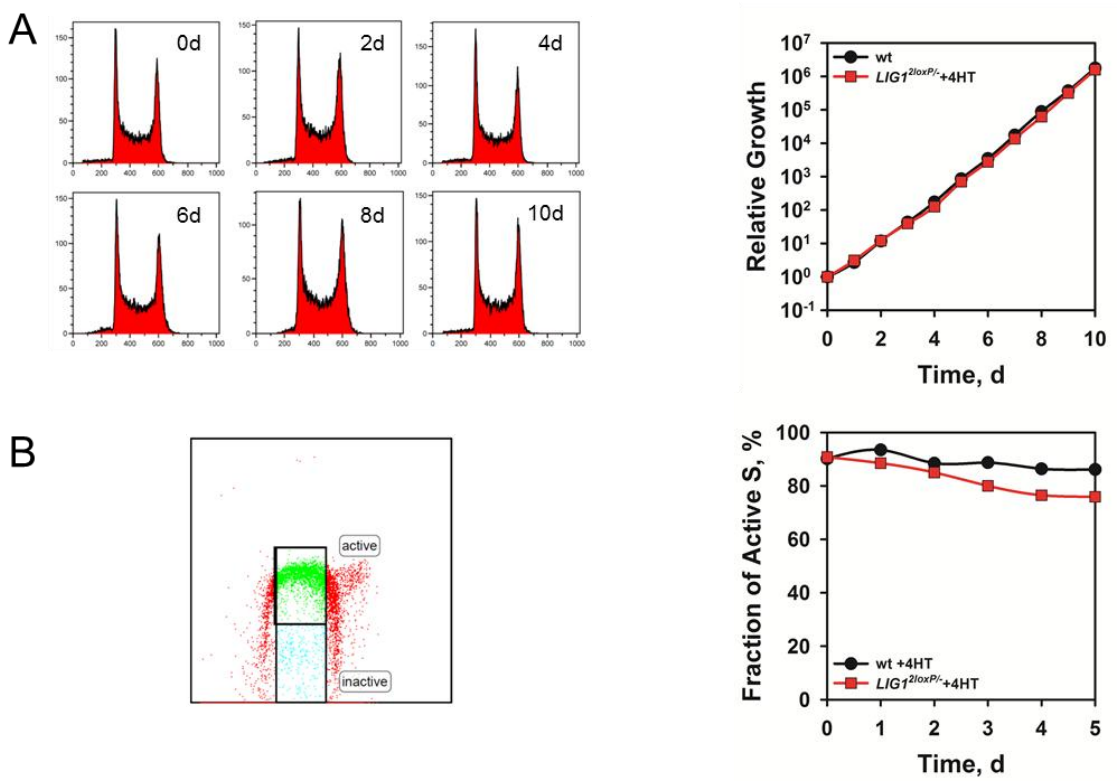

Figure 16: *LIG1* knockout has no influence on growth or the fraction of active S-phase cells A) Growth kinetics and distribution throughout the cell cycle of *LIG1*$^{2loxP/-}$ treated with 4HT and of wt cells as reference. Cells were daily diluted with fresh growth medium to maintain exponential growth. Growth is shown normalized to the initial number of cells seeded. **B)** Left: Representative dot plot of BrdU-labeled *LIG1*$^{2loxP/-}$ cells, and gates applied to calculate the active S-phase fraction Right: Fraction of actively replicating cells as a function of the treatment time.

DNA replication can also be analyzed by following the progression of G1-phase cells into S-phase. This method complements the results acquired with the 2 parametric flow cytometry as it is not affected by the fluctuations in dNTP pools and also eliminates the false negative signals, which may result from the cells undergoing apoptosis. For this purpose, a clean population of G1 DT40 cells was prepared by centrifugal elutriation. Centrifugal elutriation separates cells according to their size and allows the generation of fractions highly enriched in specific phases of the cell cycle. A G1 cell fraction was allowed to progress into the cell cycle and cells were retrieved and analyzed at different times thereafter. The resulting histograms allow estimation of cell cycle progression by comparing the initial G1 peak with the median of the progressing fraction of cells. In accordance with the above mentioned results, the *LIG1*$^{-/-}$ cells progress through the cell cycle with kinetics indistinguishable from that of wt cells

(Figure 17). Thus, even this assay could not detect any measurable effect of *LIG1* knockout on cell proliferation (Figure 17).

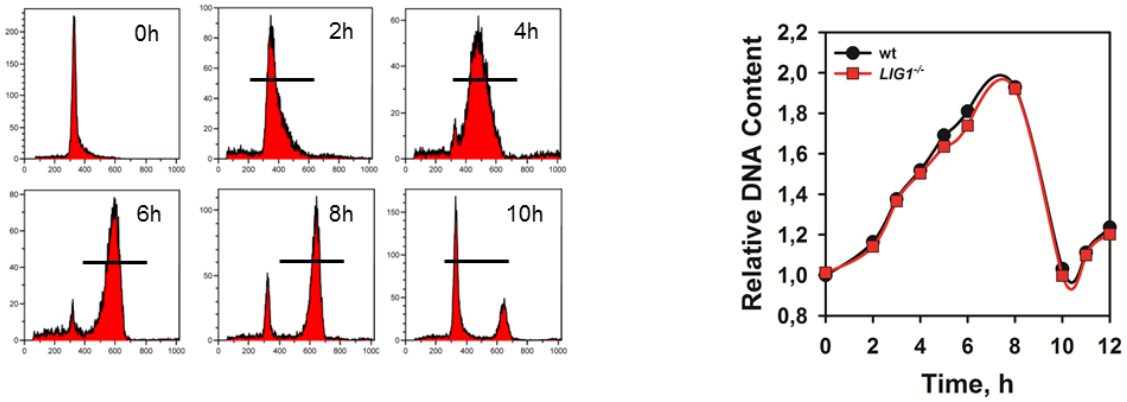

Figure 17: *LIG1* knockout has no influence on the progression through the cell cycle. Left: Representative flow-cytometric histograms of centrifugal elutriation G1 enriched *LIG1*$^{-/-}$ cells incubated to progress through the cell cycle. The horizontal bar shows the subpopulation used to estimate progression through the cycle for the population median. Right: Progression through S-phase calculated by following the relative increase in DNA content for the median of the population described in the left panel.

As already discussed, human and mouse cells carrying mutations in *LIG1* gene show a severe defect in Okazaki fragment joining. Therefore, it was tested whether in the DT40 system used, such a phenotype could also be observed (Bentley et al., 1996). This assay was consequently modified to accommodate the requirements of suspension cells, such as the DT40, and the acquired results were compared with the results obtained in parallel using 4 cell lines with different *LIG1* genetic background that have already been tested for this endpoint by others (Figure 18) (Bentley et al., 1996). No measurable defect in joining of Okazaki fragments could be detected in DT40 cells after knockout of *LIG1* (Figure 18). However, as these cells show no growth defect at all, this was not surprising.

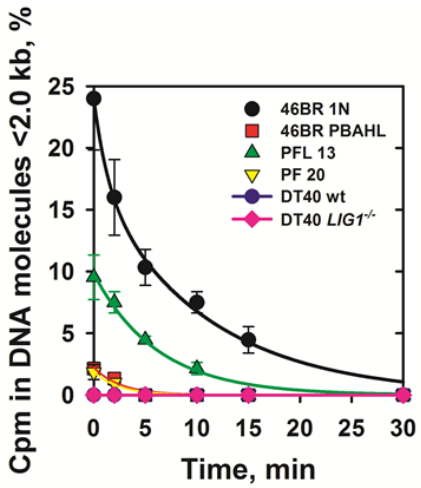

Figure 18: *LIG1* knockout has no influence on the maturation of Okazaki fragments. Accumulation of Okazaki fragments in LIG1-deficient human and mouse cells, as well as of *LIG1*$^{-/-}$ DT40 cells. The graph shows the percentage of total radioactivity present in single-stranded DNA fragments <2.0 kb for each cell line.

Also, the generation of spontaneous SCEs in the *LIG1* deficient cell line was followed (Figure 19). Notably, at this endpoint the knockout of *LIG1* did not seem to have any negative impact either. Thus, the conclusion to be drawn is that *LIG1* knockout has no measurable effect on DNA replication in DT40 cells.

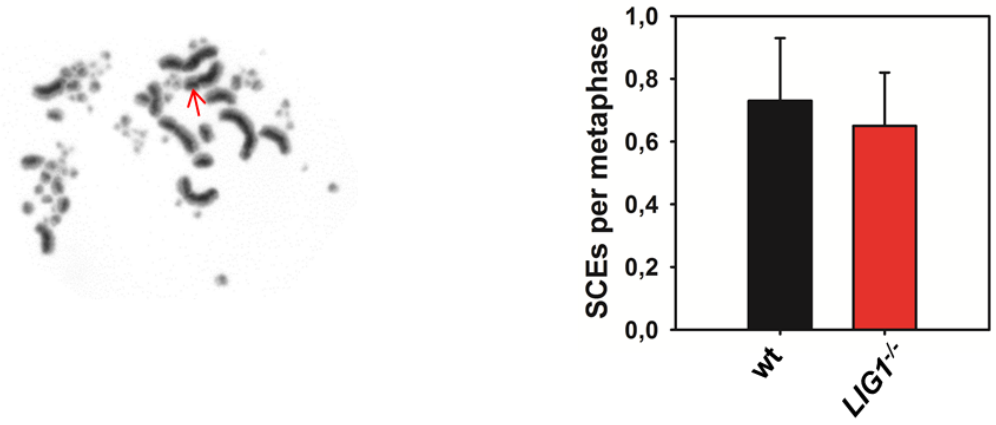

Figure 19: *LIG1* knockout has no influence on the induction of spontaneous SCEs. Left: Representative image of *LIG1*$^{-/-}$ DT40 metaphase incubated for two cell cycles with BrdU and stained afterwards with a Giemsa protocol allowing the differential visualization of sister chromatids. The red arrow points to a SCE in this exemplary metaphase. Right: Calculation of SCE frequency per metaphase. Each bar is calculated from 3 independent experiments, with 100 metaphases each. Error bars represent standard error of the mean.

4.1.3 *LIG3* knockout is lethal due to its requirement for mitochondrial function

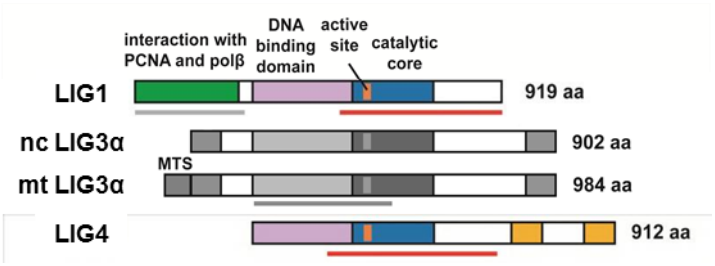

Figure 20: Schematic representation of the active ligases in 4HT treated *LIG3*$^{2loxP/-}$ cells. Deleted ligases are depicted in grey, expressed ligases are shown in color (modified from (Arakawa et al., 2012)).

Following experiments with LIG1 described above, the effects of a knockout of the evolutionarily newer LIG3 were studied. Here, the Cre/loxP conditional knockout system described above was also applied to see the impact of *LIG3* knockout on cell survival. Similar to previous results with *LIG1*$^{2loxP/-}$ cells, the targeted allele is quickly disrupted – within 12 h after treatment with 4HT (Arakawa et al., 2012).

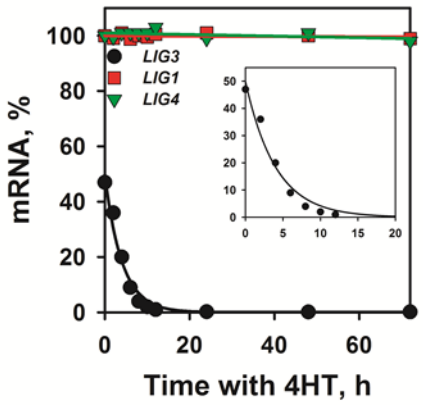

Figure 21: *LIG3* knockout does not cause compensatory overexpression of *LIG1* or *LIG4*. Measurement of *LIG1*, *LIG3* and *LIG4* mRNA levels in *LIG3*$^{2loxP/-}$ cells as a function of time after induction of the complete knockout measured by RT-PCR

The same was true for the levels of mRNA measured. The mRNA of *LIG3* dropped down to undetectable levels within 12 h (Figure 21). To examine

whether LIG3 knockout causes compensatory overexpression of the remaining ligases, the mRNA levels of *LIG1* and *LIG4* were measured. No significant decrease or increase of the mRNA levels of either ligase was noted (Figure 21).

Although the cells expressing LIG3 from only one allele (*LIG3*$^{2loxP/-}$) grow like the wt cells, the addition of 4HT in these cells resulted in complete elimination of LIG3 from the cells and had a dramatic effect on cell survival. Within 4 d after treatment the proliferation activity of the mutant decreased dramatically. This is most probably due to the inception of cell death by apoptosis (Figure 22).

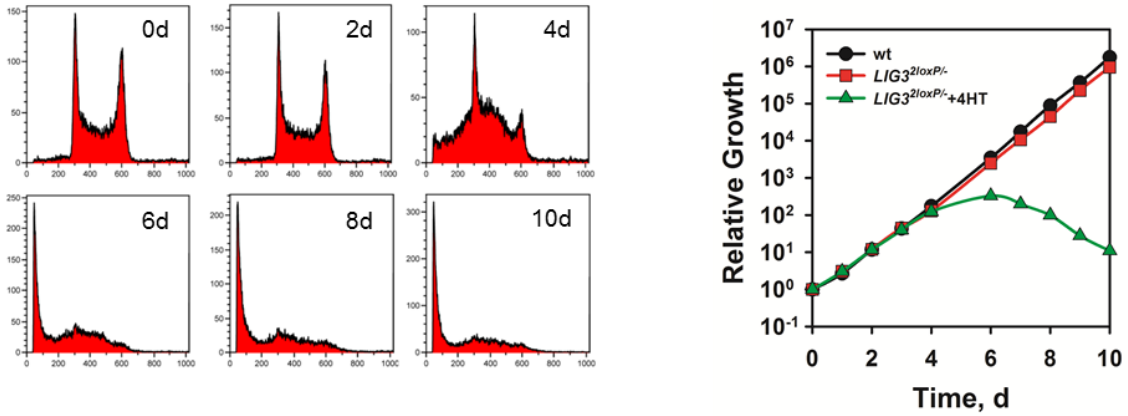

Figure 22: *LIG3* knockout has severe effects on cell survival. Growth kinetics and cell cycle distribution of *LIG3*$^{2loxP/-}$ cells with and without treatment with 4HT vis-à-vis the growth kinetics of wt cells. Cells were daily diluted with fresh growth medium to maintain exponential growth. Growth is shown normalized to the initial number of cells seeded.

We also followed LIG3 protein decay by western blotting. Surprisingly, we found that the protein concentration level remains unchanged over a period of 2 d after induction of the knockout. There was also only a slight reduction in protein level after 3 d and the corresponding protein band did not disappear completely in the measured timeframe of 5 d (Arakawa et al., 2012). This result raised the question whether the antibody is really specific and whether it recognizes another protein of the same or a comparable molecular weight as LIG3. To address these questions we introduced alternative assays to measure LIG3 activity. Indeed, for further information on the level of knockdown, we utilized an end joining assay, which preferentially measures the activity of LIG3. The results from these experiments have shown that after 3 d of treatment with 4HT, the end joining activity in whole cell extracts (WCE) prepared from these cells

was decreased to barely detectable levels. This result suggests that while the protein persists in the treated cells, it loses its catalytic activity within the first or second day of treatment (Paul et al., 2013).

Next the fraction of actively replicating cells in this mutant was measured. Here again, a decrease at day 4 after treatment was observed. This was to be expected as, at this point, the cells already started to die (Figure 23).

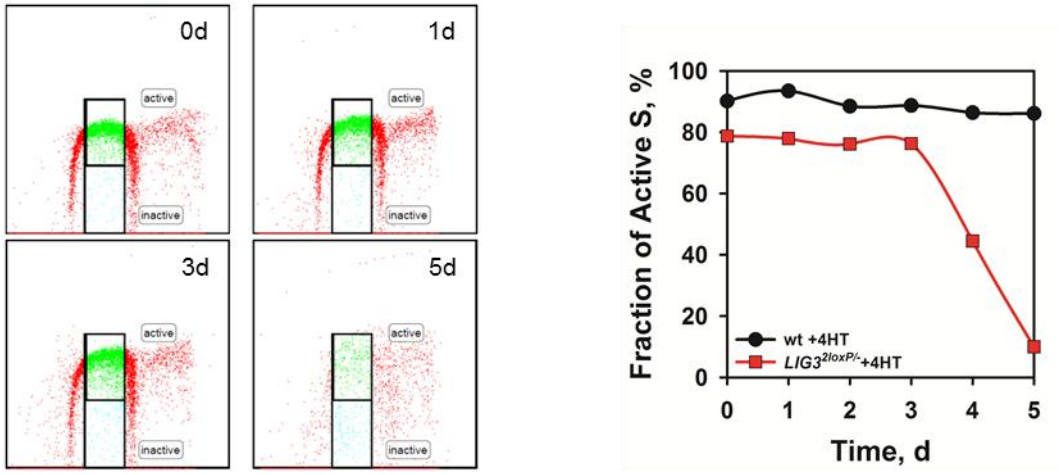

Figure 23: *LIG3* knockout leads to rapid decrease in replication activity. Left: Representative dot plots of 4HT treated BrdU-labeled *LIG3*$^{2loxP/-}$ cells and the gates applied to calculate the active S-phase fraction. Right: Fraction of actively replicating cells as a function of the treatment time.

As further support for the state of this mutant after treatment with 4HT (84 or 96 h), the progression of G1 enriched (by centrifugal elutriation) cells through the S-phase was measured. It is evident from the results obtained that untreated cells progress through the S-phase with kinetics similar to the wt cells while 4HT-treated cells significantly slowed down their progression through the cycle (Figure 24). This could be explained either by an essential function of LIG3 in DNA replication or by a secondary effect causing apoptosis. More advanced genetic systems were required to conclusively address this question and are described next.

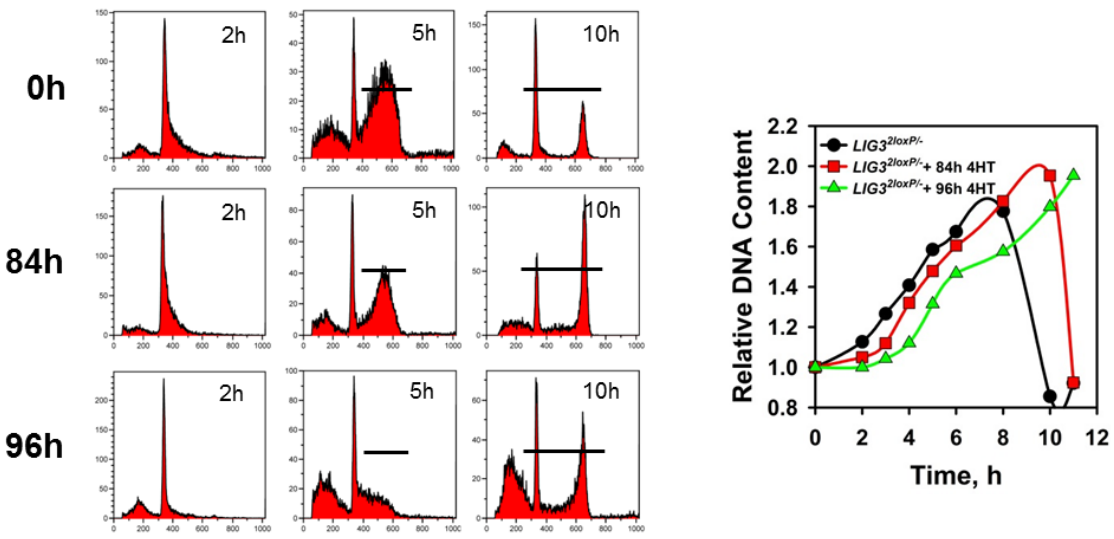

Figure 24: Induction of *LIG3* knockout leads to measurable delay in cell cycle progression. Left: Representative flow-cytometric histograms of G1 enriched *LIG3*$^{2loxP/-}$ cells with and without treatment with 4HT as they are allowed to progress through the cell cycle. The horizontal bar shows the subpopulation used to estimate progression through the cycle of the population median. Right: Progression through S-phase calculated by following the relative increase in DNA content for the median of the population described before.

To investigate whether LIG3 exerts an essential function in the cell nucleus, a mutant was constructed in which the M2 translation initiation site was inactivated and therefore only the mitochondria version of LIG3 (*LIG3*$^{2loxP/M2I}$) was expressed (Figure 25).

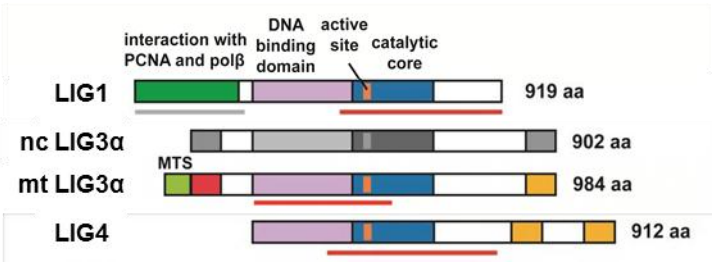

Figure 25: Schematic representation of the active ligases in 4HT treated *LIG3*$^{2loxP/-}$ cells. Deleted ligases are depicted in grey, expressed ligases are shown in color (modified from (Arakawa et al., 2012)).

During investigation of the growth characteristics of this mutant, we observed that treatment with 4HT to delete the conditional LIG3 allele did not affect the growth characteristics of the cells (Figure 26).

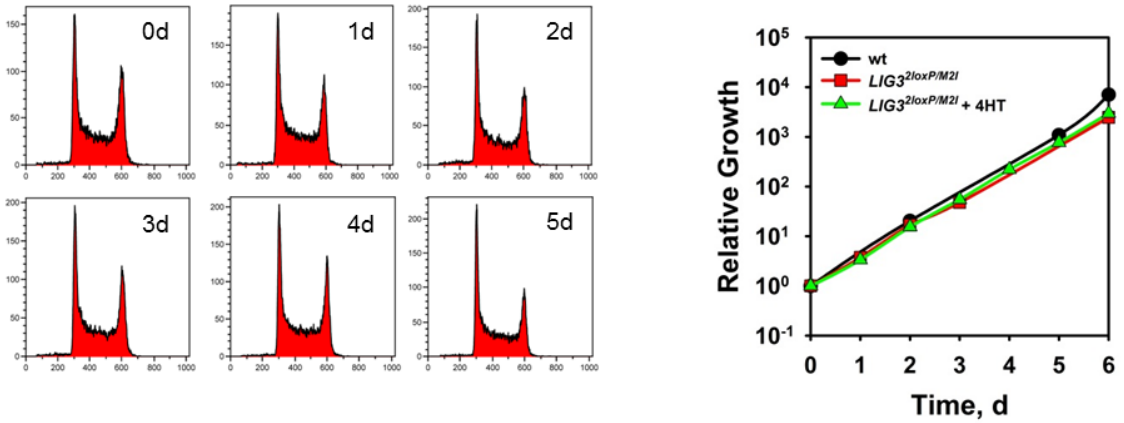

Figure 26: Treatment of *LIG3*$^{2loxP/M2I}$ cells with 4HT does not affect the growth characteristics of the cells. Growth kinetics and cell cycle distribution of *LIG3*$^{2loxP/M2I}$ with and without treatment with 4HT vis-à-vis the growth kinetics of wt cells as reference. Cells were daily diluted with fresh growth medium to maintain exponential growth. Growth is calculated normalized to the initial number of seeded cells

Yet, upon treatment with 4HT the amount of *LIG3* mRNA dropped down to the expected 50%, but cell growth remained stable and no cell killing was observed (Figure 26, 27). These observations suggest that the mitochondrial form of LIG3 together with LIG1 and LIG4 (*LIG3*$^{-/M2I}$) can fully support proliferation in DT40 cells.

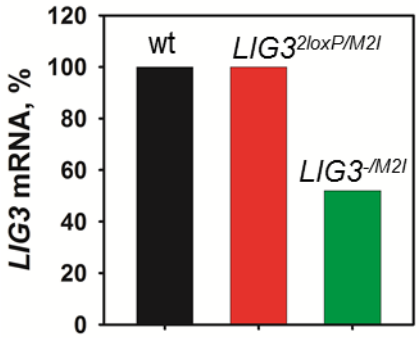

Figure 27: mRNA level of *LIG3*$^{2loxP/M2I}$ and *LIG3*$^{-/M2I}$ cells. Measurement of *LIG3* mRNA levels in wt, *LIG3*$^{2loxP/M2I}$ and *LIG3*$^{-/M2I}$ cells normalized to wt mRNA level.

The fraction of actively replicating cells was slightly reduced from 90% in the parental cell line to 80%, which might point to slight defects in replication due to the lack of nuclear LIG3 (Figure 28).

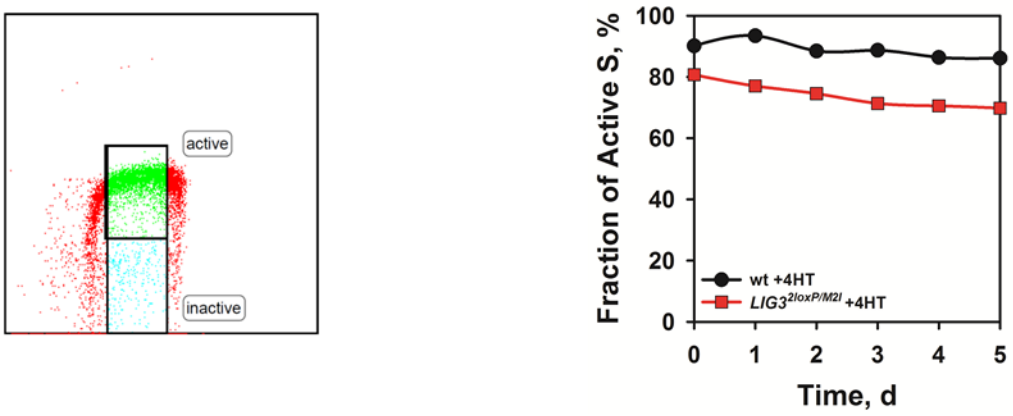

Figure 28: The fraction of actively replicating cells, decreases slightly upon induction of the knockout in *LIG3*$^{-/M2I}$ cells. Left: Representative dot plot of BrdU-labeled *LIG3*$^{2loxPM2I-}$ cells and the gates applied to calculate the active S-phase fraction. Right: Fraction of actively replicating cells as a function of the treatment time.

To confirm the above results, we attempted to rescue the lethal phenotype of *LIG3* knockout with another ligase containing a mitochondrial leader sequence. For this purpose, the yeast homolog of *LIG1*, *CDC9*, which also carries a mitochondrial leader sequence, was chosen. The gene was stably integrated in the genome of *LIG3*$^{2loxP/-}$ cells (*LIG3*$^{2loxP/-}$*cdc9*) and was associated with its own promoter to ensure stable expression (Arakawa et al., 2012).

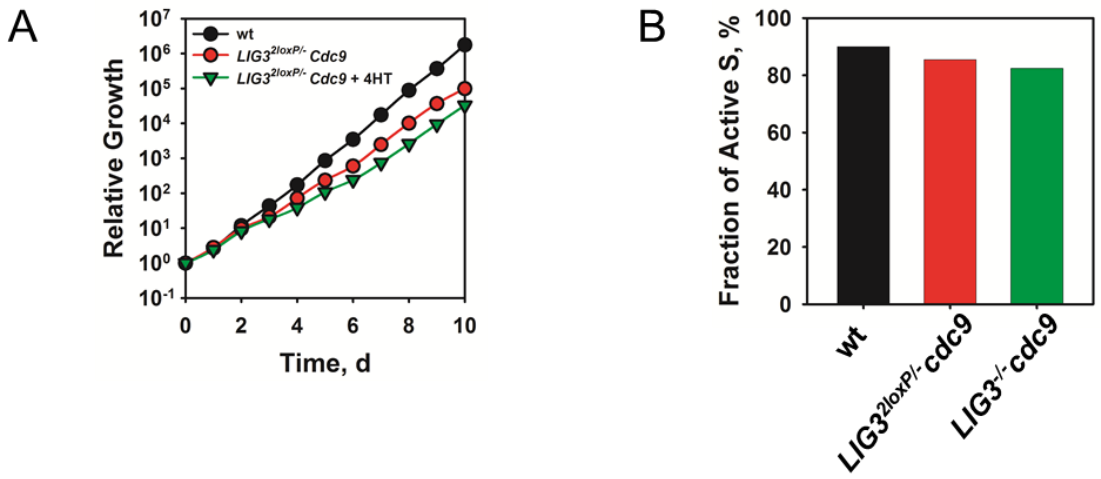

Figure 29: Expression of Cdc9 rescues the lethal phenotype observed upon *LIG3* knockout. A) Growth kinetics of *LIG3*$^{2loxP/-}$*cdc9* with and without treatment with 4HT together with the growth kinetics of wt cells as reference. Cells were daily diluted with fresh growth medium to maintain exponential growth. Growth is calculated normalized to the initial number of seeded cells. **B)** Fraction of actively replicating cells before and after treatment with 4HT.

The induction of the LIG3 knockout did not change the growth kinetics of this mutant and also had only a marginal effect on the fraction of actively replicating cells (Figure 29A, B).

Collectively, these results clearly demonstrate that the lethality of the *LIG3* knockout is not due to an essential function of LIG3 in DNA replication, but rather to its unique function in the mitochondria. Notably, this function could be fully supported by another ligase carrying a mitochondrial leader sequence from an organism evolutionarily as remote as the budding yeast. Thus, any single ligase knockout has no measurable effect on DNA replication in DT40 cells. This observation raises the possibility that both LIG1 and LIG3 support replication with similar efficiency. This aspect is investigated in greater depth in the following set of experiments.

4.1.4 Mono-ligase systems reveal that LIG1 and LIG3 support all replication functions, while LIG4 is unable to do so

The experiments with the single knockouts did not conclusively show the function of LIG3 in DNA replication. Therefore, a set of double ligase knockout mutants together with knock-in cell lines which resulted in functional mono-ligase systems was designed and tested (Arakawa et al., 2012; Paul et al., 2013).

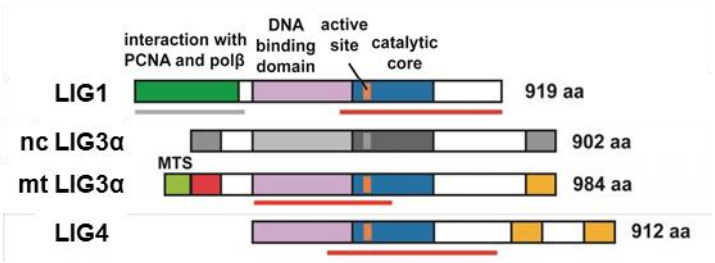

Figure 30: Schematic representation of the active ligases in *LIG3*$^{-/M2I}$ cells. Deleted ligase is depicted in grey, expressed ligases are shown in color (modified from (Arakawa et al., 2012)).

First, LIG4 was knocked out in a LIG1 deficient genetic background to generate the *LIG1*$^{-/-}$*LIG4*$^{-/-}$ double mutant (Figure 30). These cells were found to grow with slightly slower kinetics than the wt and also a bit slower than the *LIG4* single mutant (Figure 31). Nevertheless, these effects were relatively minor and demonstrated that LIG3 as a single ligase can support all ligation function of DT40 cells.

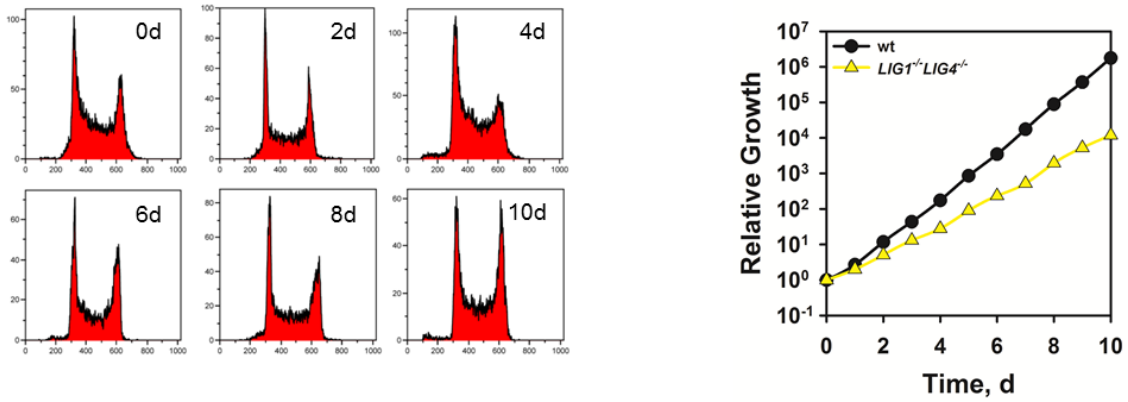

Figure 31: *LIG1* and *LIG4* knockout cells show only slightly slower growth kinetics. Growth kinetics and cell cycle distributions of *LIG1*$^{-/-}$*LIG4*$^{-/-}$ cells vis-à-vis the growth kinetics of wt cells as reference. Cells were daily diluted with fresh growth medium to maintain exponential growth. Growth is calculated normalized to the initial number of seeded cells.

The fraction of actively replicating cells was determined in this mutant and found to be at the same level as the *LIG1* knockout (Figure 32).

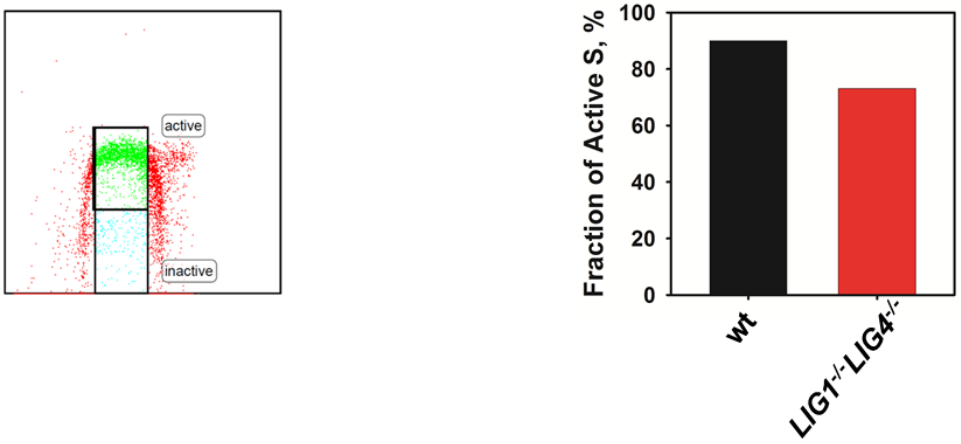

Figure 32: Knockout of *LIG4* on *LIG1* deficient background does not change fraction of actively replicating cells. Left: Representative dot plot of BrdU-labeled *LIG1*$^{-/-}$*LIG4*$^{-/-}$ cells and the gates applied to calculate the active S-phase fraction. Right: Fraction of actively replicating cells.

The effect of double knockout on the progression of cells throughout the cell cycle was also investigated by measuring the progression of elutriated *LIG1*$^{-/-}$*LIG4*$^{-/-}$ G1 cells into S-phase. This mutant also showed no defect in this assay and moved through the cell cycle with kinetics undistinguishable from the wt cells or the *LIG1*$^{-/-}$ cells (Figure 33).

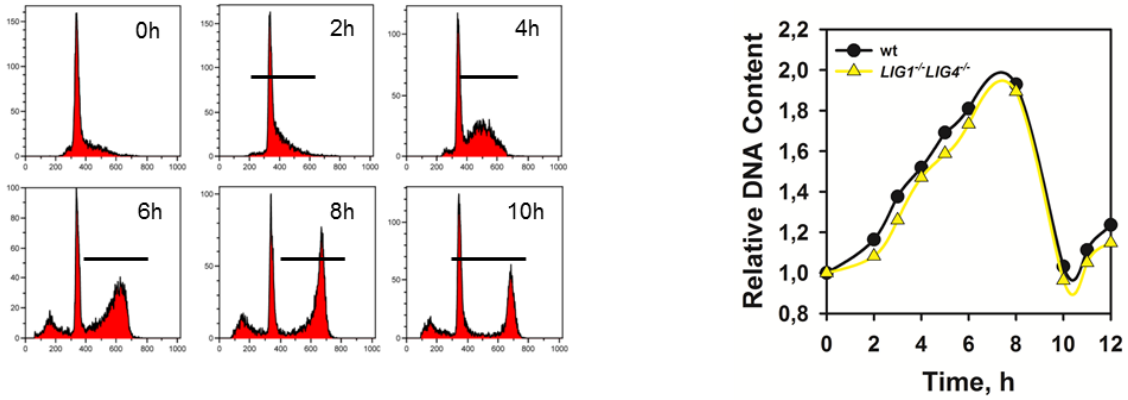

Figure 33: Knockout of *LIG4* on *LIG1* deficient background does not result in a measurable delay in cell cycle progression. Left: Representative flow-cytometric histograms of G1 enriched *LIG1*$^{-/-}$*LIG4*$^{-/-}$ cells as they progress through the cell cycle. The horizontal bar shows the subpopulation used to estimate progression through the cycle of the population median. Right: Progression through S-phase calculated by following the relative increase in DNA content for the median of the population described in the left panel.

The joining of Okazaki fragments was also tested in these cells and found to be no different from any of the other mutants tested (Figure 34).

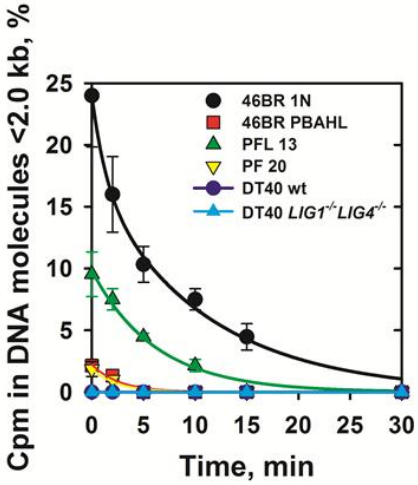

Figure 34: *LIG1* and *LIG4* knockouts have no influence on the maturation of Okazaki fragments Accumulation of Okazaki fragments in LIG1-deficient human and mouse cells as well as the indicated *LIG1*$^{-/-}$*LIG4*$^{-/-}$ DT40 cells. The graph shows the percentage of total radioactivity present in single-stranded DNA fragments <2.0 kb for each cell line.

As this mutant also represents a robust system devoid of problems associated with apoptosis, the frequency of SCEs was measured (Figure 35). It is interesting that this mutant showed a slightly higher frequency of SCEs than the wt. However, the level of SCE measured was comparable to that measured in the *LIG4*$^{-/-}$ mutant. These results conclusively show that LIG3 efficiently supports all DNA replication activities normally assigned to LIG1.

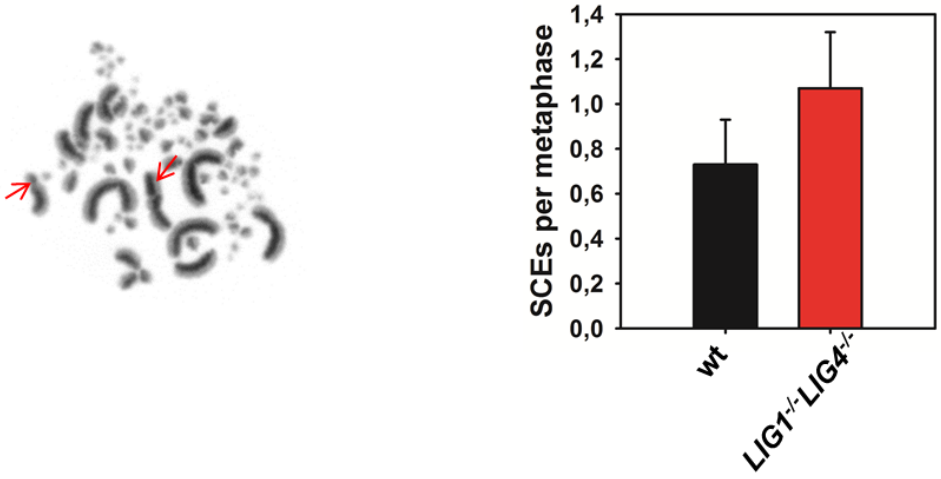

Figure 35: *LIG1* and *LIG4* knockout have no influence on the induction of spontaneous SCEs. Left: Representative image of a *LIG1*$^{-/-}$*LIG4*$^{-/-}$ metaphase incubated for two cell cycles with BrdU and stained with a Giemsa protocol allowing differential staining of the sister chromatids. The red arrows point to SCEs in this exemplary metaphase. Right: Calculation of SCE frequency per metaphase. Error bars represent standard error of the mean.

The next question that needed to be addressed was whether LIG4 can also support DNA replication in the absence of LIG3 and LIG1. It was not surprising that the cells lacking LIG1 and carrying only one conditional allele of LIG3 did not survive 4HT treatment which generates a mutant only expressing LIG4 (Figure 36). Interestingly, the mutant displayed far larger sensitivity to 4HT treatment than any of the mutants tested before with lethality manifest 1 d after treatment.

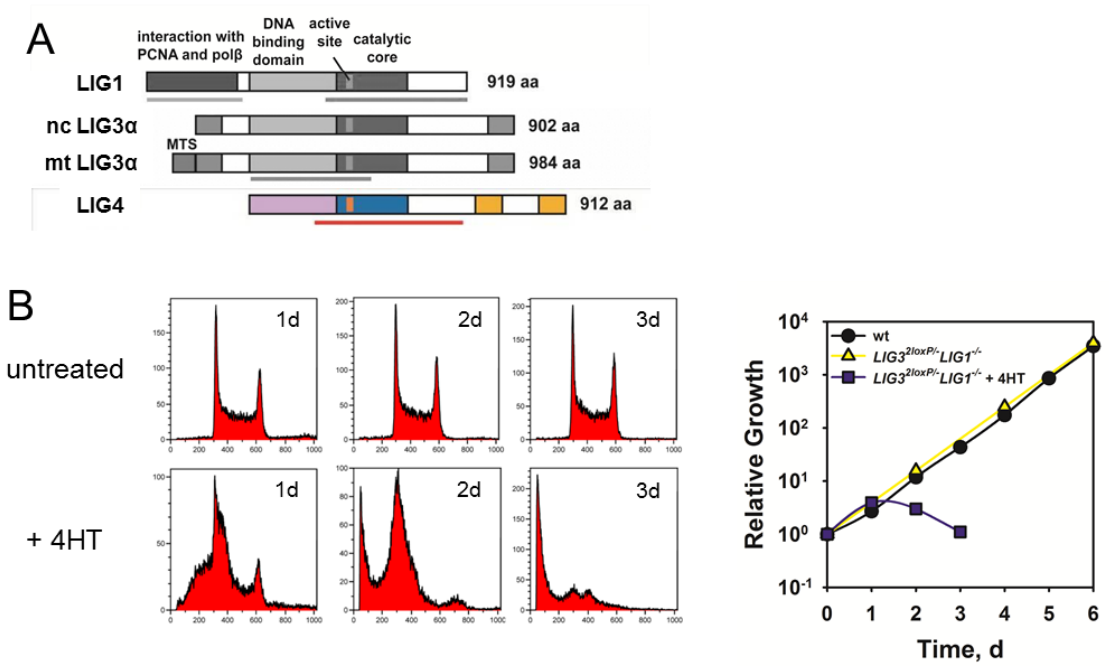

Figure 36: *LIG3*$^{2loxP/-}$*LIG1*$^{-/-}$ cells are more sensitive to 4HT treatment than any other cell line tested. A) Schematic representation of the ligases expressed in the generated mutant. Deleted ligases are depicted in grey, expressed ligases are shown in color (modified from (Arakawa et al., 2012)). **B)** Growth kinetics and cell cycle distribution of *LIG3*$^{2loxP/-}$*LIG1*$^{-/-}$ cells with and without treatment with 4HT vis-à-vis the growth kinetics of wt cells as reference. Cells were daily diluted with fresh growth medium to maintain exponential growth. Growth is calculated normalized to the initial number of seeded cells.

In line with this result, the fraction of actively replicating cells which shows a 30% lower starting point drops massively on day 1 (Figure 37).

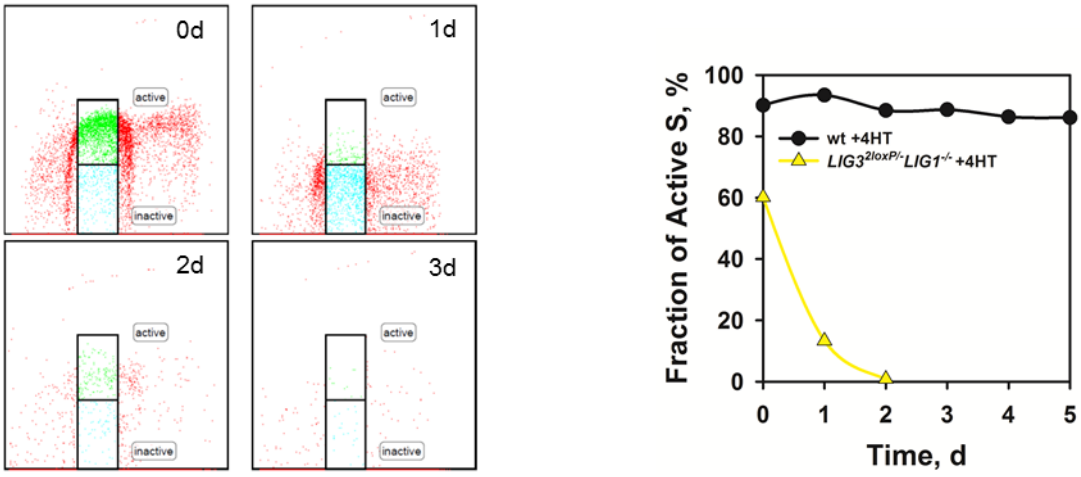

Figure 37: Impact of *LIG1* and *LIG3* knockout on DNA replication in DT40 cells. Left: Representative dot plot of BrdU-labeled *LIG3*$^{2loxP/-}$*LIG1*$^{-/-}$ cells as a function of the treatment time and the gates applied to calculate the active S-phase fraction Right: Fraction of actively replicating cells as a function of the treatment time.

This suggests that in the absence of LIG1 even slight reductions of LIG3 have severe consequences for the cells.

As already discussed, the mitochondrial function of LIG3 is essential for cell survival. This is why a mutant was designed which expresses the mitochondrial version of LIG3, but lacks the nuclear form, and, in addition, has one allele of *LIG1* flanked by 2 loxP sites to allow the conditional elimination of LIG1 (Figure 38).

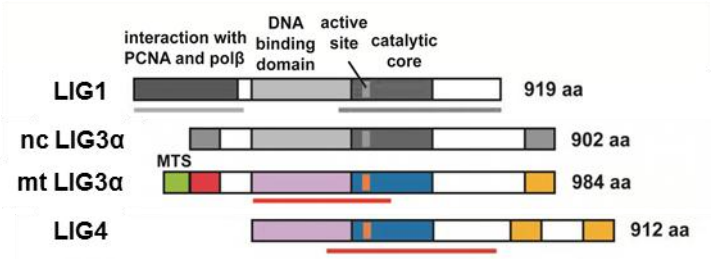

Figure 38: Schematic representation of the active ligases in 4HT treated *LIG3*$^{-/M2I}$*LIG1*$^{2loxP/-}$ cells. Deleted ligases are depicted in grey, expressed ligases are shown in color (modified from (Arakawa et al., 2012)).

Despite its greater sensitivity to 4HT in comparison to the single LIG3 mutant, this mutant did survive longer compared to the *LIG3*$^{2loxP/-}$*LIG1*$^{-/-}$ mutant (Figure 39).

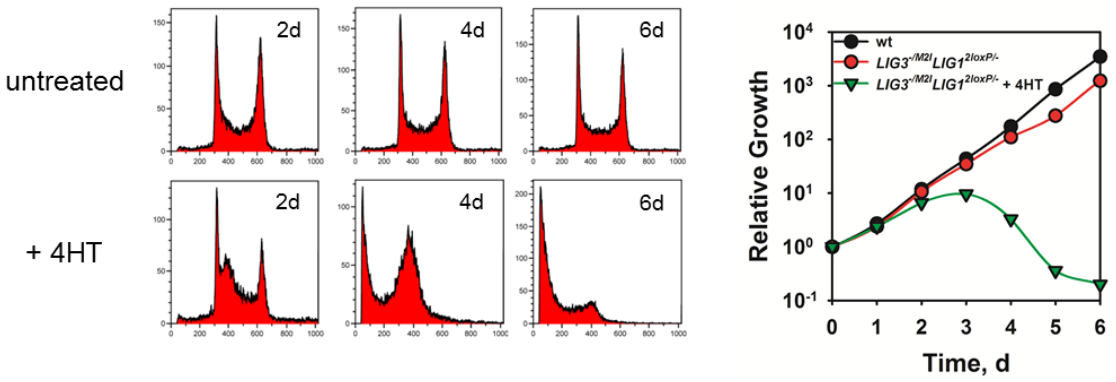

Figure 39: *LIG1* knockout on a *LIG3*$^{-/M2I}$ background has severe effects on cell survival. Growth kinetics and cell cycle distribution of *LIG3*$^{-/M2I}$*LIG1*$^{2loxP/-}$ cells with and without treatment with 4HT vis-à-vis the growth kinetics of wt cells as reference. Cells were daily diluted with fresh growth medium to maintain exponential growth. Growth is calculated normalized to the initial number of seeded cells.

Also, the initial fraction of active S-phase cells was significantly lower than that of the wt cells (Figure 40). These findings allow the conclusion that LIG4 is not able to support DNA replication, and that either LIG1 or LIG3 must be present in the nucleus to ensure cell survival.

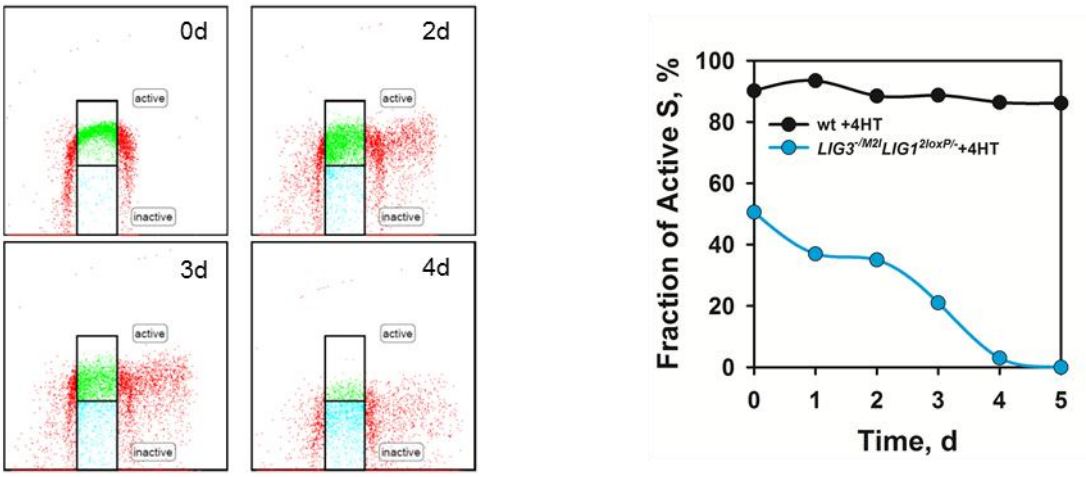

Figure 40: Impact of LIG1 and nuclear LIG3 knockout on DNA replication in DT40 cells. Left: Representative dot plot of BrdU-labeled *LIG3*$^{-/M2I}$*LIG1*$^{2loxP/-}$ cells as a function of treatment time and the gates applied to calculate the active S-phase fraction Right: Fraction of actively replicating cells as a function of treatment time.

To generate a cell line which only expresses LIG1, we constructed a knock-in system with the human *LIG1* to which a mitochondrial leader sequence was added. To get the mono-LIG1 system, we chose a mutant where *LIG4* was knocked out with a conditional *LIG3* knockout capability (*LIG3*$^{2loxP/-}$*LIG4*$^{-/-}$) as background (Figure 41) (Paul et al., 2013).

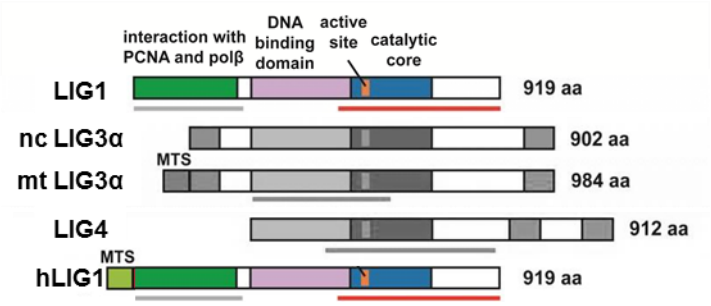

Figure 41: Schematic representation of the active ligases in *LIG3*$^{2loxP/-}$*LIG4*$^{-/-}$mts-h*LIG1* cells. Deleted ligases is depicted in grey, expressed ligases are shown in color (modified from (Arakawa et al., 2012)).

Although the targeted knock-in was not achieved, the clones were checked for protein expression by western blotting and all of the clones checked expressed the human LIG1, which could easily be distinguished from the endogenous chicken LIG1, as the latter is not recognized by the antibody used (Figure 42).

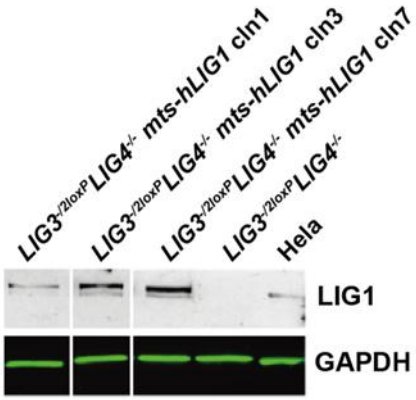

Figure 42: hLIG1 expression in *LIG3*$^{2loxP/-}$*LIG4*$^{-/-}$mts-h*LIG1* cells. Western blot analysis of LIG1 protein level in clones 1, 3 and 7 of the *LIG3*$^{-/2loxP}$*LIG4*$^{-/-}$*mts-hLIG1* mutant, of the *LIG3*$^{-/2loxP}$*LIG4*$^{-/-}$ mutant, and of HeLa cells. A mouse monoclonal antibody (10H5 GeneTex) recognizing human but not chicken LIG1 was used. GAPDH is used as loading control.

After knocking out LIG3 from this mutant we observed that cells growth was not impaired. Indeed cells grew with similar kinetics as the non-induced cells (Figure 43).

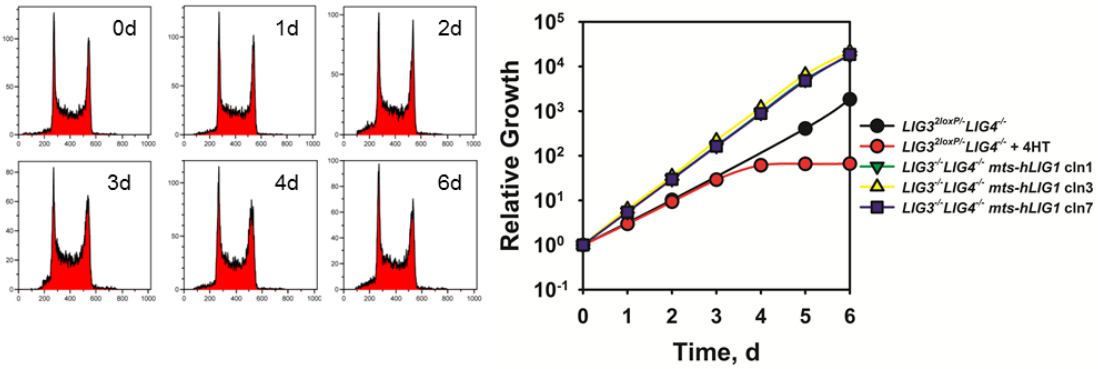

Figure 43: Knockout of both *LIG3* and *LIG4* do not change growth kinetics of mts hLIG1 expressing DT40 cells. Growth kinetics of different clones of *LIG3*$^{2loxP/-}$*LIG4*$^{-/-}$*mts-hLIG1* cells after treatment with 4HT and growth kinetics of treated and untreated parental cell lines as reference. Cells were daily diluted with fresh growth medium to maintain exponential growth. Growth is calculated normalized to the initial number of seeded cells.

The fraction of actively replicating cells was as high as in the wt cells, irrespective of the induced elimination of LIG3 (Figure 44A). In this clean knockout system the frequency of SCEs was also measured. There was no increase in this frequency compared to the wt (Figure 44B).

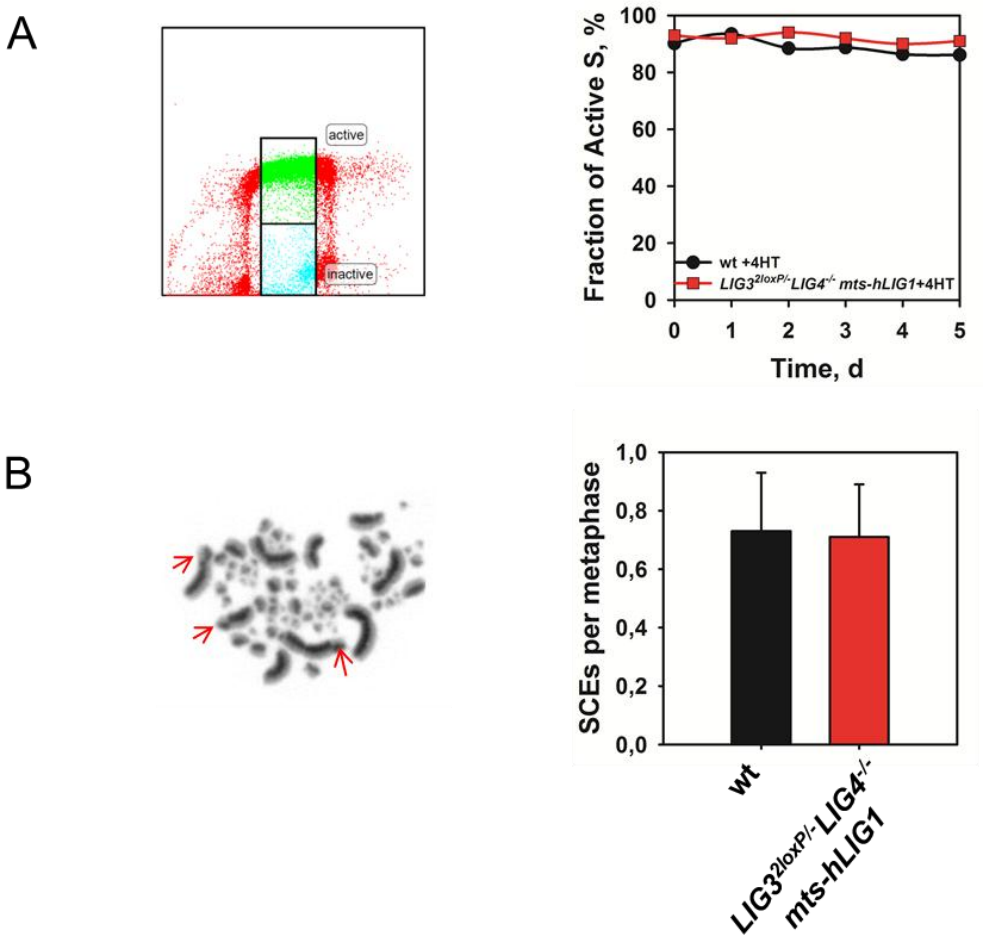

Figure 44: Knockout of both *LIG3* and *LIG4* do not change fraction of actively replicating cells or induction of spontaneous SCEs in mts hLIG1 expressing DT40 cells. A) Left: Representative dot plot of BrdU-labeled *LIG3*$^{2loxP/-}$*LIG4*$^{-/-}$*mts-hLIG1* cells and the gates applied to calculate the active S-phase fraction Right: Fraction of actively replicating cells as a function of the treatment time. **B)** Left: Representative image of *LIG3*$^{2loxP/-}$*LIG4*$^{-/-}$*mts-hLIG1* metaphase incubated for two cell cycles with BrdU and afterwards stained with Giemsa to detect SCE. The red arrows point to SCEs in this exemplary metaphase. Right: Calculation of SCE frequency per metaphase. Error bars represent standard error of the mean.

In aggregate, the results presented in this section show that LIG3 can effectively substitute for LIG1 in semi-conservative DNA replication. However,

LIG3 is not required for replication in the presence of LIG1. Indeed, LIG1 and LIG3 seem to support DNA replication with similar efficiency.

4.2 LIG3 supports DNA replication through its interaction with XRCC1, but not with PCNA

4.2.1 LIG3 does not co-immunoprecipitate with PCNA

The above results show that there is a functional overlap between LIG1 and LIG3 in functions associated with DNA replication. However, the mechanism by which LIG3 supports DNA replication remains to be elucidated. There are data showing an essential interaction between LIG3 and XRCC1 in functions associated with BER (Frosina et al., 1996; Okano et al., 2003; Okano et al., 2005). This functional interaction partner of LIG3, also interacts with PCNA, the interaction partner of LIG1 during replication and the interaction that is thought to recruit LIG1 to the DNA replication forks. Therefore, we hypothesized that the recruitment of LIG3 to DNA replication sites is mediated through the interaction of XRCC1 with PCNA. To address this possibility, immunoprecipitation (IP) experiments were performed with WCEs of LIG1 proficient (HeLa) and LIG1 deficient (46BR 1N) human cells (Figure 45).

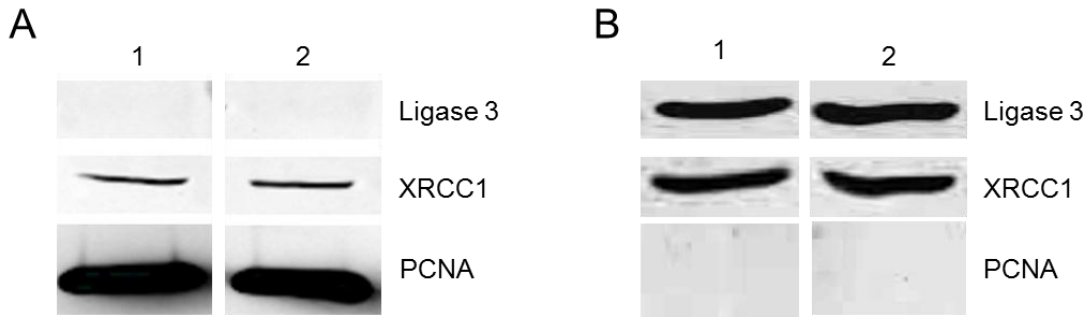

Figure 45: LIG3 and PCNA do not co-immunoprecipitate. 1 IP reactions with 46BR 1N WCE, **2** IP reactions with HeLa WCE **A)** IP reactions were performed with a monoclonal rabbit PCNA Ab (EPR3821 GeneTex). The membrane was probed with mouse anti-LIG3 (1F3 GeneTex), mouse anti-XRCC1 (33-2-5 Abcam) and mouse anti-PCNA (PC10). **B)** IP reactions were performed with a monoclonal mouse LIG3 Ab (1F3 GeneTex). The membrane was probed with mouse anti-LIG3 (1F3 GeneTex), rabbit anti-XRCC1 (GeneTex) and rabbit anti-PCNA (EPR3821 GeneTex) Ab.

The IP was performed with a monoclonal antibody (Ab) against LIG3, clone (1F3), and also with an Ab against PCNA, clone (EPR3821). In the IP reaction with the PCNA Ab, XRCC1 did co-immunoprecipitate with PCNA as expected, serving as a positive control for the IP reaction. In this reaction, there was no detectable signal for LIG3 (Figure 45A). In the IP reaction with the LIG3 Ab, XRCC1 was also co-immunoprecipitated, again, as expected, serving as positive control for the reaction. However, here again PCNA did not co-immunoprecipitate with LIG3 (Figure 45B). Surprisingly, there was no visible difference in the efficiency of co-IP between the cell lines tested either. This led to the hypothesis that LIG3 makes use of other proteins to function in DNA replication or that the replication functions of LIG3 do not require an interaction partner and are supported by the ZnFn domain instead.

4.2.2 The replication functions of LIG3 are dependent on both the BRCT and the ZnFn domains

The IP experiments did not allow conclusions about the mechanisms by which LIG3 substitutes for LIG1 functions during DNA replication. Therefore, we opted to identify the domains of LIG3 which are crucial for this function. For the purpose of these experiments, *LIG3*$^{-/M2}$*LIG1*$^{2loxP/-}$ cells were transfected with different constructs expressing the human LIG3α without the ZnFn (-ZnFn), and LIG3β in which the BRCT domain is missing anyway. The clones were selected for stable integration of the constructs and were tested for support of DNA replication by incubation of the cells with 4HT. Transfection with the *LIG3*β construct gave only one clone, while transfection with the construct encoding ZnFn free LIG3 gave 2 clones. PCR showed that none of these clones harbored a chromosome 8 targeted integration (data not shown). These clones were examined for expression of the corresponding protein by western blotting (Figure 46A). The results show that 2 of the clones showed 2 bands reacting with the anti-LIG3 Ab (Figure 46A). The lower bands probably represent the endogenous chicken LIG3α, which is also present in the wt and the parental cell lines. The upper bands in lanes 3 and 4 probably correspond to the overexpressed human LIG3β as their size matches the size of the purified

LIG3β protein, which was loaded as a control in lane 6. In lane 5, no additional band is detectable apart from the endogenous LIG3 band (Figure 46A).

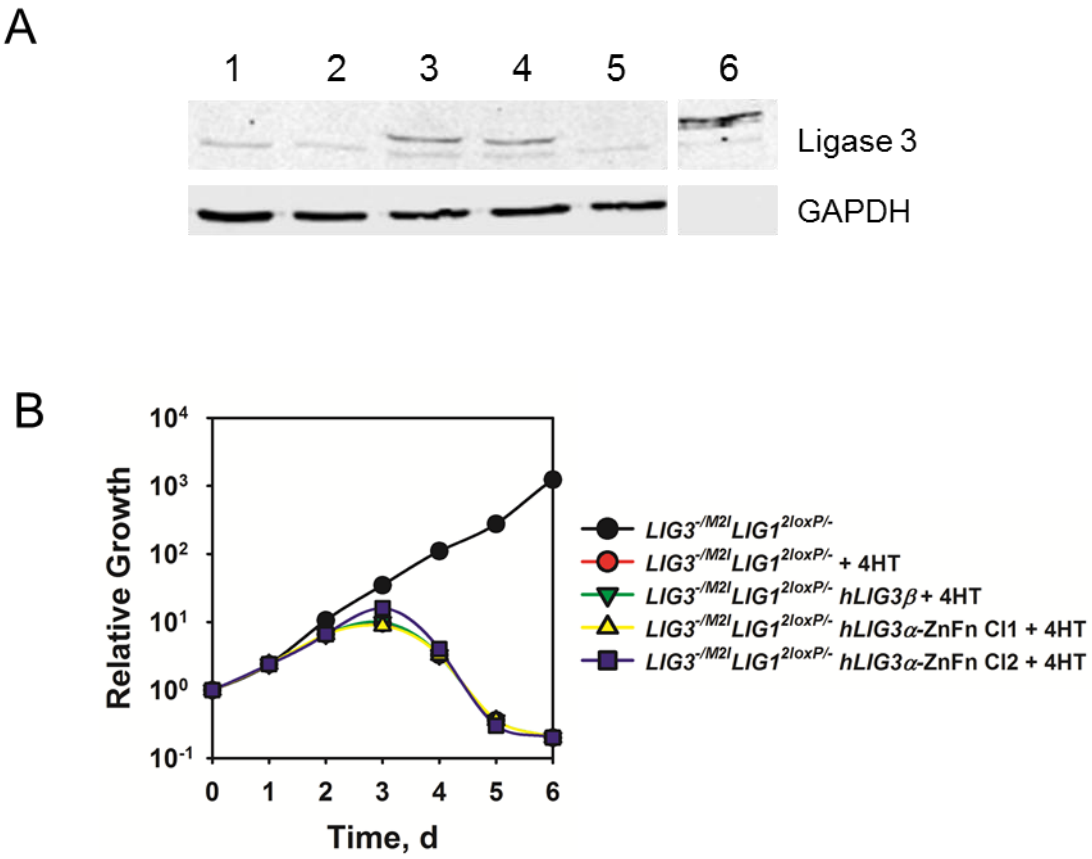

Figure 46: Characterization of *LIG3$^{-/M2}$LIG1$^{2loxP/-}$ hLIG3α* –ZnFn and of *LIG3$^{-/M2}$LIG1$^{2loxP/-}$ hLIG3β* clones. A) Western blot analysis of blasticidin resistant clones. The membrane was probed with a monoclonal mouse anti-LIG3 antibody (1F3) and a monoclonal mouse GAPDH antibody as loading control. **1.** 27 µg WCE from wt DT40 cells. **2.** 27 µg WCE from *LIG3$^{-/M2}$LIG1$^{2loxP/-}$*cells. **3.** 27 µg WCE from *LIG3$^{-/M2}$LIG1$^{2loxP/-}$ hLIG3β*.Cl1 cells. **4.** 27 µg WCE from *LIG3$^{-/M2}$LIG1$^{2loxP/-}$ hLIG3α*-ZnFn.Cl1 cells. **5.** 27 µg WCE from *LIG3$^{-/M2}$LIG1$^{2loxP/-}$ hLIG3α*-ZnFn.Cl2 cells. **6.** 24 ng purified human LIG3β. **B)** Growth kinetics of *LIG3$^{-/M2}$LIG1$^{2loxP/-}$* cells with and without 4HT treatment and clones expressing the different truncated versions of LIG3 after incubation with 4HT. Cells were daily diluted with fresh growth medium to keep them in the exponential growth phase. Growth is calculated normalized to the initial number of seeded cells.

The generated mutants were subsequently examined for sustained growth after treatment with 4HT to delete LIG1. Although the clone *LIG3$^{-/M2}$LIG1$^{2loxP/-}$ hLIG3α* –ZnFn.Cl2 did not express the truncated human LIG3α, it was included in the growth experiments to examine differences in the growth among clones following incubation with 4HT (Figure 46B). The results show that all mutants

had similar growth kinetics as the parental cell line (data not shown) and that all mutants did not survive incubation with 4HT just like the parental cell line (Figure 46B). Therefore, we conclude that LIG3 needs both the BRCT and the Zinc finger domains for its function in DNA replication. As XRCC1 interacts with the BRCT domain of LIG3 and is the only known interaction partner that uses this domain, the results essentiality suggest that XRCC1 might be involved in the replication function of LIG3, but not through an interaction with PCNA.

4.2.3 LIG3 is recruited to DNA replication sites when LIG1 is deleted

As there was no difference in the IP reactions between LIG1 wt and LIG1 mutated cell lines, we examined differences in protein localization and more specifically whether LIG3 and XRCC1 localization to replication sites changes in the presence of LIG1. Therefore, replication sites were visualized by pulse-labeling with 5-ethynyl-2'-deoxyuridine (EdU) and detected by Immunofluorescence (IF) together with LIG3, XRCC1 and PCNA. Unfortunately, this approach did not generate useful quantitative data due to the low signal to noise ratio for all Abs used, with the exception of PCNA antibody (data not shown).

To circumvent this problem live-cell imaging was introduced. For this purpose experiments were carried out with 46BR 1N cells transfected with plasmids expressing forms of LIG1, PCNA and XRCC1 tagged with different fluorescent proteins (LIG1-dsRed, PCNA-BFP and XRCC1-GFP). Before inception of imaging (24 h after transfection), the cells were also pulse-labeled with EdU for 1 h. Shorter pulses of EdU were also tried (20 min, 40 min) but did not yield satisfactory results in the 46BR 1N cells (data not shown). This might be due to the long generation time and the problems these cells have in the S-phase, as a 20 min pulse with EdU was sufficient for the control cell lines MRC5 SV and EM9.

The EdU labeled cells were subsequently stained with antibodies against EdU and GFP as the signal for GFP in contrast to BFP and dsRed was lost after fixation for unknown reasons.

Cells were either transfected with all 3 plasmids or only with the PCNA-BFP and the XRCC1-GFP plasmids to study the localization in a LIG1 mutant background as well as in the LIG1 corrected background. As expected, in the corrected background PCNA and LIG1 accumulate at sites of DNA replication marked by EdU. XRCC1 seems to be distributed throughout the nucleus with 60% co-localizing with the EdU signal (Figure 47A, C). While in the corrected cells, 67% of PCNA was found to co-localize with EdU, only 50% of total signal remained co-localized with EdU in 46BR 1N cells (Figure 47B, C). In the LIG1 mutated cells, however, a quite different distribution pattern was detected for XRCC1. The percentage of XRCC1 protein co-localizing with the EdU signal increases to 88% (Figure 47B, C). The MRC5 SV cell line and the EM9 cell line were also tested as a wt controls to examine whether the specific genetic background of the 46BR 1N cell line is the source of this interesting effect. We found that both cell lines showed a similar response (data not shown). It has to be mentioned, however, that only a small population of cells (approx. 5 per experiment, in 2 independent experiments) could be analyzed, as the cells had to express at least 2 of the fluorescent protein- tagged proteins in an analyzable amount and only S-phase cells could be used. Therefore it is necessary to increase the number of analyzed cells to get data which is statistically reliable.

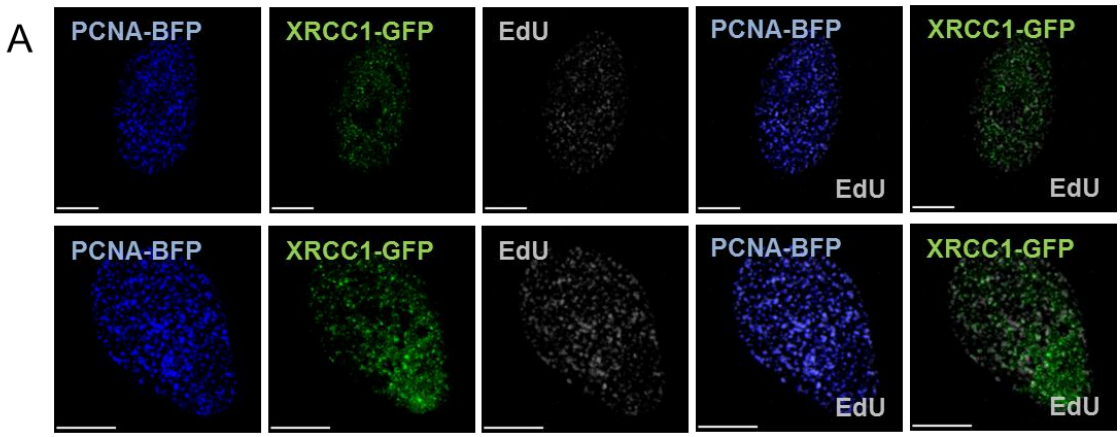

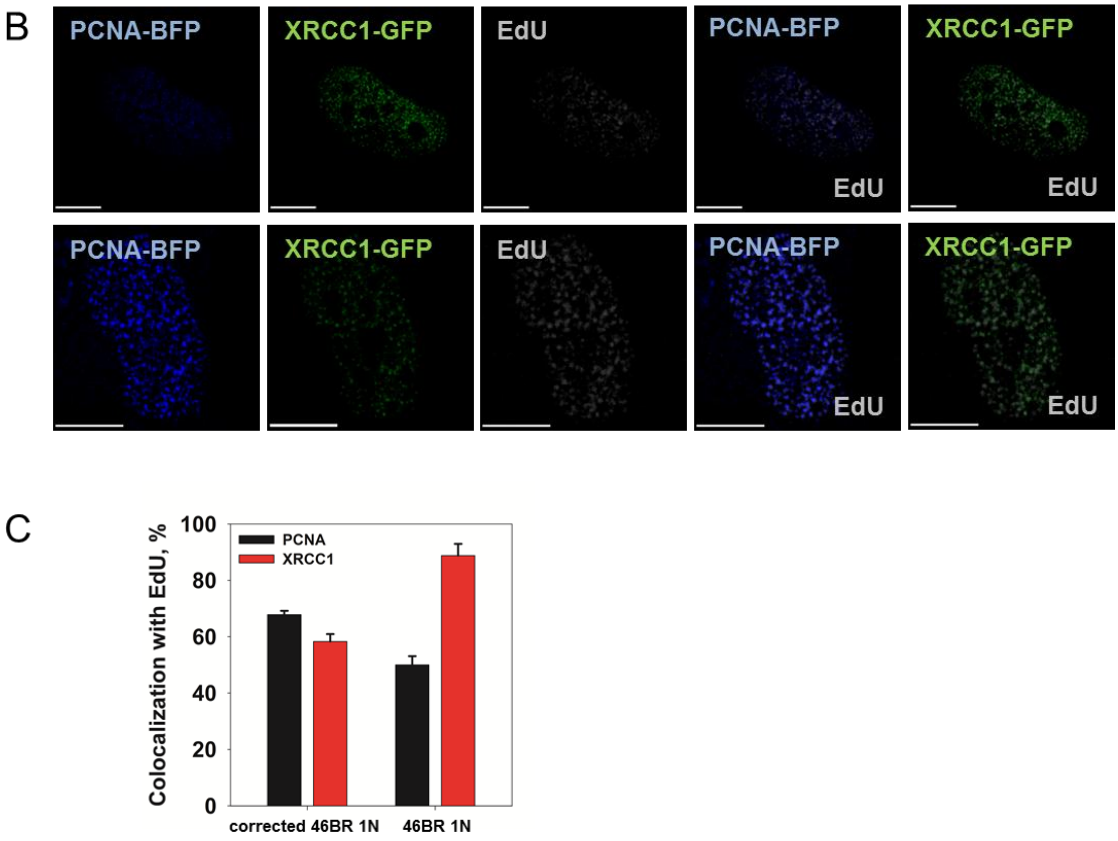

Figure 47: The localization of PCNA and XRCC1 changes depending on LIG1 functionality. A) Live cell imaging of PCNA-BFP, XRCC1-GFP and EdU in LIG1 corrected 46BR 1N cells. Twenty-four hours after transfection the cells were allowed to incorporate EdU for 1 h, fixed and stained for EdU and GFP. **B)** Localization of PCNA-BFP, XRCC1-GFP and EdU in 46BR 1N cells. Twenty-four hours after transfection the cells were allowed to incorporate EdU for 1 h, fixed and stained for EdU and GFP. **C)** Percentage of PCNA-BFP and XRCC1-GFP co-localizing with EdU in 46BR 1N cells and 46BR 1N cells transfected with a LIG1-dsRed expressing plasmid (corrected). Scale bar represents 10 µm.

Nevertheless, these results indicate that in a LIG1 mutated background, XRCC1 is recruited to the DNA replication sites, while the abundance of PCNA is reduced. Thus, interactions between ZnFn of LIG3 and an interaction with XRCC1 may co-operate to support DNA replication in LIG1 mutants.

4.3 Effects of DNA ligase knockout on DNA damage-induced cell cycle checkpoints in DT40 cells

4.3.1 Detection of S-phase checkpoint in DT40 cells

To further characterize the generated DT40 mutants we examined the impact of the various DNA ligase-knockouts on DNA damage-induced cell cycle checkpoints. To study the S-phase checkpoint, exponentially growing DT40 cells were exposed to different doses of ionizing radiation and were pulsed-labeled (15 min) with tritiated thymidine ([methyl-^{3}H]- thymidine) at different times thereafter. The degree of label incorporation reflects the DNA replication activity of the cell population at that time. To prevent DT40 cells to initiate apoptosis, a strong apoptosis inhibitor BOC-D-FMK was given 1h before irradiation. As the cells showed a pronounced accumulation in G2, the tritiated thymidine cpms were normalized to the percentage of S-phase cells (Figure 48A). We observed that after 10Gy of irradiation the replication activity of the tested cells dropped to 40% of the controls while cells exposed to 15Gy showed 80% reduction in replication activity 30 min later and did not show signs of recovery up to 8 h later (Figure 48 C). To examine whether this effect reflected a true checkpoint response 2 small molecule specific inhibitors of the major checkpoint kinases, ATR (VE-821) and ATM (Ku55933) were used. We reasoned that if the reduction in replication observed reflected the activation of the S-phase checkpoint, treatment with these inhibitors should cause a nearly complete recovery.

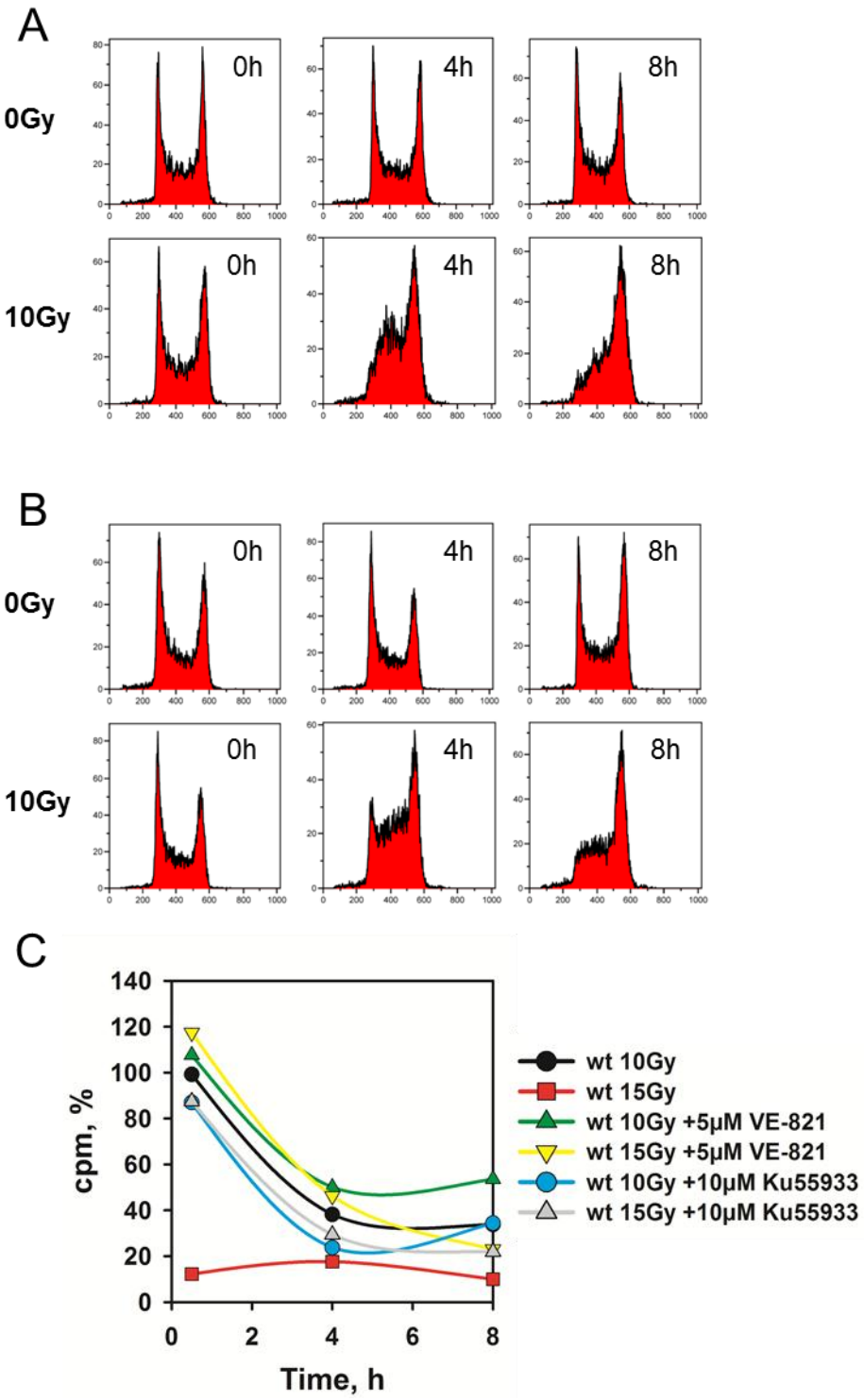

Figure 48: Study of the S-phase checkpoint in DT40 cells. A) Representative histograms of unirradiated and irradiated wt cells treated only with 50 µM BOC-F-CMK as a function of time. **B)** Representative cell cycle distribution of unirradiated and irradiated wt cells treated with 50 µM BOC-F-CMK and 5 µM VE-821 as a function of time. **C)** Incorporation of radioactive [methyl-^{3}H]-thymidine into DNA of wt cells during a 15 min pulse following the indicated treatments. All cells were treated with 50 µM BOC-F-CMK. The counts per minute (cpm) are plotted normalized to the 0Gy control at the same time point and with the same treatment.

The results obtained show that there was no significant effect from these inhibitors on the inhibition of DNA replication and accumulation of cells in G2 (Figure 48B, C). We concluded therefore that in DT40 cells a function S-phase checkpoint cannot be detected by the assays used. We postulate, though, that this observation does not reflect the absence of checkpoint response, but rather the difficulty to measure it as a result of the highly pro-apoptotic nature of DT40 cells that cause quick death in cells exposed to radiation – particularly the relatively high doses of radiation required to detect the S-phase checkpoint. The results obtained with the different ligase mutants did not differ much. The results with the *LIG1*$^{-/-}$, *LIG4*$^{-/-}$, *LIG1*$^{-/-}$*LIG4*$^{-/-}$ and *LIG3*$^{2loxP/-}$*LIG4*$^{-/-}$mts-h*LIG1* cells did show the same response. The replication activity drops to values between 40 and 20% dependent on the dose, but independent of the knockout and the cell lines tested all showed no recovery in the detected timeframe of 8 h (data not shown).

4.3.2 Knockout of various ligases does not have an effect on the G2-Checkpoint.

To further investigate the effects of DNA ligases knockout on DNA damage-induced cell cycle checkpoints, the induction of G2 checkpoint was investigated. For that purpose exponentially growing DT40 cells were exposed to different doses of irradiation and the cell cycle distribution was measured at different times thereafter. As with the results for the S-phase checkpoint, we observed that cells accumulated in G2. This accumulation could already be observed after 0.5Gy of ionizing radiation and after an exposure to 2Gy there was a higher percentage of G2 cells a few hours after irradiation in all cell lines tested.

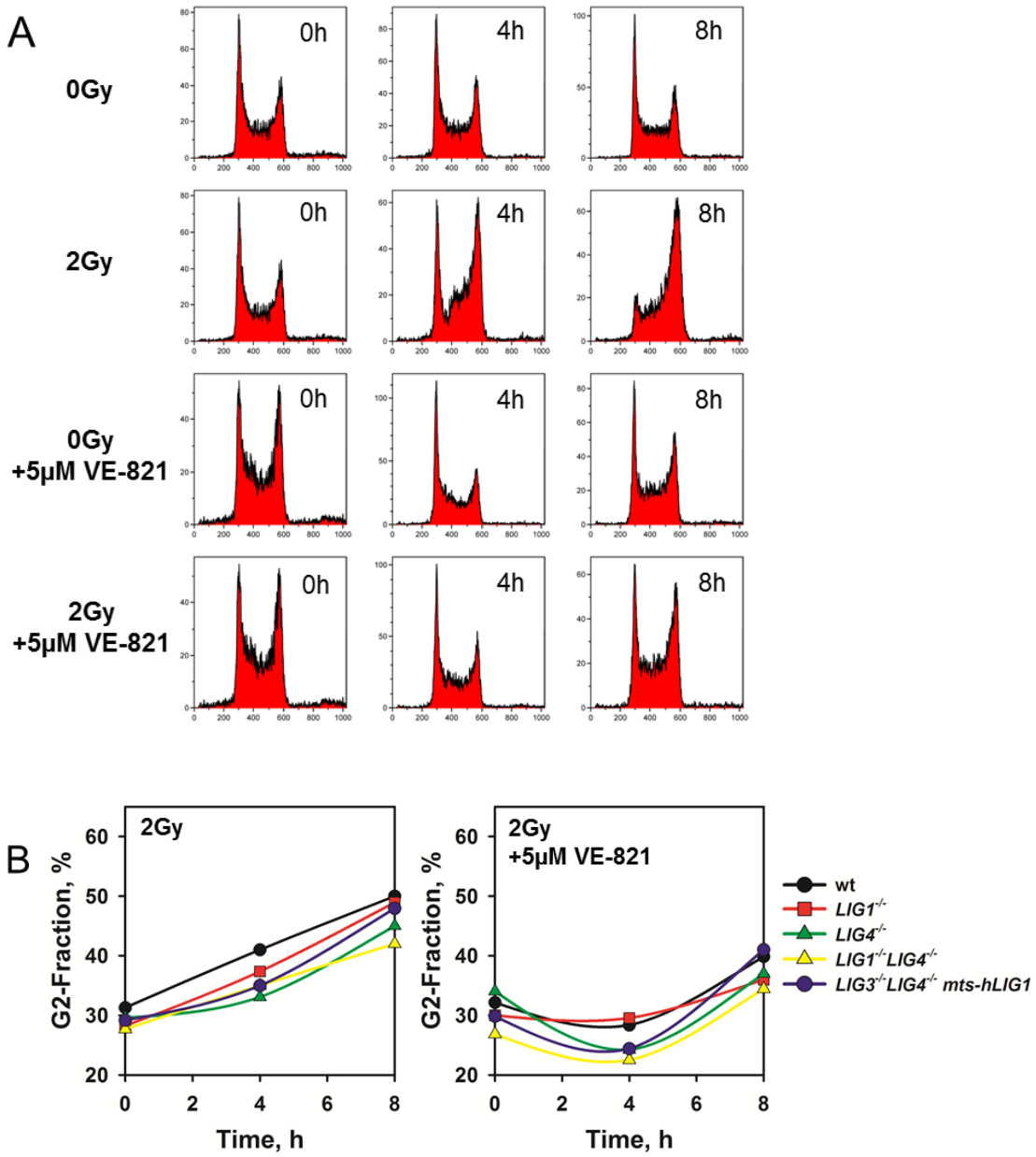

Figure 49: The development of the G2 checkpoint in DT40 cells is independent of ligase knockout. A) Representative histograms of DT40 wt cells with and without irradiation and with and without treatment with the ATR inhibitor VE-821 at different times after irradiation. **B)** Plot of G2 fraction of indicated mutants with and without treatment with VE-821

As it could not be excluded that cells arresting in G2 after radiation were in the process of undergoing apoptosis, which did not manifest due to the presence of the inhibitor, the effect of VE-821 was also tested (Figure 49). The results show that at these low doses of radiation the G2 checkpoint was indeed activated with similar kinetics in all cell lines tested (Figure 49B). This is demonstrated by the fact that the VE-821 inhibitor was, as expected in this case, able to abrogate

completely the associated accumulation of cells in the G2 phase of the cell cycle. Under these conditions, the fraction of G2 cells increased only approx. 10% as compared to the unirradiated controls. On the other hand, irradiated cells incubated without the inhibitor showed an increase in the G2 fraction by 50% at 8 h.

The slight increase in the G2 fraction observed in the presence of the ATR inhibitor might be due to dying cells, which accumulate with G2-like DNA content but are unable to further progress into mitosis (Figure 49). To test this, the percentage of apoptotic cells was analyzed by staining with DAPI and examining nuclear morphology (nuclear fragmentation) under a fluorescence microscope. Surprisingly, nearly all cells exposed to 2Gy of irradiation were observed to be apoptotic 24h later. This observation explains the incomplete abrogation of the G2 checkpoint with the ATR inhibitor and possibly also the defective recovery from this checkpoint. Interestingly, the *LIG1*$^{-/-}$, *LIG4*$^{-/-}$, *LIG1*$^{-/-}$*LIG4*$^{-/-}$ and *LIG3*$^{2loxP/-}$*LIG4*$^{-/-}$mts-h*LIG1* cells show a G2-checkpoint similar to that of the parental cell line. Although there seems to be a small effect with the *LIG1*$^{-/-}$*LIG4*$^{-/-}$ and *LIG3*$^{2loxP/-}$*LIG4*$^{-/-}$mts-h*LIG1* cells, this was not reproducible and in the 2 experiments there was no tendency for any cell line to show a stronger or weaker induction of the G2 checkpoint.

In aggregate, the above results suggest that the DT40 cells used in our study have a strong G2 checkpoint that is detectable after exposure to even low radiation doses. The knockout of one or more ligases does not seem to have a significant impact on this checkpoint.

5 Discussion

5.1 LIG3 supports DNA replication through its interaction with XRCC1, but not with PCNA

The importance of DNA ligases for the maintenance of the DNA metabolism has long been recognized and their contribution to replication, repair and recombination is documented and crucial for every organism. In spite of a large volume of information revealing the functions of these enzymes, it is clear that some of the family members are only partially characterized and their functions only incompletely understood.

Thus, in eukaryotes, the individual ligases may have overlapping activities and be not as functionally restricted as DNA ligases are in prokaryotes. In most prokaryotes and also in yeast the respective homolog of LIG1 is essential for cell survival and therefore its knockout is lethal. In higher eukaryotes on the other hand, there are clues that *LIG1* can be substituted by another ligase. The identity of this ligase, however, was unknown.

There have also been reports that LIG3 can assume work of LIG4 in double strand break repair, through a backup pathway of NHEJ, which was the first evidence that there is functional flexibility between eukaryotic ligases (Audebert et al., 2004; Cotner-Gohara et al., 2010; Liang et al., 2008; Rosidi et al., 2008; Wang et al., 2005; Wang et al., 2006). However, it should be emphasized that in the latter function LIG3 is integrated in completely different enzymatic machinery – it does not replace LIG4 in the enzymatic machinery of D-NHEJ. Very recent results have also demonstrated, that LIG1, the ligase mainly associated with DNA replication, is capable of sealing double strand breaks in the absence of LIG4 and LIG3 (Paul et al., 2013). These findings further emphasize the unexpected functional overlap between the 3 eukaryotic ligases (Paul et al., 2013).

The present thesis shows, with the help of a unique set of DT40 mutants, that the flexibility of the ligases is not limited to function in repair but also extends to DNA replication. A focus of the work was to also investigate the mechanism underpinnings of this flexibility.

Although the knockout of LIG4 is lethal in the late embryonic stages, LIG4 deficient mice have been generated by also deleting the p53 gene, which prevents massive p53-dependent neuronal apoptosis. Cell lines derived from such animals are growing well *in vitro* and have generation times similar to those of wt cells (Barnes et al., 1998; Frank et al., 1998; Frank et al., 2000; Gao et al., 2000; Gao et al., 1998; van Gent et al., 2001). In line with these results it could be shown that also in the DT40 system the knockout of LIG4 is not lethal. As expected, the replication functions of these mutants are not impaired and the maturation of Okazaki fragments remains intact. Surprisingly, the formation of SCEs is not significantly elevated in these mutants; a high number of SCEs is frequently considered as a marker for chromosomal instability (Carrano et al., 1978; Ellenberger and Tomkinson, 2008; Hoeijmakers, 2001). Certainly, it is possible that there are species specific differences in the induction of SCEs. Nevertheless, these results show that LIG4 deficient DT40 cells do not show signs of replication stress.

The knockout of LIG1, on the other hand, is potentially more directly associated with complications. Although there are human and mouse cell lines with impaired LIG1 activity, the complete knockout of *LIG1* could still have lethal consequences. In human cells there is a severe defect in Okazaki fragment ligation and the rate of spontaneous SCEs is also elevated 2.4 fold compared to the wt control (Bentley et al., 1996). Although in mouse cells the effect of LIG1 deficiency on Okazaki fragment maturation is significantly smaller, these cells show a defect in DNA replication. However, the level of SCEs remains unchanged upon the LIG1 knockout (Bentley et al., 1996). Surprisingly, LIG1 knockout in DT40 cells does not have consequences on any of the DNA replication related endpoints examined. The conditionally deficient cells showed no growth defect after induction of the knockout. Also, there was no change in the percentage of replicating cells and no effect on the maturation of Okazaki

fragments or the induction of SCEs. It cannot be ruled out of course that this lack of effect reflects a response of the DT40 cell system, particularly because effects are observed in the mouse and human systems (see above). However, there are also critical differences regarding the knockout strategy of the mouse, human and DT40 LIG1 mutant cell lines. Whereas in the DT40 system, the active site and also the whole catalytic core are completely removed, in both the mouse and the human systems there are only slight changes of those regions which lead to a functional LIG1 deficiency. In the mouse cells only the 3′ end of the gene was removed and although neither *LIG1* transcripts nor LIG1 protein could be detected in mutant embryos, it was suggested that the inactivation of the gene might not have been complete, mainly because the active site of the protein was not removed (Mackenney et al., 1997). The human cell line has a point mutation in both alleles of the *LIG1* gene, a C to T transition in the codon for Arg771, which causes this residue to be replaced by Trp (Barnes et al., 1992). This mutation does not decrease LIG1 expression, but the LIG1 activity is decreased to about 10% control, but is certainly not completely eliminated (Barnes et al., 1992). It is, therefore, possible that the effect in these mutants is not due to the knockout of LIG1 per se, but to a dominant negative effect of the mutated version of LIG1 on other ligases, like for example LIG3, that assumed the function of LIG1 when its activity is lost. It is possible that differences in the expression of such competing forms of LIG1 cause the differences in the magnitude of the defect, observed between mouse and human cells. Such complications are not likely with the DT40 cell system on the basis of the knockout strategy adopted. We consider therefore likely that we could show for the first time, in a genetically clean system that the knockout of LIG1 has no measurable effect on cell survival and replication in higher eukaryotes.

As the knockouts of LIG1 and LIG4 had no impact on DNA replication, the possibility arose that LIG3 has clear replicative functions in higher eukaryotes. However, the lethality observed upon knockout of this ligase hampered these investigations. It was therefore very important to demonstrate that this lethality is due to the mitochondrial functions of LIG3 and the cells could be rescued by just the mitochondrial version of this ligase or any other ligase which carries a mitochondrial leader sequence. In this way, it could be demonstrated that in the

presence of LIG1 the lethality observed upon LIG3 knockout was not due to any required and exclusive function of LIG3 in the cell nucleus. These results are in accordance with results obtained recently in the mouse system, where it was also shown that even ligases from viruses and bacteria can reverse the lethal LIG3 deficient phenotype (Gao et al., 2011; Simsek et al., 2011).

In other systems, however, cell survival is possible for several generations before the cells die, which could not be seen in the DT40 system where the cells undergo apoptosis directly following a decrease in LIG3 level (Gao et al., 2011). It can be speculated that this effect is due to the apoptosis-prone nature of the DT40 cell system, which tolerates far less stress than other cell systems before undergoing apoptosis. How a reduction in LIG3 levels initiates apoptosis remains to be elucidated.

Interestingly, in resting cells, LIG3 does not seem to be essential for maintaining the mitochondria, as monocytes have no detectable protein level of LIG3 and still intact mitochondria. It cannot be ruled out, however, that these cells have low levels of LIG3, as they have normal mRNA levels (Bauer et al., 2011; Bauer et al., 2012). These low levels of LIG3 might be sufficient for maintaining the mitochondrial genome as even low levels of LIG3 are able to support end-joining *in vivo* (Windhofer et al., 2007).

The direct lethality of DT40 upon LIG3 knockout, presumably due to mitochondria dysfunction is also questioned by the fact that cells without mitochondria can be generated by long-term treatment with low levels of ethidium bromide. It could also be shown that some cells tolerate the acute destruction of a fraction or even all of their mitochondria quite well (Alexeyev et al., 2013; Leibowitz, 1971). Therefore, we propose that additional mechanisms that remain to be elucidated underpin the fast lethality observed upon LIG3 knockout in DT40 cells.

Altogether, the results presented in this thesis show in a genetically “clean” manner that knockout of any of the 3 DNA ligases can be tolerated in higher eukaryotes and that single ligase depleted cells retain nearly normal DNA replication activity. Thus, there is a hitherto unexpected functional flexibility

between LIG1 and LIG3 in supporting DNA replication. Moreover, all 3 DNA ligases seem to be capable in supporting the diverse DNA repair functions of the cells.

With the help of double mutants and also with the mono-ligase systems the functional flexibility of the ligases could be evaluated in more detail. For the first time it could be shown that LIG4 is not capable to compensate for LIG1 in replication and that cells left with solely LIG4 as nuclear ligase are not viable although the mitochondria are rescued. The cells with mitochondrial LIG3 and an inducible knockout for LIG1 die sooner than the single knockout of LIG3, which suggests that optimal DNA replication requires a relatively high level of one replicative DNA ligase.

The knock-in of human LIG1 with a mitochondrial leader sequence created a system with only LIG1 left to maintain both the replication functions and the mitochondrial integrity (Paul et al., 2013). This mutant clearly showed that LIG3 has no essential function in the nucleus in the presence of LIG1. The cells proliferate even faster than the parental cell line and the fraction of actively replicating cells is also higher. Although LIG3 has been implicated in the maintenance of genomic stability, no elevated level of SCEs in the DT40 LIG3 knockout cells was found (McVey and Lee, 2008; Nussenzweig and Nussenzweig, 2007). These results in the DT40 system are in line with other studies in the mouse system, where similar observations were made (Simsek et al., 2011).

The double knockout of LIG1 and LIG4 resulted in viable clones with growth kinetics similar to the wt. The replication functions of these mutants were not changed significantly and the rate of spontaneously induced SCEs was comparable to those with only LIG4 knockout. It was also astonishing that these cells showed no defect in Okazaki fragment maturation. The results obtained with these mutants show clearly the remarkable ability of LIG3 to cope with all replication functions of LIG1, even independently of LIG4. This functional flexibility is not unexpected, as in DNA-bound state, LIG1 and LIG3 share a similar structure, forming a ring that encircles the DNA (Ellenberger and Tomkinson, 2008; Pascal et al., 2004). Also, the functional overlap in NER, the

great flexibility in the substrate choice and its unique ZnFn domain make LIG3 the obvious and ideal backup-candidate for LIG1 (Cotner-Gohara et al., 2010; Ellenberger and Tomkinson, 2008; Tomkinson and Mackey, 1998).

It is well known that LIG1 becomes integrated into DNA replication centers through interaction with PCNA (Cardoso et al., 1997; Montecucco et al., 1998; Montecucco et al., 1995). However, it remains open how LIG3 is incorporated in replication centers, but the known interaction of its closest interaction partner, XRCC1, with PCNA offers testable possibilities (Fan et al., 2004). In our experiments, there was no interaction to be seen between PCNA and LIG3 as detected by immunoprecipitation. These results confirmed the expected interaction between both PCNA and LIG3 with XRCC1 but fail to reveal any interaction whether direct or indirect with each other. Nevertheless, it is possible that PCNA and LIG3 interact indirectly with each other through XRCC1, as they do not share the same binding site, but that the sensitivity of the co-immunoprecipitation is not sufficient to detect this interaction - which is likely to occur only in S-phase. Interestingly, there was no difference between LIG1 mutated and LIG1 wt cells in signal strength for these immunoprecipitations. Overall, these results make it unlikely that there is a direct interaction between PCNA and LIG3.

The unique ZnFn domain of LIG3 makes it possible that, as proposed in the jack-knife model, LIG3 is able to do even intermolecular ligation without the help of an interaction partner (Cotner-Gohara et al., 2010). It was, therefore, worth investigating if the replication functions of LIG3 can be accomplished without the protein-protein interaction BRCT domain, or without the ZnFn domain. The experiments revealed that both the ZnFn and the BRCT domains are essential for the DNA replication functions of LIG3 in DT40. The same truncated mutants were used in the mouse system to rescue the mitochondrial functions of LIG3. However, these mutants could maintain the mitochondrial integrity, which was not unexpected, as even viral and bacterial ligases are able to rescue the mitochondria function (Simsek et al., 2011). These results show that the unique ZnFn domain of LIG3 is essential for DNA replication and that presumably the interaction with XRCC1 is also crucial for that function. Apart from giving a

deeper understanding of the functional principles underpinning the replication functions of LIG3, these results also give clues as to why LIG4 is not able to support DNA replication: it lacks the ZnFn domain.

The colocalization studies in both LIG1 mutated and LIG1 proficient cells revealed quite interesting phenomena. In LIG1 proficient cells, the distribution of the proteins studied is as expected: LIG1 and PCNA form foci at sites of ongoing replication that are marked by EdU, while XRCC1 is distributed throughout the nucleus. The distribution pattern of XRCC1 changes when LIG1 is mutated. In this case 88% of the XRCC1 protein colocalizes with EdU, which is 28% more than in the control cell lines. The fraction of PCNA colocalizing with EdU drops down by 18% to 50%. This shows that XRCC1 and with it most likely LIG3 as well, is recruited to replication sites more intensively in the absence of LIG1.

It is still possible that this recruitment is mediated by PCNA, but as the colocalization of PCNA with replication centers decreases in the absence of LIG1 it is unlikely that the replication center in which LIG3 is involved will be identical to the replication centers forming in the presence of LIG1. However, it is also possible that our observations reflect quantitative rather than qualitative differences, i.e. PCNA is still present at all DNA replication centers but at lower amounts in the absence of LIG1 that reduce its detectability by IF and live cell imaging.

The results presented here show clearly that, in the absence of LIG1, LIG3 is recruited to sites of replication due to its interaction with XRCC1. Therefore this interaction is crucial for maintaining the replication functions of LIG3. It would be interesting to examine whether other replication factors normally involved in the maturation of Okazaki fragments, like FEN1 or pol δ, are involved in this process in the absence of LIG1.

5.2 Influence of ligase knockout on DNA damage-induced cell cycle checkpoints in DT40 cells.

To further characterize the ligase mutants generated as part of this work, we studied the effect of a specific DNA ligase knockout on the activation of DNA damage-induced cell cycle checkpoints. Surprisingly, while DNA replication was promptly reduced in irradiated DT40 and their ligase deficient mutants, signs of recovery were not visible up to 8 h later. However, since this response could not be abrogated by an ATR or an ATM inhibitor, we conclude that it does not reflect the activation of the DNA damage checkpoint, but rather the irreversible entrance of the cell into a program of apoptosis. This is because either inhibitor should, if not completely abolish, at least diminish the effect of a checkpoint.

To study a possible role of apoptosis in the response, the above experiment was also performed without the caspase inhibitor to exclude side effects of the inhibitor on the endpoint measured. Although the results obtained were similar in that they showed the drop down in replication activity and no recovery, the cells started to die in this case 4 h postirradiation. Indeed, the FACS histograms could not be analyzed starting from the early time points due to an abnormal DNA content distribution and a high sub-G1 fraction, which made the normalization to the fraction of S-phase cells impossible. This observation also explains why in these cells the development of a normal S-phase checkpoint could not be studied. At the high doses used in these experiments, programmed cell death is induced soon after irradiation, and either prevents the development of a checkpoint response, or compromises our ability to detect it. Indeed, staining of nuclei 24 h after irradiation with only 2Gy revealed only fragmented nuclei. This response is ingrained in the nature of DT40 cells, which are B cell lymphocytes. Undergoing programmed cell death is an important physiological characteristic of this cell type, as B cell lymphocytes are regularly exchanged and repair of DNA damage may not be as crucial.

Interestingly however, cells in the G1 phase of the cell cycle seem to be able to enter S-phase as the G1 peak is significantly lower after 4h and absent after 8 h. It is not obvious, however, what the fate of the G1 population is. There is no

peak at the beginning of the S-phase suggesting G1 cells leaving G1 and entering S are unable to proceed beyond a certain point in the S-phase. Notably, elutriated G1 cells irradiated with 10Gy do not leave G1 phase for at least 6 h.

The G2 checkpoint could be detected at lower doses of radiation and was found to be functional in DT40 cells and their DNA ligase mutant derivatives. The cells accumulated in G2 phase as expected. Surprisingly, even a dose of 0.5Gy was sufficient to induce the checkpoint. In contrast to the S-phase checkpoint, the G2 checkpoint could be abrogated with the ATR inhibitor VE-821, which shows that the response in this case is really checkpoint related. The remaining 10% increase is most likely due to cells undergoing apoptosis as explained under Results. An effect of any of the DNA ligase knockout on the accumulation of cells in G2 phase could not be found. It could have been suspected that LIG4 knockout cells might show some differences as the repair deficiency in this case is quite pronounced (Paul et al., 2013). It is possible, however, that this defect will not affect the initiation of the checkpoint response measured here, but rather its duration.

In summary, our observation show that DT40 cells are not are not suitable for studying the intra S-phase checkpoint, but could be a useful tool for studying G2 checkpoint response on various genetic backgrounds.

6 Summary

The results show a remarkable and hitherto unexpected functional flexibility in DNA replication of LIG1 and LIG3 in vertebrates.

While the lethality of the LIG3 knockout is solely due to the mitochondrial function and not due to an essential function in the nucleus, it was conclusively shown that LIG3 can backup replication in the absence of LIG1 and that LIG4 is not capable to do so.

The results in this thesis conclusively show that the ZnFn domain of LIG3 is essential for the DNA replication function of LIG3, although it is not essential for maintaining mitochondrial integrity. Furthermore, the BRCT domain with which LIG3 interacts with XRCC1 is also essential for the replication function of LIG3.

In colocalization experiments it could be shown that LIG3 is recruited to DNA replication sites when LIG1 activity is impaired, and that the recruitment of PCNA is weakened. The results, therefore, point to a different recruitment system of LIG3 to replication factories compared to the one required for LIG1 recruitment.

Furthermore the mutants used were characterized with regard to their ability to activate checkpoint responses after induction of DNA damage. Apoptosis complicates analysis of the S-phase checkpoint which requires high doses of radiation for reliable quantification. On the other hand, DT40 cells display a normal G2 checkpoint that remains unaffected by ligase deletion.

7 References

Aboussekhra, A., Biggerstaff, M., Shivji, M.K.K., Vilpo, J.A., Moncollin, V., Podust, V.M., Protic, M., Huebscher, U., Egly, J.-M., and Wood, R.D. (1995). Mammalian DNA nucleotide excision repair reconstituted with purified protein components. Cell *80*, 859-868.

Aguilera, A., and Gomez-Gonzales, B. (2008). Genome instability: a mechanistic view of its causes and consequences. Nature Reviews Genetics *9*, 204-217.

Alexeyev, M., Shokolenko, I., Wilson, G., and LeDoux, S. (2013). The Maintenance of Mitochondrial DNA Integrity—Critical Analysis and Update. Cold Spring Harbor Perspectives in Biology *5*, a012641.

Arakawa, H., Bednar, T., Wang, M., Paul, K., Mladenov, E., Bencsik-Theilen, A.A., and Iliakis, G. (2012). Functional redundancy between DNA ligases I and III in DNA replication in vertebrate cells. Nucleic Acids Research *40*, 2599-2610.

Arakawa, H., Hauschild, J., and Buerstedde, J.-M. (2002). Requirement of the Activation-Induced Deaminase (AID) Gene for Immunoglobulin Gene Conversion. Science *295*, 1301-1306.

Arakawa, H., Lodygin, D., and Buerstedde, J.-M. (2001). Mutant lox P vectors for selectable marker recycle and conditional knockouts. BMC Biotechnology *1*, 7.

Audebert, M., Salles, B., and Calsou, P. (2004). Involvement of Poly(ADP-ribose) Polymerase-1 and XRCC1/DNA Ligase III in an Alternative Route for DNA Double-strand Breaks Rejoining. Journal of Biological Chemistry *279*, 55117-55126.

Balakrishnan, L., and Bambara, R.A. (2011). Eukaryotic Lagging Strand DNA Replication Employs a Multipathway Mechanism That Protects Genome Integrity. Journal of Biological chemistry *286*, 6865-6870.

Balakrishnan, L., Gloor, J.W., and Bambara, R.A. (2010). Reconstitution of eukaryotic lagging strand DNA replication. Methods *51*, 347-357.

Barnes, D.E., and Lindahl, T. (2004). Repair and Genetic Consequences of Endogenous DNA Base Damage in Mammalian Cells. Annual Review of Genetics *38*, 445-476.

Barnes, D.E., Stamp, G., Rosewell, I., Denzel, A., and Lindahl, T. (1998). Targeted disruption of the gene encoding DNA ligase IV leads to lethality in embryonic mice. Current Biology *8*, 1395-1398.

Barnes, D.E., Tomkinson, A.E., Lehmann, A.R., Webster, A.D.B., and Lindahl, T. (1992). Mutations in the DNA ligase 1 gene of an individual with immunodeficiencies and cellular hypersensitivity to DNA-damaging agents. Cell *69*, 495-503.

Bassing, C.H., and Alt, F.W. (2004). The cellular response to general and programmed DNA double strand breaks. DNA Repair *3*, 781-796.

Bauer, M., Goldstein, M., Christmann, M., Becker, H., Heylmann, D., and Kaina, B. (2011). Human monocytes are severely impaired in base and DNA double-strand break repair that renders them vulnerable to oxidative stress. Proceedings of the National Academy of Sciences of the United States of America *108*, 21105-21110.

Bauer, M., Goldstein, M., Heylmann, D., and Kaina, B. (2012). Human Monocytes Undergo Excessive Apoptosis following Temozolomide Activating the ATM/ATR Pathway While Dendritic Cells and Macrophages Are Resistant. PLoS ONE *7*, e39956.

Bentley, D.J., Harrison, C., Ketchen, A.-M., Redhead, N.J., Samuel, K., Waterfall, M., Ansell, J.D., and Melton, D.W. (2002). DNA ligase I null mouse cells show normal DNA repair activity but altered DNA replication and reduced genome stability. Journal of Cell Science *115*, 1551-1561.

Bentley, D.J., Selfridge, J., Millar, J.K., Samuel, K., Hole, N., Ansell, J.D., and Melton, D.W. (1996). DNA ligase I is required for fetal liver erythropoiesis but is not essential for mammlian cell viability. Nature Genetics *13*, 489-491.

Bork, P., Hofmann, K., Bucher, P., Neuwald, A.F., Altschul, S.F., and Koonin, E.V. (1997). A superfamily of conserved domains in DNA damage-responsive cell cycle checkpoint proteins. FASEB Journal *11*, 68-76.

Branzei, D., and Foiani, M. (2008). Regulation of DNA repair throughout the cell cycle. Nature Reviews Molecular Cell Biology *9*, 297-308.

Brown, E.J., and Baltimore, D. (2000). *ATR* disruption leads to chromosomal fragmentation and early embryonic lethality. Genes & Development *14*, 397-402.

Bryans, M., Valenzano, M.C., and Stamato, T.D. (1999). Absence of DNA ligase IV protein in XR-1 cells: Evidence for stabilization by XRCC4. Mutation Research *433*, 53-58.

Burgers, P.M.J. (2009). Polymerase Dynamics at the Eukaryotic DNA Replication Fork. Journal of Biological chemistry *284*, 4041-4045.

Caldecott, K., Tucker, J.D., Stanker, L.H., and Thompson, L.H. (1995). Characterization of the XRCC1-DNA ligase III complex in vitro and its absence from mutant hamster cells. Nucleic Acids Research *23*, 4836-4843.

Caldecott, K.W. (2003). XRCC1 and DNA strand break repair. DNA Repair *2*, 955-969.

Caldecott, K.W., McKeown, C.K., Tucker, J.D., Ljungquist, S., and Thompson, L.H. (1994). An Interaction between the Mammalian DNA Repair Protein XRCC1 and DNA Ligase III. Molecular and Cellular Biology *14*, 68-76.

Cardoso, M.C., Joseph, C., Rahn, H.-P., Reusch, R., Nadal-Ginard, B., and Leonhardt, H. (1997). Mapping and Use of a Sequence that Targets DNA Ligase I to Sites of DNA Replication In Vivo. Journal of Cell Biology *139*, 579-587.

Carrano, A.V., Thompson, L.H., Lindl, P.A., and Minkler, J.L. (1978). Sister chromatid exchange as an indicator of mutagenesis. Nature *271*, 551-553.

Chen, L., Trujillo, K., Sung, P., and Tomkinson, A.E. (2000). Interactions of the DNA Ligase IV-XRCC4 Complex with DNA Ends and the DNA-dependent Protein Kinase. Journal of Biological Chemistry *275*, 26196-26205.

Costanzo, V., Robertson, K., Ying, C.Y., Kim, E., Avvedimento, E., Gottesman, M., Grieco, D., and Gautier, J. (2000). Reconstitution of an ATM-dependent checkpoint that inhibits chromosomal DNA replication following DNA damage. Molecular Cell *6*, 649-659.

Cotner-Gohara, E., Kim, I.-K., Hammel, M., Tainer, J.A., Tomkinson, A.E., and Ellenberger, T. (2010). Human DNA Ligase III Recognizes DNA Ends by Dynamic Switching between Two DNA-Bound States. Biochemistry *49*, 6165-6176.

Cotner-Gohara, E., Kim, I.-K., Tomkinson, A.E., and Ellenberger, T. (2008). Two DNA-binding and Nick Recognition Modules in Human DNA Ligase III. Journal of Biological Chemistry *283*, 10764-10772.

Critchlow, S.E., Bowater, R.P., and Jackson, S.P. (1997). Mammalian DNA double-strand break repair protein XRCC4 interacts with DNA ligase IV. Current Biology *7*, 588-598.

De, A., and Campbell, C. (2007). A novel interaction between DNA ligase III and DNA polymerase γ plays an essential role in mitochondrial DNA stability. Biochemical Journal *402*, 175-186.

de Klein, A., Muijtjens, M., van Os, R., Verhoeven, Y., Smit, B., Carr, A.M., Lehmann, A.R., and Hoeijmakers, J.H.J. (2000). Targeted disruption of the cell-cycle checkpoint gene ATR leads to early embryonic lethality in mice. Current Biology *10*, 479-482.

Dulic, A., Bates, P.A., Zhang, X., Martin, S.R., Freemont, P.S., Lindahl, T., and Barnes, D.E. (2001). BRCT Domain Interactions in the Heterodimeric DNA Repair Protein XRCC! - DNA Ligase III. Biochemistry *40*, 5906-5913.

Ellenberger, T., and Tomkinson, A.E. (2008). Eukaryotic DNA Ligases: Structural and Functional Insights. Annual Review of Biochemistry *77*, 313-338.

Fan, J., Otterlei, M., Wong, H.-K., Tomkinson, A.E., and Wilson III, D.M. (2004). XRCC1 co-localizes and physically interacts with PCNA. Nucleic Acids Research *32*, 2193-2201.

Ferrari, G., Rossi, R., Arosio, D., Vindigni, A., Biamonti, G., and Montecucco, A. (2003). Cell Cycle-dependent Phosphorylation of Human DNA Ligase I at the Cyclin-dependent Kinase Sites. Journal of Biological Chemistry *278*, 37761-37767.

Frank, K.M., Sekiguchi, J.M., Seidl, K.J., Swat, W., Rathbun, G.A., Cheng, H.-L., Davidson, L., Kangaloo, L., and Alt, F.W. (1998). Late embryonic lethality and impaired *V*(D)*J* recombination in mice lacking DNA ligase IV. Nature *396*, 173-177.

Frank, K.M., Sharpless, N.E., Gao, Y., Sekiguchi, J.M., Fergson, D.O., Zhu, C., Manis, J.P., Horner, J., DePinho, R.A., and Alt, F.W. (2000). DNA ligase IV deficiency in mice leads to defective neurogenesis and embryonic lethality via the p53 pathway. Molecular Cell *5*, 993-1002.

Friedberg, E.C. (2003). DNA damage and repair. Nature *421*, 436-440.

Frosina, G., Fortini, P., Rossi, O., Carrozzino, F., Raspaglio, G., Cox, L.S., Lane, D.P., Abbondandolo, A., and Dogliotti, E. (1996). Two Pathways for Base Excision Repair in Mammalian Cells. Journal of Biological Chemistry *271*, 9573-9578.

Gao, Y., Ferguson, D.O., Xie, W., Manis, J.P., Sekiguchi, J.A., Frank, K.M., Chaudhuri, J., Horner, J., DePinho, R.A., and Alt, F.W. (2000). Interplay of p53 and DNA-repair protein XRCC4 in tumorigenesis, genomic stability and development. Nature *404*, 897-900.

Gao, Y., Katyal, S., Lee, Y., Zhao, J., Rehg, J.E., Russell, H.R., and McKinnon, P.J. (2011). DNA ligase III is critical for mtDNA integrity but not Xrcc1-mediated nuclear DNA repair. Nature *471*, 240-244.

Gao, Y., Sun, Y., Frank, K.M., Dikkes, P., Fujiwara, Y., Seidl, K.J., Sekiguchi, J.M., Rathbun, G.A., Swat, W., Wang, J.*, et al.* (1998). A Critical Role for DNA End-Joining Proteins in Both Lymphogenesis and Neurogenesis. Cell *95*, 891-902.

Gloor, J.W., Balakrishnan, L., and Bambara, R.A. (2010). Flap endonuclease 1 mechanism analysis indicates flap base binding prior to threading. Journal of Biological chemistry *285*, 34922-34931.

Grawunder, U., Wilm, M., Wu, X., Kulesza, P., Wilson, T.E., Mann, M., and Lieber, M.R. (1997). Activity of DNA ligase IV stimulated by complex formation with XRCC4 protein in mammalian cells. Nature *388*, 492-495.

Grawunder, U., Zimmer, D., Fugmann, S., Schwarz, K., and Lieber, M.R. (1998a). DNA ligase IV is essential for V(D)J recombination and DNA double-strand break repair in human precursor lymphocytes. Molecular Cell *2*, 477-484.

Grawunder, U., Zimmer, D., and Lieber, M.R. (1998b). DNA ligase IV binds to XRCC4 via a motif located between rather than within its BRCT domains. Current Biology *8*, 873-876.

Gu, J., Lu, H., Tippin, B., Shimazaki, N., Goodman, M.F., and Lieber, M.R. (2007). XRCC4: DNA ligase IV can ligate incompatible DNA ends and can ligate across gaps. EMBO Journal *26*, 1010-1023.

Harrison, J.C., and Haber, J.E. (2006). Surviving the breakup: the DNA damage checkpoint. Annual Review of Genetics *40*, 209-235.

Hartwell, L.H. (1974). Saccharomyces cerevisiae cell cycle. Bacteriological Reviews *38*, 164-198.

Hartwell, L.H., and Kastan, M.B. (1994). Cell cycle control and cancer. Science *266*, 1821-1828.

Henderson, L.M., Arlett, C.F., Harcourt, S.A., Lehmann, A.R., and Broughton, B.C. (1985). Cells from an immunodeficient patient (46BR) with a defect in DNA ligation are hypomutable but hypersensitive to the induction of sister chromatid

exchanges. Proceedings of the National Academy of Sciences of the United States of America *82*, 2044-2048.

Hoeijmakers, J.H.J. (2001). Genome maintenance mechanisms for preventing cancer. Nature *411*, 366-374.

Hsu, H.-L., Yannone, S.M., and Chen, D.J. (2002). Defining interactions between DNA-PK and ligase IV/XRCC4. DNA Repair *1*, 225-235.

Huschtscha, L.I., and Holliday, R. (1983). Limited and unlimited growth of SV40-transformed cells from human diploid MRC-5 fibroblasts. Journal of Cell Science *63*, 77-99.

Johnston, L.H. (1979). The DNA Repair Capability of *cdc9*, the *Saccharomyces cerevisiae* Mutant Defective in DNA Ligase. Molecular & General Genetics *170*, 89-92.

Johnston, L.H., and Nasmyth, K.A. (1978). *Saccharomyces cerevisiae* cell cycle mutant *cdc9* is defective in DNA ligase. Nature *274*, 891-893.

Kelman, Z. (1997). PCNA: structure, functions and interactions. Oncogene *14*, 629-640.

Kysela, B., Doherty, A.J., Chovanec, M., Stiff, T., Ameer-Beg, S.M., Vojnovic, B., Girard, P.-M., and Jeggo, P.A. (2003). Ku Stimulation of DNA Ligase IV-dependent Ligation Requires Inward Movement along the DNA Molecule. Journal of Biological Chemistry *278*, 22466-22474.

Lakshmipathy, U., and Campbell, C. (1999). The Human DNA Ligase III Gene Encodes Nuclear and Mitochondrial Proteins. Molecular and Cellular Biology *19*, 3869-3876.

Lee, Y., Barnes, D.E., Lindahl, T., and McKinnon, P.J. (2000). Defective neurogenesis resulting from DNA ligase IV deficiency requires Atm [In Process Citation]. Genes & Development *14*, 2576-2580.

Lehman, I.R. (1974). DNA ligase: Structure, mechanism, and function. Science *186*, 790-797.

Leibowitz, R.D. (1971). The effect of ethidium bromide on mitochondrial DNA synthesis and mitochondrial DNA structure in HeLa cells. Journal of Cell Biology *51*, 116-122.

Levin, D.S., Bai, W., Yao, N., O'Donnell, M., and Tomkinson, A.E. (1997). An interaction between DNA ligase I and proliferating cell nuclear antigen: Implications for Okazaki fragment synthesis and joining. Proceedings of the National Academy of Sciences of the United States of America *94*, 12863-12868.

Levin, D.S., McKenna, A.E., Motycka, T.A., Matsumoto, Y., and Tomkinson, A.E. (2000). Interaction between PCNA and DNA ligase I is critical for joining of Okazaki fragments and long-patch base-excision repair. Current Biology *10*, 919-922, S911-S912.

Levin, D.S., Vijayakumar, S., Liu, X., Bermudez, V.P., Hurwitz, J., and Tomkinson, A.E. (2004). A Conserved Interaction between the Replicative Clamp Loader and DNA Ligase in Eukaryotes: IMPLICATIONS FOR OKAZAKI FRAGMENT JOINING. Journal of Biological Chemistry *279*, 55196-55201.

Li, X., Li, J., Harrington, J., Lieber, M.R., and Burgers, P.M.J. (1995). Lagging Strand DNA Synthesis at the Eukaryotic Replication Fork Involves Binding and Stimulation of FEN-1 by Proliferating Cell Nuclear Antigen. Journal of Biological chemistry *270*, 22109-22112.

Liang, L., Deng, L., Nguyen, S.C., Zhao, X., Maulion, C.D., Shao, C., and Tischfield, J.A. (2008). Human DNA ligases I and III, but not ligase IV, are required for microhomology-mediated end joining of DNA double-strand breaks. Nucleic Acids Research *36*, 3297-3310.

Lindahl, T., and Barnes, D.E. (1992). Mammalian DNA ligases. Annual Review of Biochemistry *61*, 251-281.

Lönn, U., Lönn, S., Nylen, U., and Winblad, G. (1989). Altered formation of DNA replication intermediates in human 46 BR fibroblast cells hypersensitive to 3-aminobenzamide. Carcinogenesis *10*, 981-985.

Mackenney, V.J., Barnes, D.E., and Lindahl, T. (1997). Specific Function of DNA Ligase I in Simian Virus 40 DNA Replication by Human Cell-free Extracts Is Mediated by the Amino-terminal Non-catalytic Domain. Journal of Biological Chemistry *272*, 11550-11556.

Mackey, Z.B., Niedergang, C., Menissier-de Murcia, J., Leppard, J., Au, K., Chen, J., de Murcia, G., and Tomkinson, A.E. (1999). DNA Ligase III Is Recruited to DNA Strand Breaks by a Zinc Finger Motif Homologous to That of Poly (ADP-ribose) Polymerase. Journal of Biological Chemistry *274*, 21679-21687.

Mackey, Z.B., Ramos, W., Levin, D.S., Walter, C.A., McCarrey, J.R., and Tomkinson, A.E. (1997). An Alternative Splicing Event Which Occurs in Mouse Pachytene Spermatocytes Generates a Form of DNA Ligase III with Distinct Biochemical Properties That May Function in Meiotic Recombination. Molecular and Cellular Biology *17*, 989-998.

Matsumoto, Y., and Kim, K. (1995). Excision of deoxyribose phosphate residues by DNA polymerase β during DNA repair. Science *269*, 699-700.

McElhinny, S.A., Snowden, C.M., McCarville, J., and Ramsden, D. (2000). Ku recruits the XRCC4-ligase IV complex to DNA ends. Molecular and Cellular Biology *20*, 2996-3003.

McVey, M., and Lee, S.E. (2008). MMEJ repair of double-strand breaks (director's cut): deleted sequences and alternative endings. Trends in Genetics *24*, 529-538.

Melo, J., and Toczyski, D. (2002). A unified view of the DNA-damage checkpoint. Current Opinion in Cell Biology *14*, 237-245.

Montecucco, A., Rossi, R., Levin, D.S., Gary, R., Park, M.S., Motycka, T.A., Ciarrocchi, G., Villa, A., Biamonti, G., and Tomkinson, A.E. (1998). DNA ligase I is recruited to sites of DNA replication by an interaction with proliferating cell nuclear antigen: identification of a common targeting mechanism for the assembly of replication factories. EMBO Journal *17*, 3786-3795.

Montecucco, A., Savini, E., Weighardt, F., Rossi, R., Ciarrocchi, G., Villa, A., and Biamonti, G. (1995). The N-terminal domain of human DNA ligase I contains the nuclear localization signal and directs the enzyme to sites of DNA replication. EMBO Journal *14*, 5379-5386.

Moser, J., Kool, H., Giakzidis, I., Caldecott, K., Mullenders, L.H.F., and Fousteri, M.I. (2007). Sealing of Chromosomal DNA Nicks during Nucleotide Excision Repair Requires XRCC1 and DNA Ligase III[alpha] in a Cell-Cycle-Specific Manner. Molecular Cell *27*, 311-323.

Mossi, R., Jónsson, Z., Allen, B., Hardin, S., and Hübscher, U. (1997). Replication factor C interacts with the C-terminal side of proliferating cell nuclear antigen. Journal of Biological chemistry *272*, 1769-1776.

Nandakumar, J., Shuman, S., and Lima, C.D. (2006). RNA Ligase Structures Reveal the Basis for RNA Specificity and Conformational Changes that Drive Ligation Forward. Cell *127*, 71-84.

Nash, R.A., Caldecott, K.W., Barnes, D.E., and Lindahl, T. (1997). XRCC1 Protein Interacts with One of Two Distinct Forms of DNA Ligase III. Biochemistry *36*, 5207-5211.

Nussenzweig, A., and Nussenzweig, M.C. (2007). A Backup DNA Repair Pathway Moves to the Forefront. Cell *131*, 223-225.

O'Driscoll, M., Ruiz-Perez, V.L., Woods, C.G., Jeggo, P.A., and Goodship, J.A. (2003). A splicing mutation affecting expression of ataxia-telangiectasia and Rad3-related protein (ATR) results in Seckel syndrome. Nature Genetics *33*, 497-501.

Okano, S., Lan, L., Caldecott, K.W., Mori, T., and Yasui, A. (2003). Spatial and Temporal Cellular Responses to Single-Strand Breaks in Human Cells. Molecular and Cellular Biology *23*, 3974-3981.

Okano, S., Lan, L., Tomkinson, A.E., and Yasui, A. (2005). Translocation of XRCC1 and DNA ligase IIIα from centrosomes to chromosomes in response to DNA damage in mitotic human cells. Nucleic Acids Research *33*, 422-429.

Okazaki, R., Okazaki, T., Sakabe, K., Sugimoto, K., and Sugino, A. (1968). Mechanism of DNA chain growth. I. Possible discontinuity and unusual secondary structure of newly synthesized chains. Proceedings of the National Academy of Sciences of the United States of America *59*, 598-605.

Painter, R.B. (1980). A replication model for sister-chromatid exchange. Mutation Research/Fundamental and Molecular Mechanisms of Mutagenesis *70*, 337-341.

Pandey, M., Syed, S., Donmez, I., Patel, G., Ha, T., and Patel, S.S. (2009). Coordinating DNA replication by means of priming loop and differential synthesis rate. Nature *462*, 940-943.

Pascal, J.M., O'Brien, P.J., Tomkinson, A.E., and Ellenberger, T. (2004). Human DNA ligase I completely encircles and partially unwinds nicked DNA. Nature *432*, 473-478.

Paul, K., Wang, M., Mladenov, E., Bencsik-Theilen, A.A., Bednar, T., Wu, W., Arakawa, H., and Iliakis, G. (2013). DNA ligases I and III cooperate in alternative non-homologous end-joining in vertebrates. PLoS One *8*, e59505.

Perez-Jannotti, R.M., Klein, S.M., and Bogenhagen, D.F. (2001). Two Forms of Mitochondrial DNA Ligase III Are Produced in Xenopus laevis Oocytes. Journal of Biological Chemistry *276*, 48978-48987.

Petrini, J.H.J., Xiao, Y., and Weaver, D.T. (1995). DNA Ligase I Mediates Essential Functions in Mammalian Cells. Molecular and Cellular Biology *15*, 4303-4308.

Prasad, R., Singhal, R., Srivastava, D., Molina, J., Tomkinson, A., and Wilson, S. (1996). Specific Interaction of DNA Polymerase β and DNA Ligase I in a Multiprotein Base Excision Repair Complex from Bovine Testis. Journal of Biological chemistry *271*, 16000-16007.

Puebla-Osorio, N., Lacey, D.B., Alt, F.W., and Zhu, C. (2006). Early Embryonic Lethality Due to Targeted Inactivation of DNA Ligase III. Molecular and Cellular Biology *26*, 3935-3941.

Rosidi, B., Wang, M., Wu, W., Sharma, A., Wang, H., and Iliakis, G. (2008). Histone H1 functions as a stimulatory factor in backup pathways of NHEJ. Nucleic Acids Research *36*, 1610-1623.

Rossi, R., Villa, A., Negri, C., Scovassi, I., Ciarrocchi, G., Biamonti, G., and Montecucco, A. (1999). The replication factory targeting sequence/PCNA-binding site is required in G_1 to control the phosphorylation status of DNA ligase I. EMBO Journal *18*, 5745-5754.

Sambrook, J., Fritsch, E.F., and Maniatis, T. (1989). Molecular Cloning: A Laboratory Manual. In, C.S.H. Press, ed. (Plainview, New York).

Sancar, A., Lindsey-Boltz, L.A., Ünsal-Kacmaz, K., and Linn, S. (2004). Molecular Mechanisms of Mammalian DNA Repair and the DNA Damage Checkpoints. Annual Review of Biochemistry *73*, 39-85.

Santocanale, C., and Diffley, J.F.X. (1998). A Mec1-and Rad53-dependent checkpoint controls late-firing origins of DNA replication. Nature *395*, 615-618.

Schär, P., Herrmann, G., Daly, G., and Lindahl, T. (1997). A newly identified DNA ligase of Saccharomyces cerevisiae involved in RAD52-independent repair of DNA double-strand breaks. Genes & Development *11*, 1912-1924.

Sekiguchi, J.M., Ferguson, D.O., Chen, H.T., Yang, E.M., Earle, J., Frank, K., Whitlow, S., Gu, Y., Xu, Y., Nussenzweig, A.*, et al.* (2001). Genetic interactions between ATM and the nonhomologous end-joining factors in genomic stability and development. Proceedings of the National Academy of Sciences of the United States of America *98*, 3243-3028.

Shiloh, Y. (2003). ATM and related protein kinases: Safeguarding genome integrity. Nature Reviews Cancer *3*, 155-168.

Shiloh, Y., and Kastan, M.B. (2001). ATM: Genome stability, neuronal development, and cancer cross paths. In Advances in Cancer Research (Academic Press), pp. 209-254.

Shuman, S. (2009). DNA Ligases: Progress and Prospects. Journal of Biological Chemistry *284*, 17365-17369.

Sibanda, B., Critchlow, S.E., Begun, J., Pei, X.Y., Jackson, S.P., Blundell, T.L., and Pellegrini, L. (2001). Crystal structure of an Xrcc4-DNA ligase IV complex. Nature Structural Biology *8*, 1015-1019.

Simsek, D., Furda, A., Gao, Y., Artus, J., Brunet, E., Hadjantonakis, A.-K., Van Houten, B., Shuman, S., McKinnon, P.J., and Jasin, M. (2011). Crucial role for DNA ligase III in mitochondria but not in Xrcc1-dependent repair. Nature *471*, 245-248.

Simsek, D., and Jasin, M. (2011). DNA ligase III: A spotty presence in eukaryotes, but an essential function where tested. Cell Cycle *10*, 3636-3644.

Song, W., Levin, D.S., Varkey, J., Post, S., Bermudez, V.P., Hurwitz, J., and Tomkinson, A.E. (2007). A Conserved Physical and Functional Interaction between the Cell Cycle Checkpoint Clamp Loader and DNA Ligase I of Eukaryotes. Journal of Biological Chemistry *282*, 22721-22730.

Sonoda, E., Sasaki, M.S., Morrison, C., Yamaguchi-Iwai, Y., Takata, M., and Takeda, S. (1999). Sister chromatid exchanges are mediated by homologous recombination in vertebrate cells. Molecular and Cellular Biology *19*, 5166-5169.

Sriskanda, V., and Shuman, S. (1998). Chlorella virus DNA ligase: nick recognition and mutational analysis. Nucleic Acids Research *26*, 525-531.

Teo, S.-H., and Jackson, S.P. (1997). Identification of *Saccharomyces cerevisiae* DNA ligase IV: involvement in DNA double-strand break repair. EMBO Journal *16*, 4788-4795.

Tercero, J.A., and Diffley, J.F.X. (2001). Regulation of DNA replication fork progression through damaged DNA by the Mec1/Rad53 checkpoint. Nature *412*, 553-557.

Thompson, L.H., Brookman, K.W., Jones, N.J., Allen, S.A., and Carrano, A.V. (1990). Molecular Cloning of the Human XRCC1 Gene, Which Corrects Defective DNA Strand Break Repair and Sister Chromatid Exchange. Molecular and Cellular Biology *10*, 6160-6171.

Thompson, L.H., Rubin, J.S., Cleaver, J.F., Whitmore, G.F., and Brookman, K. (1980). A screening method for isolating DNA repair-deficient mutants of CHO cells. Somatic Cell Genetics *6*, 391-405.

Tom, S., Henricksen, L.A., Park, M.S., and Bambara, R.A. (2001). DNA Ligase I and Proliferating Cell Nuclear Antigen Form a Functional Complex. Journal of Biological chemistry *276*, 24817-24825.

Tomkinson, A.E., and Mackey, Z.B. (1998). Structure and function of mammalian DNA ligases. Mutation Research *407*, 1-9.

Tomkinson, A.E., Vijayakumar, S., Pascal, J.M., and Ellenberger, T. (2006). DNA Ligases: Structure, Reaction Mechanism, and Function. Chemical Reviews *106*, 687-699.

Tsurimoto, T., Melendy, T., and Stillman, B. (1990). Sequential initiation of lagging and leading strand synthesis by two different polymerase complexes at the SV40 DNA replication origin. Nature *346*, 534-539.

van Gent, D.C., Hoeijmakers, J.H.J., and Kanaar, R. (2001). Chromosomal stability and the DNA double-stranded break connection. Nature Reviews Genetics *2*, 196-206.

Waga, S., Bauer, G., and Stillman, B. (1994). Reconstitution of complete SV40 DNA replication with purified replication factors. Journal of Biological Chemistry *269*, 10923-10934.

Waga, S., and Stillman, B. (1994). Anatomy of a DNA Replication fork revealed by reconstitution of SV40 DNA replication in vitro. Nature *369*, 207-212.

Wang, H., Rosidi, B., Perrault, R., Wang, M., Zhang, L., Windhofer, F., and Iliakis, G. (2005). DNA Ligase III as a Candidate Component of Backup Pathways of Nonhomologous End Joining. Cancer Research *65*, 4020-4030.

Wang, M., Wu, W., Wu, W., Rosidi, B., Zhang, L., Wang, H., and Iliakis, G. (2006). PARP-1 and Ku compete for repair of DNA double strand breaks by distinct NHEJ pathways. Nucleic Acids Research *34*, 6170-6182.

Wang, Y.-G., Nnakwe, C., Lane, W.S., Modesti, M., and Frank, K.M. (2004). Phosphorylation and Regulation of DNA Ligase IV Stability by DNA-dependent Protein Kinase. Journal of Biological Chemistry *279*, 37282-37290.

Ward, J.F. (1988). DNA damage produced by ionizing radiation in mammalian cells: Identities, mechanisms of formation, and reparability. Progress in Nucleic Acid Research *35*, 95-125.

Webster, A.D.B., Barnes, D.E., Arlett, C.F., Lehmann, A.R., and Lindahl, T. (1992). Growth retardation and immunodeficiency in a patient with mutations in the DNA ligase 1 gene. Lancet *339*, 1508-1509.

Wei, Y.-F., Robins, P., Carter, K., Caldecott, K., Pappin, D.J.C., Yu, G.-L., Wang, R.-P., Shell, B.K., Nash, R.A., Schar, P.*, et al.* (1995). Molecular cloning and expression of human cDNAs encoding a novel DNA ligase IV and DNA ligase III, an enzyme active in DNA repair and recombination. Molecular and Cellular Biology *15*, 3206-3216.

Willer, M., Rainey, M., Pullen, T., and Stirling, C.J. (1999). The yeast CDC9 gene encodes both a nuclear and a mitochondrial form of DNA ligase I. Current Biology *9*, 1085-1094.

Wilson, T.E., Grawunder, U., and Lieber, M.R. (1997). Yeast DNA ligase IV mediates non-homologous DNA end joining. Nature *388*, 495-498.

Windhofer, F., Wu, W., and Iliakis, G. (2007). Low Levels of DNA Ligases III and IV Sufficient for Effective NHEJ. Journal of Cellular Physiology *213*, 475-483.

Wold, M.S. (1997). Replication Protein A: A heterotrimeric, single-stranded DNA-binding protein required for eukaryotic DNA metabolism. Annual Review of Biochemistry *66*, 61-92.

Wolff, S. (1977). Sister Chromatid Exchange. Annual Review of Genetics *11*, 183-201.

Yao, S.-L., Akhtar, A.J., McKenna, K.A., Bedi, G.C., Sidransky, D., Mabry, M., Ravi, R., Collector, M.I., Jones, R.J., Sharkis, S.J.*, et al.* (1996). Selective

radiosensitization of p53-deficient cells by caffeine-mediated activation of p34cdc2 kinase. Nature Medicine *2*, 1140-1143.

Zhang, Y., Riesterer, C., Ayrall, A.M., Sablitzky, F., Littlewood, T.D., and Reth, M. (1996). Inducible site-directed recombination in mouse embryonic stem cells. Nucleic Acids Research *24*, 543-548.

Zheng, L., and Shen, B. (2011). Okazaki fragment maturation: nucleases take centre stage. Journal of Molecular Cell Biology *3*, 23-30.

Zhou, B.B., and Elledge, S.J. (2000). The DNA damage response: putting checkpoints in perspective. Nature *408*, 433-439.

Acknowledgements

Writing this work I realized how many people have made various contributions to my work and also my personal life during these last years, which is why I would like to take this opportunity to express my gratitude.

First I would like to thank for the financial support from Bundesministerium für Bildung und Forschung (BMBF) 02NUK001B. This project was integrated into the Kompetenzverbund Strahlenforschung (KVSF).

If the supervisor is no good, the laboratory won't be for sure. That is why I would like to thank Prof. George Iliakis for the brilliant and motivating environment he created in his lab. Thank you very much for always having an open ear for problems and for your ability to motivate in every possible situation. It has been a great pleasure to work in your lab.

Special thanks go to Dr. Hiroshi Arakawa for his brilliant expertise in gene targeting, as well as for the development of the well thought out targeting strategies that led to the generation of the mutants used in the present work.

I am very grateful to Prof. Wolfgang-Ulrich Müller and Drs. Veronika and Emil Mladenov for their critical reading and their helpful suggestions on this thesis.

I would also like to thank Minli and Katja for giving me insights into the miracles of experiments with DT40 cells and Katja especially for the many experiments we performed together and for the helpful discussions throughout my work.

New friends are hard to find. Special thanks therefore go to Maria and Vlado, for introducing me to Metin and Mici and for solving starting problems in these relationships.

It has been a pleasure to work in this fantastic team for the last years. I would like to thank everyone for their contribution to the wonderful atmosphere in this lab. For all the laughs we shared and the inspiring discussions. Thank you everyone!

The last years would not have been the same without the regular “meetings” in the evenings where we exchanged “protocols” and tried to improve our skills in the lab by practicing in the kitchen. It has always been a great experience with you girls!

Above all I would like to thank my family and friends. Thank you all for accepting the many “maybe”s and “no, sorry”s I had to give you in the last months. Especially I thank my parents for always being supportive and encouraging, Maren who has always been my personal cheerleader, Hen who always has the right words in every situation and of course Benni who had to endure several sleepless nights, never stopped being motivating or calming depending on the situation and was always patient during difficult time periods.

Curriculum vitae

ENTFÄLLT aus Datenschutzgründen

ENTFÄLLT aus Datenschutzgründen

ENTFÄLLT aus Datenschutzgründen

Erklärungen

Erklärung:

Hiermit erkläre ich, gem. § 6 Abs. (2) f) der Promotionsordnung der Fakultäten für Biologie, Chemie und Mathematik zur Erlangung der Dr. rer. nat., dass ich das Arbeitgebiet, dem das Thema „Efficient support of DNA replication functions by DNA ligase 3 in vertebrate cells“ zuzuordnen ist, in Forschung und Lehre vertrete und den Antrag von Frau Theresa Bednar befürworte und die Betreuung auch im Falle eines Weggangs, wenn nicht wichtige Gründe dem entgegenstehen, weiterführen werde.

Essen, _____ _____

Unterschrift eines Mitglieds der Universität Duisburg-Essen

Erklärung:

Hiermit erkläre ich, gem. § 7 Abs. (2) c) + e) der Promotionsordnung Fakultäten für Biologie, Chemie und Mathematik zur Erlangung des Dr. rer. nat., dass ich die vorliegende Dissertation selbständig verfasst und mich keiner anderen als der angegebenen Hilfsmittel bedient habe.

Essen, _____ _____

Unterschrift der Doktorandin

Erklärung:

Hiermit erkläre ich, gem. § 7 Abs. (2) d) + f) der Promotionsordnung der Fakultäten für Biologie, Chemie und Mathematik zur Erlangung des Dr. rer. nat., dass ich keine anderen Promotionen bzw. Promotionsversuche in der Vergangenheit durchgeführt habe und dass diese Arbeit von keiner anderen Fakultät/Fachbereich abgelehnt worden ist.

Essen, _____ _____

Unterschrift der Doktorandin